Search for four-top-quark production in the single-lepton and opposite-sign dilepton final states in pp collisions at $\sqrt{s} = 13$ TeV with the ATLAS detector

M. Aaboud *et al.*[*]
(ATLAS Collaboration)

(Received 7 November 2018; published 26 March 2019)

A search for four-top-quark production, $t\bar{t}t\bar{t}$, is presented. It is based on proton-proton collision data with a center-of-mass energy $\sqrt{s} = 13$ TeV collected by the ATLAS detector at the Large Hadron Collider during the years 2015 and 2016, corresponding to an integrated luminosity of 36.1 fb^{-1}. Data are analyzed in both the single-lepton and opposite-sign dilepton channels, characterized by the presence of one or two isolated electrons or muons with high-transverse momentum and multiple jets. A data-driven method is used to estimate the dominant background from top-quark pair production in association with jets. No significant excess above the Standard Model expectation is observed. The result is combined with the previous same-sign dilepton and multilepton searches carried out by the ATLAS Collaboration and an observed (expected) upper limit of 5.3 (2.1) times the four-top-quark Standard Model cross section is obtained at 95% confidence level. Additionally, an upper limit on the anomalous four-top-quark production cross section is set in the context of an effective field theory model.

DOI: 10.1103/PhysRevD.99.052009

I. INTRODUCTION

With a mass close to the scale of electroweak symmetry breaking, the top quark, besides having a large coupling to the Standard Model (SM) Higgs boson [1,2], is predicted to have large couplings to new particles hypothesized in many models beyond the Standard Model (BSM) [3–5]. Possible new phenomena may enhance the cross sections over SM predictions for various processes involving top quarks, and in particular for the production of four top quarks [6–15]. This paper focuses on a search for four-top-quark ($t\bar{t}t\bar{t}$) production via the SM processes in proton-proton (pp) collisions at the Large Hadron Collider (LHC) and the results are interpreted in the context of an effective field theory (EFT) approach where the BSM contribution is represented via a four-top-quarks contact interaction [10].

The SM four-top-quark production cross section ($\sigma_{\mathrm{SM}}^{t\bar{t}t\bar{t}}$) in pp collisions at a center-of-mass energy $\sqrt{s} = 13$ TeV is predicted to be $\sigma_{\mathrm{SM}}^{t\bar{t}t\bar{t}} = 9.2$ fb at next-to-leading-order (NLO) accuracy in QCD, with scale and parton distribution function (PDF) uncertainties of the order of 30% and 6%, respectively [16,17]. Previous searches for four-top-quark production using LHC Run 2 data at $\sqrt{s} = 13$ TeV were performed by both the ATLAS [18–20] and CMS [21–24] Collaborations. Among them, the most sensitive one is a CMS search [24] obtaining an observed (expected) 95% confidence level (C.L.) upper limit of 4.5 (2.3) times the SM expectation. Searches for anomalous $t\bar{t}t\bar{t}$ production via an EFT model were recently performed by the ATLAS Collaboration [19,20], which set an observed (expected) upper limit of 16 fb (31 fb) on the production cross section at 95% C.L.

The four-top-quark production events can give rise to different final states depending on the hadronic or semileptonic decay mode of each of the top quarks. The four-top-quark decay topology considered in this search corresponds to either single-lepton events with one isolated charged lepton (electron or muon)[1] or dilepton events with two opposite-sign charged leptons (electrons or muons). The event topology also features high jet multiplicity and high multiplicity of jets containing b-hadrons. Signal events are characterized by high scalar sum of the jet transverse momenta ($H_{\mathrm{T}}^{\mathrm{had}}$), which provides good discrimination against the dominant background, i.e., top-quark

[*]Full author list given at the end of the article.

[1]The τ-leptons are not reconstructed; however, isolated electron and muon by-products of the leptonically decaying τ-leptons are considered in the analysis.

pair production in association with jets ($t\bar{t}+$ jets). Given that the four-top-quark production events are expected to contain hadronically decaying top-quark candidates with collimated or partially collimated topologies, the analysis makes use of "mass-tagged reclustered large-R (RCLR) jets" [25,26], which will be described in Sec. III.

Selected events in each of the two channels are classified into several categories according to the number of jets, b-tagged jets and mass-tagged RCLR jets. A data-driven method is developed to estimate the dominant $t\bar{t}+$ jets background. The Monte Carlo (MC) simulation is used in order to estimate correction factors and evaluate the systematic uncertainties of the data-driven estimate.

The paper is organized as follows: the ATLAS detector is described in Sec. II. Section III summarizes the selection criteria applied to events and reconstructed objects. The simulation-based signal and background modeling, together with the data-driven estimation of nonprompt and fake lepton backgrounds are discussed in Sec. IV. Section V is devoted to the search strategy and classification of event topologies, while the $t\bar{t}+$ jets background estimation technique using data is described in Sec. VI. The systematic uncertainties are summarized in Sec. VII. Section VIII presents the results and the combination with the same-sign dilepton and multilepton final-states search [20] carried out by ATLAS.

II. ATLAS DETECTOR

The ATLAS detector [27] at the LHC is a multipurpose particle detector with a forward-backward symmetric cylindrical geometry and nearly 4π coverage in solid angle.[2] It consists of an inner tracking detector (ID), electromagnetic and hadronic calorimeters, and a muon spectrometer. The inner detector, including the insertable B-layer [28,29], provides charged-particle tracking from silicon pixel and microstrip detectors in the pseudorapidity region $|\eta| < 2.5$, surrounded by a transition radiation tracker that enhances electron identification in the region $|\eta| < 2.0$. The ID is surrounded by a thin superconducting solenoid providing an axial 2 T magnetic field, and by a fine-granularity lead/liquid-argon electromagnetic calorimeter covering $|\eta| < 3.2$, which provides energy measurements of electromagnetic showers. Hadron calorimetry is also based on the sampling technique and covers $|\eta| < 4.9$, with either scintillator tiles or liquid argon as the active medium and with steel, copper or tungsten as the absorber material. An extensive muon spectrometer with an air-core toroid magnet system surrounds the calorimeters. It includes three layers of high-precision tracking chambers, which provide coverage in the range $|\eta| < 2.7$. The field integral of the toroid magnets ranges from 2.0 to 6.0 Tm across most of the detector. A two-level trigger system [30], the first level using custom hardware and followed by a software-based level, is used to reduce the event rate to a maximum of around one kHz for offline storage.

[2]ATLAS uses a right-handed coordinate system with its origin at the nominal interaction point (IP) in the center of the detector. The positive x axis is defined by the direction from the IP to the center of the LHC ring, with the positive y axis pointing upwards, while the beam direction defines the z axis. Cylindrical coordinates (r, ϕ) are used in the transverse plane, ϕ being the azimuthal angle around the z axis. The pseudorapidity η is defined in terms of the polar angle θ by $\eta = -\ln\tan(\theta/2)$. Unless stated otherwise, the angular distance is defined as $\Delta R \equiv \sqrt{(\Delta\eta)^2 + (\Delta\phi)^2}$.

III. OBJECT AND EVENT SELECTION

Events are selected from pp collisions with $\sqrt{s} = 13$ TeV recorded by the ATLAS detector in 2015 and 2016. Only events for which all relevant subsystems were operational are considered. The data set corresponds to an integrated luminosity of 36.1 ± 0.8 fb^{-1} [31]. The event reconstruction is affected by multiple inelastic pp collisions in a single bunch crossing and by collisions in neighboring bunch crossings, referred to as "pileup." The number of interactions per bunch crossing in this data set ranges from about 8 to 45 interactions. Events are required to have at least one reconstructed vertex with two or more associated tracks with transverse momentum $p_{\mathrm{T}} > 0.4$ GeV. If multiple vertices are reconstructed, the vertex with the largest sum of the squares of the transverse momenta of associated tracks is taken as the primary vertex [32].

Events in both the single-lepton and dilepton channels were recorded using single-lepton triggers. Events were selected using triggers with either low p_{T} thresholds and a lepton-isolation requirement, or with higher thresholds but with a looser identification criterion and without any isolation requirement. The lowest p_{T} threshold used for muons is 20 (26) GeV in 2015 (2016), while the higher p_{T} threshold is 50 GeV in both years. For electrons, triggers with a p_{T} threshold of 24 (26) GeV in 2015 (2016) and isolation requirements are used along with triggers with a 60 GeV threshold and no isolation requirement, and with a 120 (140) GeV threshold with looser identification criteria.

Electron candidates are reconstructed [33,34] from an isolated electromagnetic calorimeter energy deposit, matched to a track in the ID, within the fiducial region of $|\eta_{\mathrm{cluster}}| < 2.47$, where η_{cluster} is the pseudorapidity of the calorimeter energy deposit associated with the electron candidate. Candidates within the transition region between the barrel and end cap electromagnetic calorimeters, $1.37 < |\eta_{\mathrm{cluster}}| < 1.52$, are excluded. The electron candidates are required to have $p_{\mathrm{T}} > 30$ GeV and to satisfy "tight" likelihood-based identification criteria [34] based on calorimeter, tracking and combined variables that provide good separation between electrons and jets. Muon candidates are reconstructed [35] by combining tracks reconstructed in both the ID and the muon

spectrometer. Candidates are required to pass the "medium" identification criteria [35] and to have $p_{\mathrm{T}} > 30$ GeV and $|\eta| < 2.5$. To reduce the contribution from nonprompt leptons (e.g., from semileptonic b- or c-hadron decays), photon conversions and hadrons, lepton candidates are also required to be isolated. The lepton isolation is estimated using the scalar sum of all tracks excluding the lepton candidate itself ($I_R = \sum p_{\mathrm{T}}^{\mathrm{trk}}$) within a cone defined by $\Delta R < R_{\mathrm{cut}}$ along the direction of the lepton. The value of R_{cut} is the smaller of r_{min} and $10\ \mathrm{GeV}/p_{\mathrm{T}}^{\ell}$, where r_{min} is set to 0.2 (0.3) for electron (muon) candidates, and p_{T}^{ℓ} is the lepton p_{T}. All lepton candidates are required to satisfy $I_R/p_{\mathrm{T}}^{\ell} < 0.06$. Finally, lepton tracks must match the primary vertex of the event: the longitudinal impact parameter z_0 is required to satisfy $|z_0 \sin\theta| < 0.5$ mm, where θ is the polar angle of the track. The transverse impact parameter significance $|d_0|/\sigma(d_0)$ must be less than 5 for electrons and 3 for muons, where d_0 is the transverse impact parameter and $\sigma(d_0)$ is its uncertainty.

Jet candidates are reconstructed from three-dimensional topological energy clusters [36] in the calorimeter using the anti-k_t jet algorithm [37–39] with a radius parameter of 0.4, and these are referred to as "small-R jets". Each topological cluster is calibrated to the electromagnetic energy scale prior to jet reconstruction [40]. The reconstructed jets are then calibrated to the particle level by the application of a jet energy scale derived from simulation [41]. After energy calibration, jets are required to satisfy the $p_{\mathrm{T}} > 25$ GeV and $|\eta| < 2.5$ selection. Quality criteria are imposed to identify jets arising from noncollision sources or detector noise and any event containing such a jet is removed [42]. Finally, to reduce the effect of pileup, an additional requirement is made on the jet vertex tagger (JVT) discriminant [43] for jets with $p_{\mathrm{T}} < 60$ GeV and $|\eta| < 2.4$.

Jets are tagged as containing a b-hadron via a multivariate b-tagging algorithm [44,45]. For each jet, a value for the multivariate b-tagging discriminant is calculated, and the jet is considered b-tagged if this value is above a given threshold. The threshold used in this search corresponds to an average 77% efficiency to tag a jet containing a b-hadron, with a light-jet rejection factor of ∼134 and a charm-jet rejection factor of ∼6, as determined for jets with $p_{\mathrm{T}} > 20$ GeV and $|\eta| < 2.5$ in simulated $t\bar{t}$ events [46–48].

To avoid assigning a single detector response to more than one reconstructed object, a sequential overlap-removal procedure is adopted. Electron candidates that lie within $\Delta R = 0.01$ of a muon candidate are removed to suppress contributions from bremsstrahlung. To prevent double-counting of electron energy deposits as jets, the closest jet within $\Delta R_y = \sqrt{(\Delta y)^2 + (\Delta\phi)^2} = 0.2$ of a selected electron is removed.[3] If the nearest jet surviving that selection is within $\Delta R_y = 0.4$ of an electron, the electron is discarded. The overlap removal procedure between the remaining jet candidates and muon candidates is designed to remove those muons that are likely to have arisen in the decay chain of hadrons and to retain the overlapping jet instead. Jets and muons may also appear in close proximity. For example, a muon with high-p_{T} bremsstrahlung radiation inside the calorimeter may be reconstructed as a jet. In such cases, the jet should be removed and the muon retained. Such jets are characterized by having very few matching inner-detector tracks. Selected muons that satisfy $\Delta R(\mu, \mathrm{jet}) < 0.04 + 10\ \mathrm{GeV}/p_{\mathrm{T}}^{\mu}$ are rejected if the jet has at least three tracks originating from the primary vertex; otherwise the jet is removed and the muon is kept.

The selected and calibrated small-R jets with $p_{\mathrm{T}} > 25$ GeV and passing both the requirement on the JVT and the overlap removal with leptons are used as inputs for further jet reclustering [25] using the anti-k_t algorithm with a radius parameter of $R = 1.0$. These reclustered large-R jets are referred to as RCLR jets. The calibration corrections and uncertainties in the RCLR jets are automatically inherited from the small-R jets [26]. In order to further suppress contributions from pileup and other soft radiation, the RCLR jets are trimmed [49] by removing all small-R jets within a reclustered jet that have p_{T} below 5% of the p_{T} of the reclustered jet. Due to the pileup suppression and $p_{\mathrm{T}} > 25$ GeV requirements made on the small-R jets, the probability for a small-R jet to be removed from the corresponding reclustered jet by the trimming requirement is less than 1%. The resulting RCLR jets are used to identify hadronically decaying top-quark candidates. RCLR jets that have $p_{\mathrm{T}} > 200$ GeV, $|\eta| < 2.0$, mass[4] larger than 100 GeV and at least one constituent small-R jet are referred to as "mass-tagged RCLR jets."

The missing transverse momentum in the event, whose magnitude will be denoted in the following by $E_{\mathrm{T}}^{\mathrm{miss}}$, is defined as the negative vector sum of the p_{T} of reconstructed and calibrated objects in the event, where only primary objects enter the sum (e.g., RCLR jets are not used). This sum includes a term to account for energy from low-momentum particles in the event that are not associated with any of the selected objects, which is calculated from inner detector tracks matched to the reconstructed primary vertex in the event [50].

Events of interest are required to have at least one reconstructed lepton that matches, within $\Delta R < 0.15$, the lepton with the same flavor reconstructed by the trigger algorithm. Events in the opposite-sign dilepton channel are retained if they contain exactly two opposite-sign charged leptons (electrons or muons) and at least four jets satisfying the quality and kinematic criteria discussed

[3]The rapidity is defined as $y = \frac{1}{2}\ln\frac{E+p_z}{E-p_z}$, where E is the energy and p_z is the longitudinal component of the momentum along the beam pipe.

[4]The reclustered jet mass is computed from the sum of the four-momenta of the associated small-R jets [26].

TABLE I. Summary of preselection requirements for the single-lepton and dilepton channels. Here m_{T}^{W} is the transverse mass of the lepton and the $E_{\mathrm{T}}^{\mathrm{miss}}$ vector, and $m_{\ell\ell}$ denotes the dilepton invariant mass in the ee and $\mu\mu$ channels.

Preselection requirements		
Requirement	Single-lepton	Dilepton
Trigger	Single-lepton triggers	
Leptons	1 isolated	2 isolated, opposite-sign
Jets	≥ 5 jets	≥ 4 jets
b-tagged jets	≥ 2 b-tagged jets	
Other	$E_{\mathrm{T}}^{\mathrm{miss}} > 20$ GeV	$m_{\ell\ell} > 50$ GeV
	$E_{\mathrm{T}}^{\mathrm{miss}} + m_{\mathrm{T}}^{W} > 60$ GeV	$\lvert m_{\ell\ell} - 91\ \mathrm{GeV}\rvert > 8$ GeV

above, of which at least two must be b-tagged. In both the ee and $\mu\mu$ channels, the dilepton invariant mass ($m_{\ell\ell}$) must be above 50 GeV and outside the Z mass window 83–99 GeV. Events not in the opposite-sign dilepton channel may enter the single-lepton channel if they contain exactly one lepton and at least five jets, of which at least two are b-tagged. The above selection criteria imply that events containing two leptons with the same charge, or three or more leptons of any charge are excluded from the selection. This is done in order to maintain orthogonality with the complementary search with same-sign dilepton and multilepton final states [20] carried out by ATLAS, as these results are combined with the results presented here (Sec. VIII). Additional requirements are made to suppress the background from multijet production in the single-lepton channel. Requirements are made on $E_{\mathrm{T}}^{\mathrm{miss}}$ as well as on the transverse mass of the combined lepton and $E_{\mathrm{T}}^{\mathrm{miss}}$ system[5] (m_{T}^{W}): $E_{\mathrm{T}}^{\mathrm{miss}} > 20\,\mathrm{GeV}$ and $E_{\mathrm{T}}^{\mathrm{miss}} + m_{\mathrm{T}}^{W} > 60$ GeV.

The above requirements are referred to as "preselection" and are summarized in Table I. Events satisfying either the single-electron or single-muon selections are combined and treated as a "single-lepton" analysis channel, and events satisfying any of the opposite-sign lepton selections (ee, $\mu\mu$ or $e\mu$) are combined and treated as a "dilepton" analysis channel.

IV. SIGNAL AND BACKGROUND MODELING

After the event preselection, the main background processes arise from the SM production of $t\bar{t}$ + jets and single top-quarks, as well as W- or Z-boson production in association with jets. Small contributions arise from the associated production of a vector boson V ($V = W, Z$) or a Higgs boson and a $t\bar{t}$ pair ($t\bar{t} + V$ and $t\bar{t} + H$) and from diboson (WW, WZ, ZZ) production. Multijet events contribute to the selected sample via the misidentification of hadronic objects (jets, hadrons) as leptons or the presence of a nonprompt electron or muon. These events are referred to as the "fake and nonprompt lepton" background in the remainder of this paper.

MC simulation samples are used to model the expected distributions of the signal and most of the background processes. The fake and nonprompt lepton background in the single-lepton channel is estimated with a fully data-driven method. The $t\bar{t}$ + jets background, which is dominant in regions with very high jet and b-jet multiplicities, is estimated via a dedicated data-driven method, with some correction factors taken from the MC simulation, as described in Sec. VI. The MC samples were processed either through the full ATLAS detector simulation [51] based on GEANT4 [52], or through a faster simulation making use of parametrized showers in the calorimeters [53]. To model the effects of pileup, events from minimum-bias interactions were generated using the PYTHIA 8.186 [54] event generator and overlaid on the simulated hard-scatter events according to the luminosity profile of the recorded data. All simulated samples were processed through the same reconstruction algorithms and analysis chain as the data. In the simulation, the top-quark mass was assumed to be $m_{\mathrm{top}} = 172.5$ GeV. The heavy-flavor decays were modeled using the EVTGEN 1.2.0 [55] program, except for processes modeled using the SHERPA generator [56].

A. Signal modeling

Simulated events for the main signal process, i.e., the four-top-quark production with SM kinematics, were generated at leading order (LO) with the MADGRAPH5_aMC@NLO 2.2.2 [17] generator and the NNPDF2.3 LO PDF set [57], interfaced to PYTHIA 8.186 using the A14 set of tuned parameters [58], which will be denoted in the following by A14 tune. The SM $t\bar{t}t\bar{t}$ sample is normalized to a cross section of 9.2 fb, computed at NLO in QCD [17].

This search also probes a BSM model with kinematic characteristics similar to those of the SM $t\bar{t}t\bar{t}$ events: the $t\bar{t}t\bar{t}$ production via an effective field theory involving a four-fermion contact interaction [10]. The EFT $t\bar{t}t\bar{t}$ sample was generated at LO with the MADGRAPH5_aMC@NLO 2.2.2 generator and the NNPDF2.3 LO PDF set, interfaced to PYTHIA 8.186 with the A14 tune. It is normalized assuming $|C_{4t}|/\Lambda^2 = 4\pi\ \mathrm{TeV}^{-2}$, where C_{4t} denotes the coupling constant and Λ the energy scale of new physics, which yields a cross section of 926.3 fb computed using MADGRAPH5_aMC@NLO. Details of this BSM scenario can be found in Refs. [19,20].

B. Background modeling

The dominant $t\bar{t}$ + jets background estimation relies on the data-driven technique described in Sec. VI. The

[5] $m_{\mathrm{T}}^{W} = \sqrt{2 p_{\mathrm{T}}^{\ell} E_{\mathrm{T}}^{\mathrm{miss}} (1 - \cos\Delta\phi)}$, where p_{T}^{ℓ} is the transverse momentum of the lepton and $\Delta\phi$ is the azimuthal angle separation between the lepton and the direction of the missing transverse momentum.

validation of this technique and the extraction of the corresponding correction factors were performed with simulated MC $t\bar{t}+$ jets events, generated with POWHEG-BOX v2 [59–62], which provides NLO accuracy in QCD for the $t\bar{t}$ process and uses the CT10 PDF set [63]. Showering was performed using PYTHIA 6.428 [64] with the CTEQ6L PDF set [65] and the PERUGIA2012 tune [66]. The hard-process factorization scale μ_{F} and renormalization scale μ_{R} were set to the default POWHEG value: $\mu=\sqrt{m_{\mathrm{top}}^2+p_{\mathrm{T,top}}^2}$, where $p_{\mathrm{T,top}}$ is the transverse momentum of the top quark in the $t\bar{t}$ center-of-mass reference frame. The POWHEG model resummation damping parameter, h_{damp}, which controls the matching of matrix elements to parton showers and regulates the high-p_{T} parton radiation, was set to m_{top} [67]. The sample is normalized to the theoretical cross-section value for the inclusive $t\bar{t}$ process of 832^{+40}_{-46} pb obtained with TOP++ [68], calculated at next-to-next-to-leading order (NNLO) in QCD, and including resummation of next-to-next-to-leading logarithmic soft gluon terms [69–73].

Samples of $W/Z+$ jets events were generated with the SHERPA 2.2 [56] generator. The matrix element calculation was performed with up to two partons at NLO in QCD and up to four partons at LO using matrix elements from COMIX [74] and OPENLOOPS [75]. The matrix element calculation was merged with the SHERPA [76] parton shower (PS) using the ME + PS@NLO prescription [77]. The PDF set used for the matrix element calculation is NNPDF3.0nnlo with a dedicated PS tuning developed by the SHERPA authors. The $W+$ jets and $Z+$ jets samples are normalized to their inclusive production cross section estimates at NNLO in QCD, calculated with FEWZ [78,79].

Samples of single-top-quark backgrounds, corresponding to the Wt and s-channel production mechanisms, were generated with POWHEG-BOX v1 [80] at NLO accuracy using the CT10 PDF set. Overlaps between the $t\bar{t}$ and Wt final states were removed using the "diagram removal" scheme [81]. Samples of t-channel single-top-quark events were generated using the POWHEG-BOX v1 [82,83] NLO generator that uses the four-flavor scheme. The fixed four-flavor PDF set CT10f4 [63] was used for the matrix element calculations. Showering was performed using PYTHIA 6.428 with the PERUGIA2012 tune. The single-top-quark samples are normalized to the approximate NNLO cross sections [84–86].

Diboson processes with one of the bosons decaying hadronically and the other leptonically were simulated using the SHERPA 2.1.1 generator. They were calculated for up to one (ZZ) or zero (WW, WZ) additional partons at NLO, and up to three additional partons at LO, using the same procedure as for $W/Z+$ jets. The CT10 PDF set was used together with a dedicated PS tuning of the SHERPA fragmentation model. All diboson samples are normalized to their NLO cross sections provided by SHERPA.

Samples of $t\bar{t}+V$ (with $V=W$ or Z, including nonresonant Z/γ^* contributions) were generated with MADGRAPH5_aMC@NLO 2.3.2, using NLO in QCD matrix elements and the NNPDF3.0NLO [87] PDF set. Showering was performed using PYTHIA 8.210 and the A14 tune. The $t\bar{t}+V$ events are normalized to their NLO cross section [17]. A sample of $t\bar{t}+H$ events was generated using MADGRAPH5_aMC@NLO 2.3.2 generator and the NNPDF3.0NLO PDF set. Showering was performed using PYTHIA 8.210 and the A14 tune. Inclusive decays of the Higgs boson are assumed in the generation of the $t\bar{t}+H$ sample, which is normalized to the corresponding cross section calculated at NLO [88,89]. Rare backgrounds, such as $t\bar{t}+WW$ and triple-top-quark production ($t\bar{t}+t$, $t\bar{t}+tW$), were generated at LO with MADGRAPH5_aMC@NLO 2.2.2 with no additional partons and interfaced with PYTHIA 8.186. They are normalized using cross sections computed at NLO in QCD [17,90].

C. Estimation of nonprompt and fake lepton backgrounds

In the single-lepton channel, the background from events with a fake or nonprompt lepton is estimated from data using a "matrix method" technique [91,92]. Events are selected using looser isolation or identification requirements for the lepton and are then weighted according to the efficiencies for both prompt and background (fake and nonprompt) leptons to pass the tighter default selection. These efficiencies are measured in data using dedicated control regions. The contribution from events with a fake or nonprompt lepton is found to be consistent with zero in regions defined by the presence of two or more mass-tagged RCLR jets, as well as in the regions requiring the presence of at least one mass-tagged RCLR jet and at least four b-tagged jets. The contribution is at most 6% in the rest of the signal regions (described in Sec. V).

In the dilepton channel, the majority (90%) of events containing one prompt lepton and one background lepton, arising from either a heavy-flavor hadron decay, photon conversion, jet misidentification or light-meson decay, originate from the single-lepton $t\bar{t}+$ jets background. This contribution is included in the estimation via the data-driven technique described in Sec. VI, while the small fraction of fake and nonprompt leptons events arising from $W+$ jets and $t\bar{t}+V$ events is estimated from MC simulation.[6] The total contribution is found to be less than 8% of the total background in the signal regions.

[6]No data-driven estimation was attempted due to the statistical overlap with the same-sign dilepton and multilepton final-states search [20].

V. SEARCH STRATEGY

Signal events from SM four-top-quark production in the single lepton (opposite-sign dilepton) decay channel are characterized by the presence of one charged lepton (two opposite-sign charged leptons), missing transverse momentum from the escaping neutrino(s) and a high number of high-p_{T} jets. At LO the single-lepton (opposite-sign dilepton) decay will potentially have an event topology with ten (eight) jets, when each parton from a top-quark decay gives rise to a separate jet: six (four) jets are light-jets and four are b-quark jets. However, the topology of a reconstructed event could differ due to the limited detector acceptance, the b-tagging efficiency, and the possible presence of jets arising either from additional radiation and multiple parton interactions (MPI) or from collimated partons not resolved as separate objects. Events are classified in several regions to optimize the sensitivity of the search, to perform a data-driven estimate of the $t\bar{t}+$ jets background (described in Sec. VI) and to validate the background prediction.

Preselected events in each of the two channels are classified according to their event topology, defined by the number of jets with $p_{\mathrm{T}} > 25$ GeV and the number of b-jets. Several regions are split according to the mass-tagged RCLR jet multiplicity in addition to the jet and b-tagged jet multiplicities. In the following, a region with m jets (j), of which n are b-tagged jets (b) and from which p separate mass-tagged RCLR jets (J) are reconstructed is referred to as "mj, nb, pJ." When no mass-tagged RCLR jet multiplicity is specified, no selection on these objects is performed.

The following regions are defined to be orthogonal using the classification described above: 20 "signal regions," 16 "validation regions," 18 "source regions" and 2 "efficiency extraction regions," as shown in Fig. 1.

Twelve regions in the single-lepton channel and eight regions in the dilepton channel with the largest signal-to-background ratios (up to 5.7% in the single-lepton channel and 7.0% in the dilepton channel), assuming SM $t\bar{t}t\bar{t}$ production cross section and kinematics, are referred to as signal regions. These regions are included in the simultaneous fit to extract the signal cross section and have high jet multiplicities ($\geq$ 9j and $\geq$ 7j for single-lepton and dilepton respectively) and high b-tagged jet multiplicities ($\geq$ 3b). Since events from the main $t\bar{t}+$ jets background are characterized by at most one hadronically decaying top quark in the single-lepton channel and no hadronically decaying top quarks in the dilepton channel, the signal regions are split into 0, 1 and $\geq$ 2J in the single-lepton case, and into 0 and $\geq$ 1J in the dilepton case.

Twelve validation regions in the single-lepton channel and four validation regions in the dilepton channel are defined. These regions do not overlap with the signal region selections and feature low expected signal-to-background ratios (less than 1%). They are not included in the fit nor used to extract information from the data. These regions are designed primarily to validate the data-driven estimate of the $t\bar{t}+$ jets background (introduced in Sec. VI) and to confirm the validity of the assumption that the $t\bar{t}+$ jets data-driven estimate can be extrapolated to the signal regions. The validation regions in the single-lepton channel contain exactly seven or exactly eight jets of which three or at least four are b-tagged. In the dilepton channel, the validation regions have exactly six jets of which three or at least four are b-tagged. In each of the two channels these validation regions are split according to the mass-tagged RCLR jet multiplicity in the same way as the corresponding signal regions.

With the goal of estimating the $t\bar{t}+$ jets background in the signal regions, data events with lower jet and/or b-jet

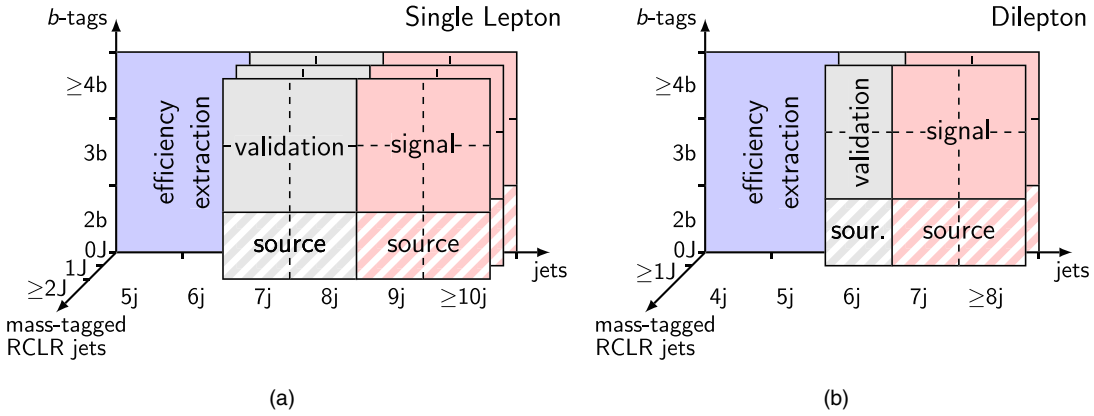

FIG. 1. Schematic view of the different analysis regions in (a) the single-lepton and (b) the dilepton channels. The three axes represent the jet multiplicity, the b-tagged jet multiplicity and the mass-tagged RCLR jet multiplicity. The efficiency extraction region in each channel is defined inclusively in the mass-tagged RCLR jet multiplicity.

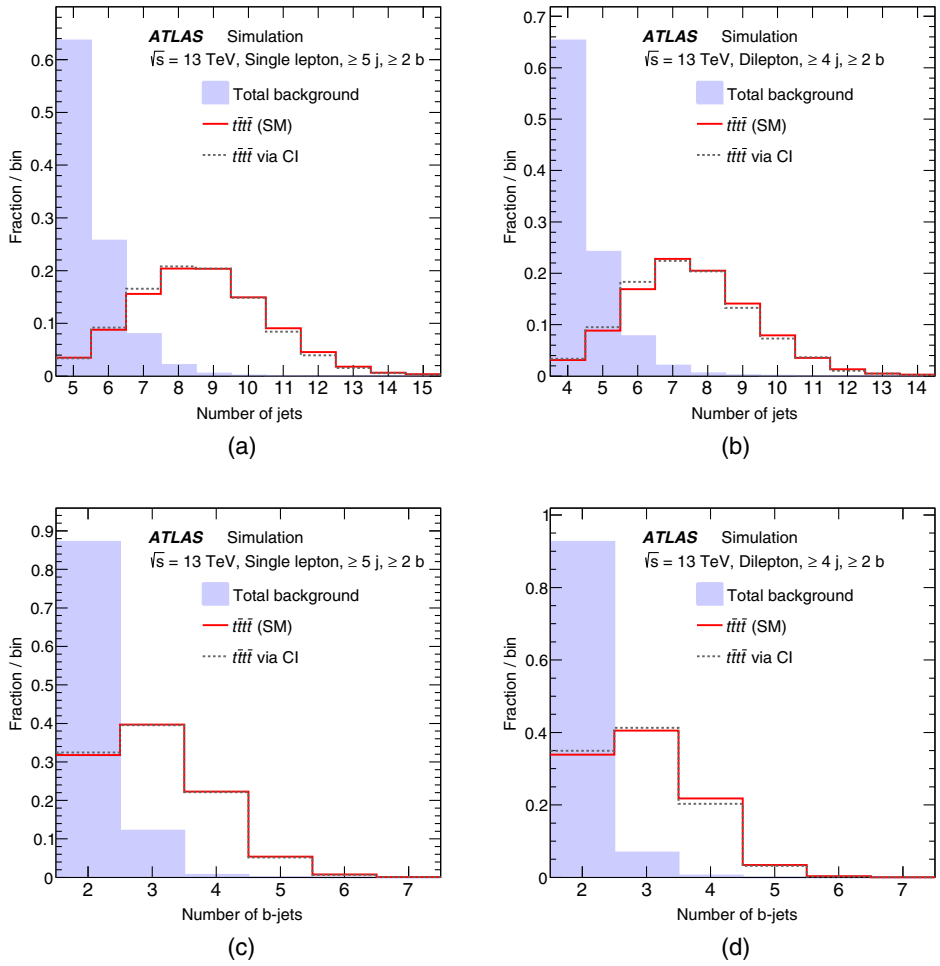

FIG. 2. (a), (b) The jet multiplicity and (c), (d) the b-jet multiplicity distributions after preselection for the total predicted background with the $t\bar{t}$ + jets background estimated via MC simulation (shaded histogram) and the signal scenarios considered in this search in the single-lepton (a), (c) and the dilepton (b), (d) channels. The signals shown correspond to four-top-quark production with SM kinematics (solid) and $t\bar{t}t\bar{t}$ production involving a four-fermion contact interaction (dashed). The distributions are normalized to unit area. The last bin in each distribution contains the overflow.

multiplicities are used in the data-driven method described in Sec. VI. The 18 source regions are built using events with high jet multiplicity: 7, 8, 9, ≥ 10 for the single-lepton channel and 6, 7, ≥ 8 for the dilepton channel, out of which exactly 2 jets are b-tagged. They are used to build pseudodata event samples in the signal and validation regions with same jet multiplicities but higher number of b-tagged jets. Efficiency extraction regions are characterized by lower jet multiplicities: five or six jets for the single-lepton channel and four or five for the dilepton channel, out of which 2, 3 or ≥ 4 are b-tagged. They are used to extract the b-tagging probabilities, since they provide a sample depleted of signal and dominated by $t\bar{t}$ + jets. Neither the efficiency extraction regions nor the source regions are included in the final fit to data.

Figure 2 shows the expected shapes of the jet and b-jet multiplicity distributions after preselection in the single-lepton and dilepton channels. The distributions shown are for the total predicted background, with the $t\bar{t}$ + jets background estimated via MC simulation, and for the considered four-top-quark signal scenarios. Figures 3(a) and 3(b) show the same distributions but for the mass-tagged RCLR jet multiplicity.

Figures 3(c) and 3(d) compare the expected shapes of the scalar sum of the jet transverse momenta, considering all selected jets ($H_{\mathrm{T}}^{\mathrm{had}}$), between the different four-top-quark signal scenarios and the total predicted background. Given the different kinematic features, the $H_{\mathrm{T}}^{\mathrm{had}}$ distribution provides a suitable discrimination between events from the signal hypotheses and the background, and is used as the main discriminating variable in each of the regions. The signal-to-background discrimination is therefore provided by the combination of the event categorization and the $H_{\mathrm{T}}^{\mathrm{had}}$ distribution in each category.

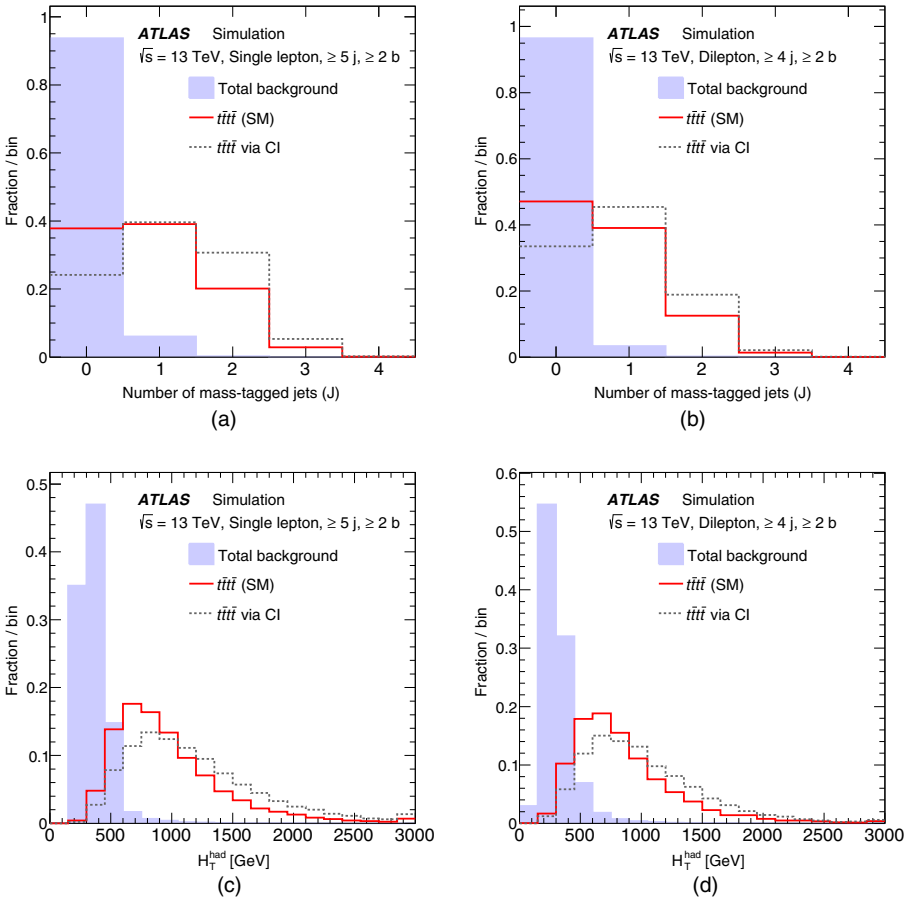

FIG. 3. (a), (b) The mass-tagged RCLR jet multiplicity distributions and (c), (d) the $H_{\mathrm{T}}^{\mathrm{had}}$ distributions after preselection for the total predicted background with the $t\bar{t}+$ jets background estimated via MC simulation (shaded histogram) and signals for the single-lepton (a), (c) and the dilepton (b), (d) channels. The signals shown correspond to four-top-quark production with SM kinematics (solid) and $t\bar{t}t\bar{t}$ production involving a four-fermion contact interaction (dashed). The distributions are normalized to unit area. The last bin in each distribution contains the overflow.

VI. $t\bar{t}+$ jets BACKGROUND ESTIMATION USING DATA: THE TRF$_{t\bar{t}}$ METHOD

The MC simulation-based approach at NLO accuracy in QCD for the prediction of the inclusive $t\bar{t}$ background is not expected to model well the very high jet and b-jet multiplicity regions exploited in this search. Given the lack of multileg calculations, the MC simulation-based approach relies on the description of such large multiplicities through the parton-shower formalism with consequently large uncertainties. Therefore, a data-driven method is used to estimate the dominant background from $t\bar{t}+$ jets in regions with very high jet and b-jet multiplicities. This method provides a more accurate prediction of this background than a purely simulation-based approach and avoids the need to estimate modeling uncertainties (documented in Sec. VII) by extrapolation from kinematic regimes with different numbers of jets and b-tagged jets.

The estimate is based on a method introduced in Ref. [93] and is referred to as "tag rate function for $t\bar{t}+$ jets events," which will be denoted in the following by TRF$_{t\bar{t}}$. The method assumes that the probability of b-tagging an additional[7] jet in a $t\bar{t}+$ jets event, where the additional jets can include c- and b-jets, is essentially independent of the number of additional jets. With this assumption, the tagging probability, as a function of the kinematic properties of the jet, can be estimated in lower jet-multiplicity events and then applied to data events with the same jet multiplicity as signal-region events, but lower b-tagged jet multiplicity, where the signal contamination is negligible. These b-tagging probabilities are measured and applied as a function of some of the jet and event properties. Simulation-based corrections are then applied in order to correct for the fact that the assumptions stated above may not be completely valid. Systematic uncertainties in these corrections are propagated through the final estimate.

[7]Additional refers to all jets in addition to the $b(\bar{b})$-jets originating from the $t\bar{t}$ decay. This includes the jets possibly originating from hadronically decaying W bosons.

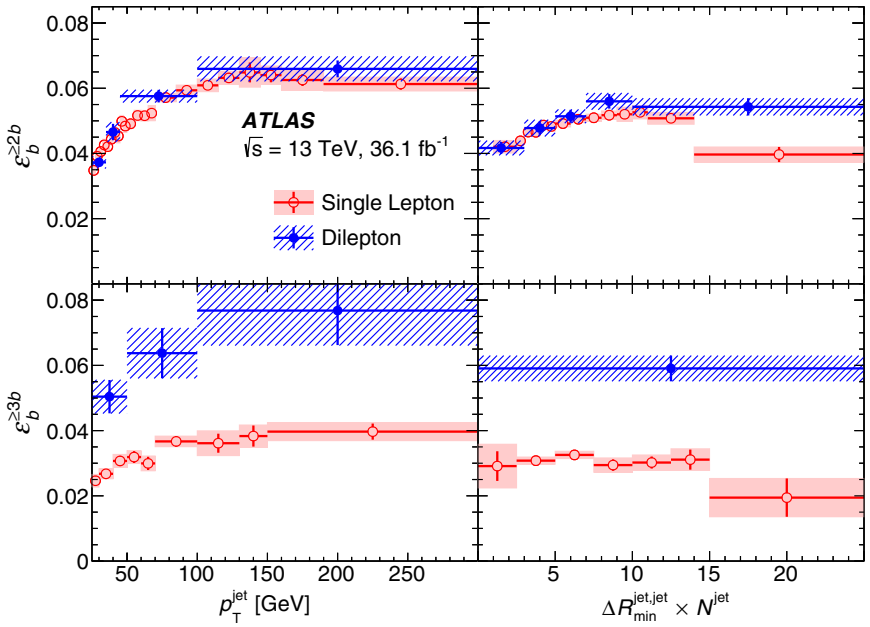

FIG. 4. Values of the per-jet b-tagging probability for $t\bar{t}$ + jets events as a function of the jet transverse momentum (p_T^{jet}) and the minimum ΔR between the considered jet and the other jets in the event, scaled by the jet multiplicity ($\Delta R_{min}^{jet,jet} \times N^{jet}$), as measured in data requiring the presence of at least two b-jets ($\varepsilon_b^{\geq 2b}$) and least three b-jets ($\varepsilon_b^{\geq 3b}$). b-tagging probabilities are shown separately for single-lepton and dilepton events. The vertical error bars indicate the statistical uncertainties, while the shaded (hatched) areas indicate the combined statistical and systematic uncertainties. In the dilepton case, a constant b-tagging probability is assumed as a function of $\Delta R_{min}^{jet,jet} \times N^{jet}$ for $\varepsilon_b^{\geq 3b}$.

The per-jet b-tagging probabilities ε_b are measured in the efficiency extraction regions (described in Sec. V), after subtracting the contribution from all non-$t\bar{t}$ processes modeled with MC simulation, amounting to 8%–14% of the total background, depending on the channel and on the signal region considered. In order to take into account the correlation of ε_b with the b-tagged jet multiplicities, two sets of probabilities $\varepsilon_b^{\geq 2b}$ and $\varepsilon_b^{\geq 3b}$ are extracted separately for each of the two analysis channels. The measurement of $\varepsilon_b^{\geq 2b}$ ($\varepsilon_b^{\geq 3b}$) is done from events with ≥ 2 (≥ 3) b-tagged jets. The two (three) b-tagged jets with the highest values of the multivariate b-tagging discriminant in the event are excluded from the computation. All probabilities ε_b are measured both as a function of jet p_T and as a function of the quantity $\Delta R_{min}^{jet,jet} \times N^{jet}$: the minimum distance in the η-ϕ plane between the given jet and all the other jets in the event, multiplied by the jet multiplicity[8] N^{jet}, chosen in order to take into account the correlation between the b-tagging probability and the presence of nearby jets (see Ref. [93]).

Figure 4 shows the measured values of the b-tagging probability in the single-lepton and dilepton channels. It can be seen how the $\varepsilon_b^{\geq 3b}$ are systematically lower than the $\varepsilon_b^{\geq 2b}$ in the case of the single-lepton channel, while they are systematically higher in the case of the dilepton channel. This effect is due to the presence of hadronically decaying W bosons only in the single-lepton channel, which can give rise only to light-jets or c-jets. In the dilepton case, when $\varepsilon_b^{\geq 3b}$ is computed in the dominant four jet multiplicity, this leaves only one jet where this b-tagging probability can be sampled, and this jet is likely to be a b-jet or c-jet, neglecting the mistag probability and considering the relative contributions of $t\bar{t}$ + single and double c/b through gluon splitting. This is not the case in the single-lepton channel, where, instead, three tagged jets out of five can easily be the consequence of tagging a c-jet from the W boson, hence reducing the probability of tagging an additional jet. In the dilepton case, the dependence on $\Delta R_{min}^{jet,jet} \times N^{jet}$ for the $\geq 3b$ selection was found to be compatible with a constant value within statistics.

These b-tagging probabilities are then used to build "pseudodata samples" in validation and signal regions: this is done by applying the information derived from the measured ε_b to the data in the source regions containing the same number of jets and mass-tagged RCLR jets, accounting for the fact that this starting sample contains two

[8]Assuming a uniform random distribution of jets across the η-ϕ plane, $\Delta R_{min}^{jet,jet}$ is inversely proportional to N^{jet}. Variables parametrizing the b-tagging probability should be chosen to be mostly independent of N^{jet}, to allow the extrapolation of the b-tagging probabilities from low to high multiplicity regions.

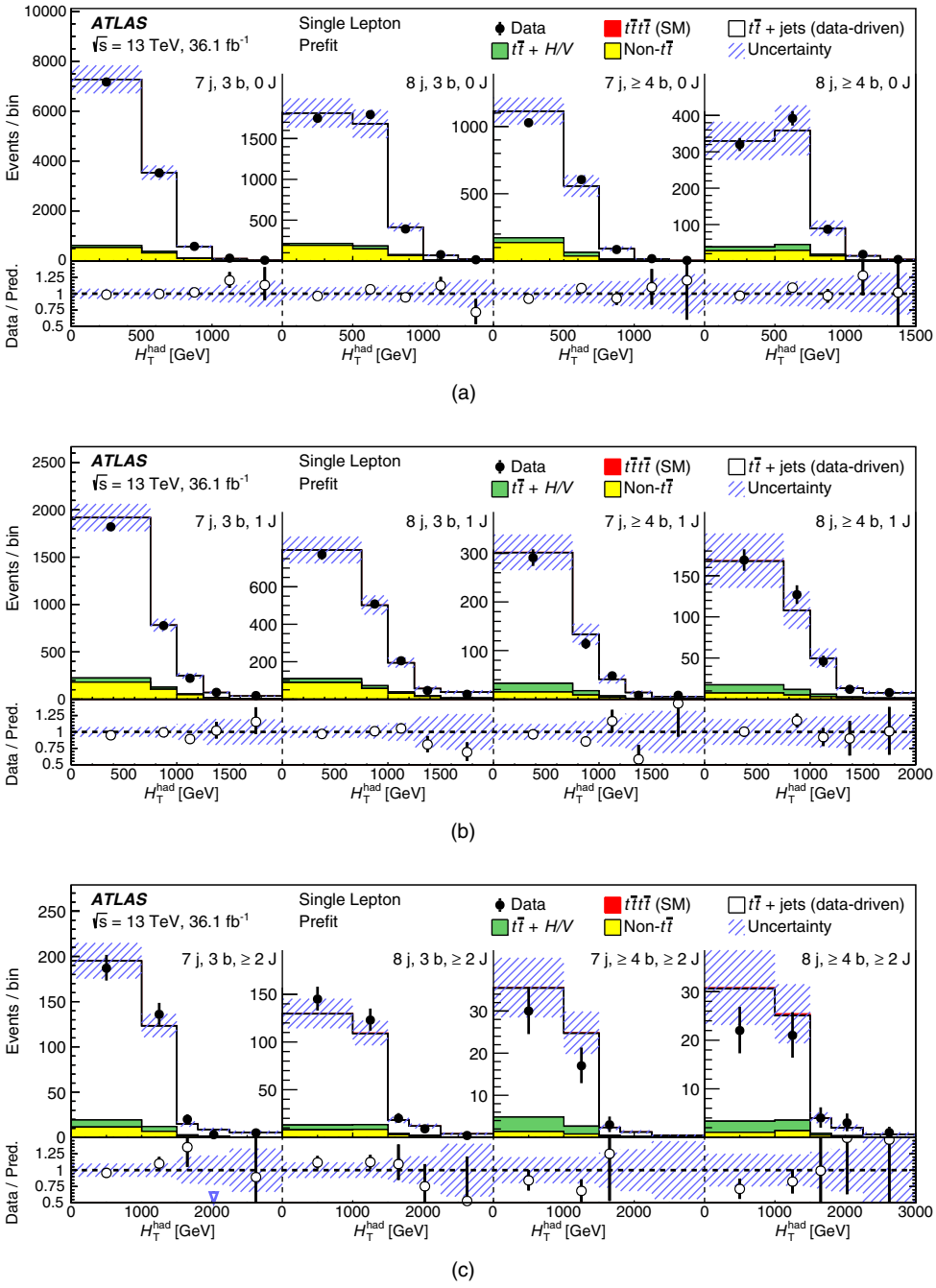

FIG. 5. Comparison between data and prediction of the $H_{\mathrm{T}}^{\mathrm{had}}$ distributions in the single-lepton validation regions prior to the combined fit to data in the single-lepton and dilepton channels. The $t\bar{t}+$ jets background is estimated with the data-driven method. The $t\bar{t}+V$ and $t\bar{t}+H$ processes are denoted $t\bar{t}+H/V$. Contributions from $W/Z+$ jets, single-top, diboson and multijet backgrounds are combined into a single background source referred to as "Non-$t\bar{t}$". The hashed area represents the combined statistical and systematic uncertainties of the prediction. The last bin in all figures contains the overflow. The lower panel shows the ratio between the data and the total prediction, including the SM $t\bar{t}t\bar{t}$ signal. An arrow indicates that the point is off scale.

b-tagged jets [93]. The small non-$t\bar{t}+$ jets background contribution is subtracted, analogously to the procedure described in Ref. [94]. In this way, jets that were not b-tagged in the original data sample can be promoted to b-tagged jets in a given pseudodata events sample, with a weight determined by ε_b, which accounts for the corresponding probability. For the estimate in the $3b$ categories, the procedure above is applied using only b-tagging probabilities extracted from events in the $\geq 2b$ region ($\varepsilon_b^{\geq 2b}$). For the estimate in the $\geq 4b$ categories, a two-step procedure is applied: the estimates in the corresponding $3b$ categories are used as the starting point to

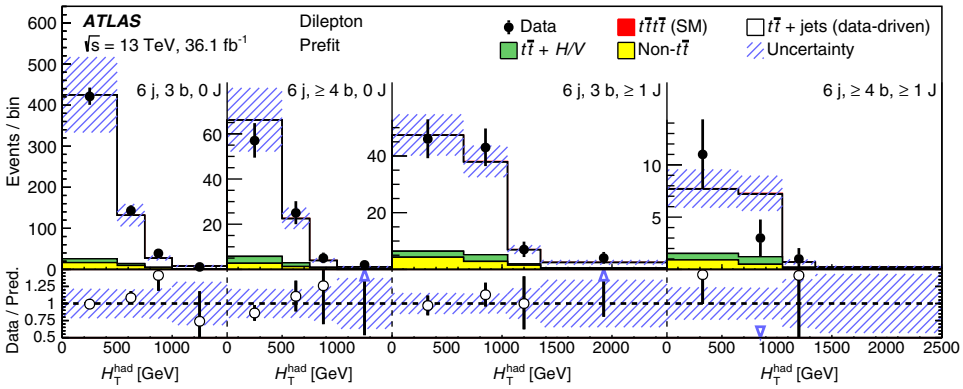

FIG. 6. Comparison between data and prediction of the $H_{\mathrm{T}}^{\mathrm{had}}$ distributions in the dilepton validation regions prior to the combined fit to data in the single-lepton and dilepton channels. The $t\bar{t}+\mathrm{jets}$ background is estimated with the data-driven method. The $t\bar{t}+V$ and $t\bar{t}+H$ processes are denoted $t\bar{t}+H/V$. Contributions from $W/Z+\mathrm{jets}$, single-top, diboson and multijet backgrounds are combined into a single background source referred to as "Non-$t\bar{t}$". The hashed area represents the combined statistical and systematic uncertainties of the prediction. The last bin in all figures contains the overflow. The lower panel shows the ratio between the data and the total prediction, including the SM $t\bar{t}t\bar{t}$ signal. An arrow indicates that the point is off scale.

apply again the same procedure, now using b-tagging probabilities extracted from events in the $\geq 3b$ region ($\varepsilon_b^{\geq 3b}$).

The last step of the method relies on the MC simulation to correct the estimate in each of the considered bins and to assign a set of systematic uncertainties. In order to achieve this, all the steps described above are applied to MC simulated $t\bar{t}+\mathrm{jets}$ events: the b-tagging probability ε_b is extracted from simulated events in the efficiency extraction regions and is then used to reweight simulated events in the source regions, obtaining an estimate in the signal and validation regions. The resulting estimate in bin i of $H_{\mathrm{T}}^{\mathrm{had}}$ distributions, $B_i^{\mathrm{TRF}_{t\bar{t}},\mathrm{MC}}$, is then compared with the prediction from simulated events selected in the signal and validation regions, B_i^{MC}, extracting a correction factor for each considered bin, defined as $C_i = B_i^{\mathrm{MC}}/B_i^{\mathrm{TRF}_{t\bar{t}},\mathrm{MC}}$. The correction is then applied bin-by-bin to the purely data-driven estimate, $B_i^{\mathrm{TRF}_{t\bar{t}},\mathrm{Data}}$ to obtain a corrected estimate in each bin, $B_i^{\mathrm{TRF}_{t\bar{t}}} = C_i \times B_i^{\mathrm{TRF}_{t\bar{t}},\mathrm{Data}}$. These corrections reweight $B_i^{\mathrm{TRF}_{t\bar{t}},\mathrm{Data}}$ by less than 20% on average, varying in magnitude region by region, and are primarily aimed to account for effects such as the dependence of the b-tagging probability on other jet or event properties than the ones used in the parametrization.

A full set of systematic uncertainties is then derived for the estimate $B_i^{\mathrm{TRF}_{t\bar{t}}}$ by repeating the described procedure on MC simulated events with systematic variations applied. For each considered source of systematic uncertainty affecting the $t\bar{t}+\mathrm{jets}$ MC prediction (see Sec. VII), a new set of correction factors C_i' is derived. In this ratio, systematic variations ΔB_i partially cancel out since $C_i' = (B+\Delta B)_i^{\mathrm{MC}}/(B+\Delta B)_i^{\mathrm{TRF}_{t\bar{t}},\mathrm{MC}} \simeq C_i \times [1+(\Delta B_i/B_i)^{\mathrm{MC}} - (\Delta B_i/B_i)^{\mathrm{TRF}_{t\bar{t}},\mathrm{MC}}]$. The cancellation is exact for some uncertainties, e.g., overall normalization. Besides the systematic uncertainties, two sources of statistical uncertainties are considered. The first is the statistical uncertainty affecting the purely data-driven estimate, due to the limited numbers of data events in the source regions. The second source comes from the MC correction factor, given the limited number of simulated events both in the source regions and in the signal and validation regions.

Validation regions are designed primarily to validate the $\mathrm{TRF}_{t\bar{t}}$ data-driven estimate of the dominant $t\bar{t}+\mathrm{jets}$ background and confirm the validity of the assumption that the estimate can be extrapolated to the signal regions. Comparisons of the $H_{\mathrm{T}}^{\mathrm{had}}$ distributions between data and the total SM prediction (including the SM four-top-quark signal) in the validation regions prior to the fit to data are presented in Fig. 5 for the single-lepton channel and in Fig. 6 for the dilepton channel. The $t\bar{t}+\mathrm{jets}$ background is estimated with the data-driven method, including the MC correction factors and the systematic uncertainties. Data agree well with the SM expectation within the uncertainties, validating the overall data-driven procedure and the assumptions made.

VII. SYSTEMATIC UNCERTAINTIES

Several sources of systematic uncertainties that can affect the normalization of signal and background and the shape of the $H_{\mathrm{T}}^{\mathrm{had}}$ distributions are considered. The systematic uncertainties of the data-driven estimate for the $t\bar{t}+\mathrm{jets}$ background are propagated as described in Sec. VI. For each considered source of systematic uncertainty affecting the $t\bar{t}+\mathrm{jets}$ MC prediction, a new set of correction factors C_i' is derived, by coherently replacing the nominal MC prediction with the systematic variation in all regions. The usage of this data-driven technique to estimate the $t\bar{t}+\mathrm{jets}$ background, as

opposed to a purely simulation-based approach, allows to reduce significantly the uncertainty on its prediction in the high jet and b-tagged jet multiplicity topologies exploited by this search.

A. Experimental uncertainties

The uncertainty in the combined 2015+2016 integrated luminosity affecting the overall normalisation of all processes estimated from the simulation is 2.1%. It is derived, following a methodology similar to that detailed in Ref. [31], and using the LUCID-2 detector for the baseline luminosity measurements [95], from calibration of the luminosity scale using x-y beam-separation scans. This systematic uncertainty is applied to all processes modeled using MC simulations.

Uncertainties associated with jets primarily arise from the jet energy scale. The jet energy scale (JES) and its uncertainty are derived by combining information from test-beam data, LHC collision data and simulation [41]. The JES uncertainty is split into 21 uncorrelated sources, which have different dependencies on jet p_{T} and η. In particular, three uncertainties account for differences in the jet response and simulated jet composition of light-quark, b-quark, and gluon-initiated jets. The flavor response uncertainties are derived by comparing the average jet response for each jet flavor using Pythia and Herwig++. The flavor composition uncertainty is assumed to be a 50% quark and 50% gluon composition with a conservative 100% uncertainty. Uncertainties in the jet mass scale, the jet energy resolution and the efficiency to pass the JVT requirement are also considered.

The efficiency of the b-tagging algorithm is measured for each jet flavor using control samples in data and in simulation. From these measurements, correction factors are derived to match the tagging rates in the simulation [44,47,48]. Uncertainties in these corrections include a total of six independent sources affecting b-jets and four independent sources affecting c-jets. Each uncertainty has a different dependence on jet p_{T}. Seventeen uncertainties are considered for the light-jet tagging, which depend on the jet p_{T} and η. These systematic uncertainties are taken as uncorrelated between b-jets, c-jets, and light-flavor jets. An additional uncertainty is included due to the extrapolation of these corrections to jets with p_{T} beyond the kinematic reach of the data calibration samples used ($p_{\mathrm{T}} > 300$ GeV for b- and c-jets and $p_{\mathrm{T}} > 750$ GeV for light-jets) and is taken to be correlated among the three jet flavors.

Uncertainties associated with leptons arise from the trigger, reconstruction, identification, and isolation efficiencies, as well as the lepton momentum scale and resolution. These are measured in data using leptons in $Z \to \ell^+\ell^-$ and $J/\psi \to \ell^+\ell^-$ events at $\sqrt{s} = 13$ TeV [34,35].

All uncertainties in energy scales and resolutions are propagated to the missing transverse momentum. Additional small uncertainties associated with the modeling of the underlying event affecting the reconstruction of the missing transverse momentum are also taken into account.

B. Modeling uncertainties

As mentioned in Sec. VI, common normalization uncertainties for $t\bar{t}+$jets that equally affect B_i^{MC} and $B_i^{\mathrm{TRF}_{t\bar{t}},\mathrm{MC}}$ have no impact on their ratios C_i, and consequently on the total $\mathrm{TRF}_{t\bar{t}}$ prediction. Instead, uncertainties in the $t\bar{t}+$jets heavy-flavor content or kinematics can have residual systematic effects on the $\mathrm{TRF}_{t\bar{t}}$ prediction. Therefore, no uncertainty is assigned to the inclusive $t\bar{t}$ production cross section in the search, while variations of the relative fractions of $t\bar{t}$ events with additional jets originating from b- and c- quarks, as well as comparisons of $t\bar{t}+$jets kinematics with alternative predictions, are considered as systematic uncertainties related to the theory modeling of the $t\bar{t}+$jets process, as described below. A categorization of $t\bar{t}+$jets events is performed for the purpose of assigning systematic uncertainties associated with the modeling of heavy-flavor production in different topologies [96]. Events are categorized depending on the flavor content of additional particle jets and labeled either $t\bar{t}+\geq 1b$ or $t\bar{t}+\geq 1c$, while the remaining events are labeled as $t\bar{t}+$light-jets events, including those with no additional jets.

Detailed comparisons of $t\bar{t}+\geq 1b$ production between the nominal NLO Powheg-Box v2 + Pythia 6.428 $t\bar{t}$ inclusive MC sample and an NLO prediction based on Sherpa + OpenLoops [56,75] (referred to as SherpaOL) have shown that the cross sections agree within 50% [97]. Therefore, a normalization uncertainty of 50% is applied to the $t\bar{t}+\geq 1b$ component of the $t\bar{t}+$jets background obtained from the Powheg-Box v2 + Pythia 6.428 MC simulation. In the absence of an NLO prediction for the $t\bar{t}+\geq 1c$ background, a 50% systematic uncertainty is also applied to the $t\bar{t}+\geq 1c$ component, and the uncertainties in the $t\bar{t}+\geq 1b$ and $t\bar{t}+\geq 1c$ background normalizations are taken as uncorrelated. The overall normalization of all systematic uncertainties in the $t\bar{t}+$jets prediction, except these explicit uncertainties in the $t\bar{t}+\geq 1c$ and $t\bar{t}+\geq 1b$ normalizations, is fixed to the nominal one and only migrations across categories and distortions to the shape of the kinematic distributions are considered.

To provide a comparison with a different parton-shower model, an alternative $t\bar{t}$ sample was generated using the same Powheg model setup as for the nominal sample described in Sec. IV, except the PS, hadronization, underlying-event (UE) and MPI are simulated using Herwig++ (version 2.7.1) [98] with the UEEE5 tune [99] and the corresponding CTEQ6L1 PDF set. To assess the systematic uncertainties related to the use of different models for the hard-scattering generation, while maintaining the same PS model, a sample using MadGraph5_aMC@NLO [17] interfaced to Herwig++ 2.7.1 was

generated. The effects of initial- and final-state radiation (ISR/FSR) are explored using two alternative POWHEG-BOX v2 + PYTHIA 6.428 samples, one with h_{damp} set to $2 \times m_{\mathrm{top}}$, the renormalization and factorization scales set to half the nominal value and using the PERUGIA2012 high-variation UE tune, giving more radiation, and one with the PERUGIA2012 low-variation UE tune, $h_{\mathrm{damp}} = m_{\mathrm{top}}$ and the renormalization and factorization scales set to twice the nominal value, giving less radiation [100]. The μ_{R} and μ_{F} scale variations and the h_{damp} variations are kept correlated, since the two proposed variations cover the full set of uncertainties obtained by changing the scales and the resummation damping parameter independently.

Previous studies have seen that NNLO calculations provide better agreement with data than NLO calculation, particularly for the top-quark p_{T} distribution [101]. Hence, an uncertainty in the modeling of the top-quark p_{T} distribution is evaluated by taking the full difference between applying and not applying the reweighting to match the predictions at NNLO accuracy in QCD [102,103] of the top-quark p_{T} distribution. This uncertainty only affects the $t\bar{t}$ + light-jets and $t\bar{t}+ \geq 1c$ events, for which NNLO predictions have been derived in literature.

In the case of $t\bar{t}+ \geq 1b$ events, an uncertainty is assigned by comparing the NLO prediction in the four-flavor scheme of $t\bar{t}+ \geq 1b$ including parton shower [97] based on SHERPAOL with the nominal NLO POWHEG-BOX v2 + PYTHIA 6.428 inclusive $t\bar{t}$ MC sample with a five-flavor scheme, by means of a generator-level reweighting, as detailed in Ref. [96]. This reweighting is performed separately for each of the $t\bar{t}+ \geq 1b$ subcategories in such a way that their inter-normalization and the shape of the relevant kinematic distributions are at NLO accuracy, while preserving the nominal $t\bar{t}+ \geq 1b$ cross section in POWHEG-BOX v2 + PYTHIA 6.428. Additional uncertainties are assessed for those contributions of $t\bar{t}+ \geq 1b$ background which are not part of the NLO prediction, namely from MPI or FSR from top-quark decay products. They are assessed via the alternative radiation samples described above.

Uncertainties affecting the modeling of the W/Z + jets background include 5% scale uncertainty from their respective normalizations to the theoretical NNLO cross sections [104]. An additional 24% normalization uncertainty is added in quadrature for each additional inclusive jet-multiplicity bin, based on a comparison among different algorithms for merging LO matrix elements and parton showers [105]. Therefore, normalization uncertainties of 54% and 59% are assigned for events with exactly five jets and at least six jets, respectively. These normalization uncertainties are taken as correlated (uncorrelated) across jet multiplicities within signal regions (efficiency extraction regions). Uncertainties affecting the modeling of the single-top-quark background include an uncertainty of +5% and −4% in the total cross section estimated as a weighted average of the theoretical uncertainties in t-, Wt- and s-channel production [84–86].

Uncertainties in the diboson background normalization include 5% from the NLO cross sections [106], as well as an additional 24% normalization uncertainty added in quadrature for each additional inclusive jet multiplicity bin: this assumes that two of the jets originate from the W/Z decays, as in $WW/WZ \to \ell\nu jj$. Recent comparisons between data and SHERPA 2.1.1 for $WZ(\to \ell\nu\ell\ell)+ \geq 4$ jets show agreement within the experimental uncertainty of approximately 40% [107], which further justifies the above uncertainties. Uncertainties in the $t\bar{t} + V$ and $t\bar{t} + H$ normalizations are ±15% and $^{+10}_{-13}$%, respectively, from the uncertainties in their respective NLO cross sections [88,89,108,109].

For the determination of the SM $t\bar{t}t\bar{t}$ production signal strength, no uncertainty is assigned to the theoretical cross section for this process. In the extraction of the exclusion limits on $t\bar{t}t\bar{t}$ production via BSM models, the SM $t\bar{t}t\bar{t}$ process is considered as background and a conservative 50% normalization uncertainty is assigned to the total $t\bar{t}t\bar{t}$ cross section, taking into account the uncertainties in both its production cross section and possible acceptance and shape variations [16,17].

Uncertainties in the data-driven fake or nonprompt lepton background estimate include contributions from the limited sample size in data, particularly at high jet and b-tag multiplicities, from the uncertainty in the real and fake efficiencies extracted from data in dedicated control regions (e.g., selected with a requirement on either the maximum $E_{\mathrm{T}}^{\mathrm{miss}}$ or m_{T}^{W}), as well as from the extrapolation from these control regions to the analysis regions, as detailed in Ref. [92]. Based on comparisons between data and the total prediction in these control regions, the normalization uncertainties assumed for this background are 50% (100%) for events with a central (forward) electron, and 50% for muons, taken to be uncorrelated across regions with different mass-tagged RCLR jet multiplicities and between electron and muon channels. No explicit shape uncertainty is assigned due to the associated large statistical uncertainties. These uncertainties are uncorrelated between bins in the final discriminant distribution and effectively cover possible shape uncertainties.

VIII. RESULTS

Following the statistical method presented below, four-top-quark production signals are searched for by performing a binned profile likelihood fit to the $H_{\mathrm{T}}^{\mathrm{had}}$ distribution simultaneously in the 12 signal regions in the single-lepton channel and 8 signal regions in the dilepton channel, using a total of 20 final-state topologies. The single-lepton and dilepton channels are combined in order to gain sensitivity to different four-top-quark production signals.

A. Statistical interpretation

For each search, the $H_{\mathrm{T}}^{\mathrm{had}}$ distributions across all regions considered are jointly analyzed to test for the presence of a signal predicted by the benchmark scenarios. The statistical interpretation uses a binned likelihood function $\mathcal{L}(\mu, \boldsymbol{\theta})$ constructed as a product of Poisson probability terms over all bins considered in each search (namely, all $H_{\mathrm{T}}^{\mathrm{had}}$ bins in the 20 signal regions defined in Fig. 1). The likelihood function depends on the signal-strength parameter μ, a multiplicative factor that scales the number of expected signal events, and $\boldsymbol{\theta}$, a set of nuisance parameters (NPs) that encode the effect of systematic uncertainties on the signal

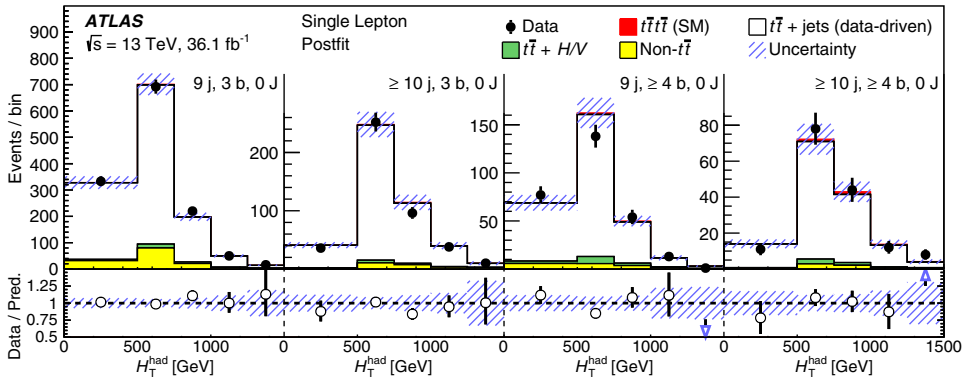

(a)

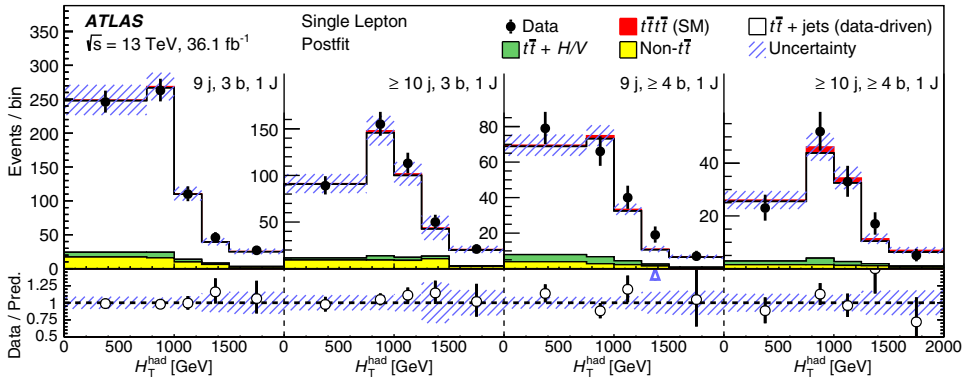

(b)

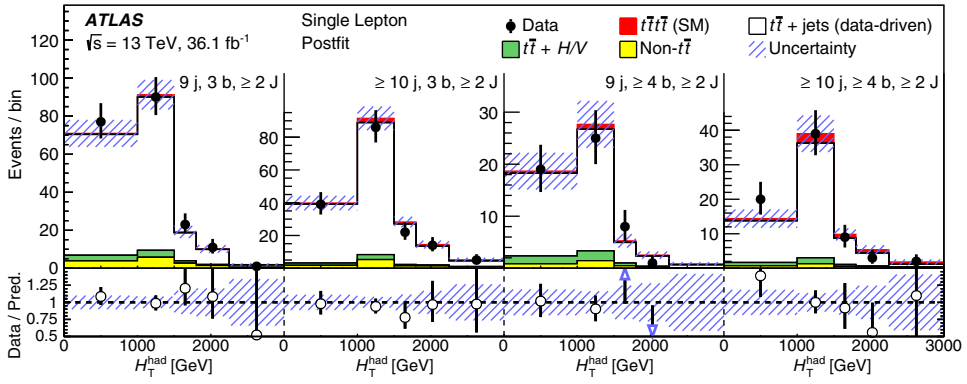

(c)

FIG. 7. Comparison between data and prediction of the $H_{\mathrm{T}}^{\mathrm{had}}$ distributions in the single-lepton signal regions after the combined fit to data in both the single-lepton and dilepton channels. The $t\bar{t}$ + jets background is estimated with the data-driven method. The $t\bar{t} + V$ and $t\bar{t} + H$ processes are denoted $t\bar{t} + H/V$. Contributions from W/Z + jets, single-top, diboson and multijet backgrounds are combined into a single background source referred to as "Non-$t\bar{t}$". The hashed area represents the combined statistical and systematic uncertainties of the prediction. The last bin in all figures contains the overflow. The lower panel shows the ratio between the data and the total prediction, including the SM $t\bar{t}t\bar{t}$ signal scaled by the best-fit signal strength. An arrow indicates that the point is off scale.

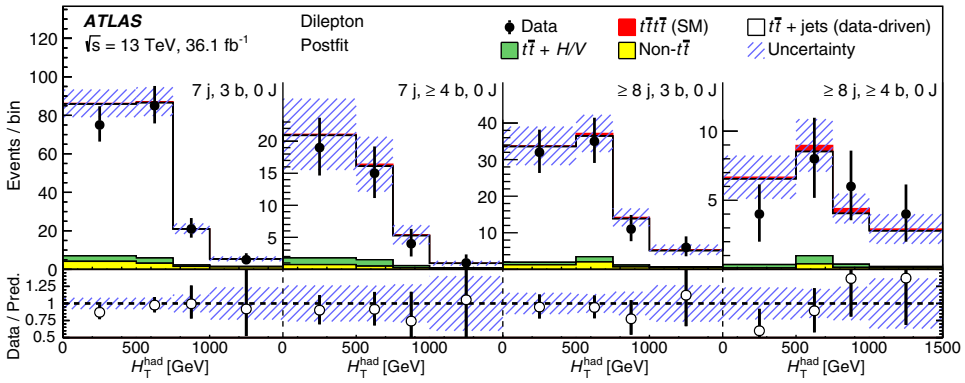

(a)

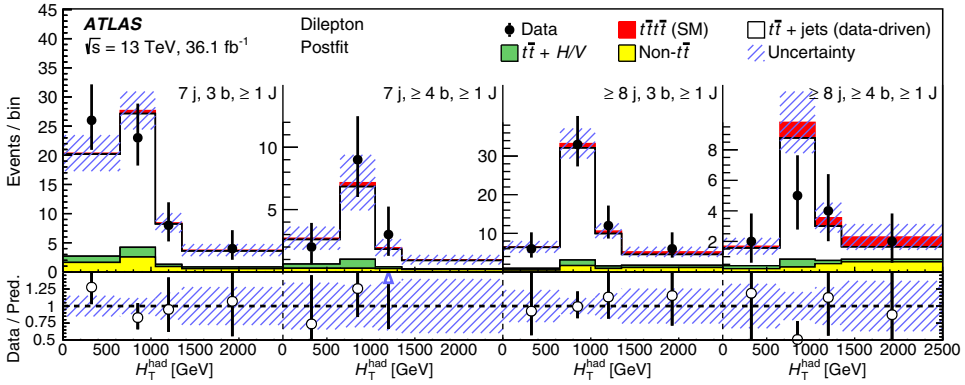

(b)

FIG. 8. Comparison between data and prediction of the $H_{\mathrm{T}}^{\mathrm{had}}$ distributions in the dilepton signal regions after the combined fit to data in both the single-lepton and dilepton channels. The $t\bar{t}+\mathrm{jets}$ background is estimated with the data-driven method. The $t\bar{t}+V$ and $t\bar{t}+H$ processes are denoted $t\bar{t}+H/V$. Contributions from $W/Z+\mathrm{jets}$, single-top, diboson and multijet backgrounds are combined into a single background source referred to as "Non-$t\bar{t}$". The hashed area represents the combined statistical and systematic uncertainties of the prediction. The last bin in all figures contains the overflow. The lower panel shows the ratio between the data and the total prediction, including the SM $t\bar{t}t\bar{t}$ signal scaled by the best-fit signal strength. An arrow indicates that the point is off scale.

and background expectations, which are implemented in the likelihood function as Gaussian, log-normal or Poisson constraints. Individual sources of systematic uncertainty are considered to be uncorrelated. Correlations of a given systematic uncertainty are maintained across processes and channels. The statistical uncertainty of the prediction, which incorporates the statistical uncertainty of the MC events and of the data-driven fake and nonprompt lepton estimate, is included in the likelihood in the form of additional nuisance parameters, one for each of the included bins.

The test statistic q_μ is defined as the profile likelihood ratio: $q_\mu = -2\ln(\mathcal{L}(\mu,\hat{\hat{\boldsymbol{\theta}}}_\mu)/\mathcal{L}(\hat{\mu},\hat{\boldsymbol{\theta}}))$, where $\hat{\mu}$ and $\hat{\boldsymbol{\theta}}$ are the values of the parameters that maximize the likelihood function (with the constraint $0 \le \hat{\mu} \le \mu$), and $\hat{\hat{\boldsymbol{\theta}}}_\mu$ are the values of the NPs that maximize the likelihood function for a given value of μ. The test statistic q_μ is implemented in the RooFit package [110,111]. In the absence of any significant excess above the background expectation, upper limits on the signal production cross section for each of the signal scenarios considered in Sec. IV A are derived by using q_μ and the $\mathrm{CL_s}$ method [112,113]. For a given signal scenario, values of the production cross section (parametrized by μ) yielding $\mathrm{CL_s} < 0.05$, where $\mathrm{CL_s}$ is computed using the asymptotic approximation [114], are excluded at $> 95\%$ C.L.

B. Comparison between data and prediction in signal regions after the fit to data

A binned likelihood fit to the data is performed in the 12 signal regions in the single-lepton channel and 8 signal regions in the dilepton channel, leading to good agreement between data and postfit estimates. Comparisons of the $H_{\mathrm{T}}^{\mathrm{had}}$ distributions between data and the total SM

TABLE II. Breakdown of the contributions to the uncertainties on μ. The quoted uncertainties $\Delta\mu$ are obtained by repeating the fit with certain sets of nuisance parameters fixed to their postfit values, and subtracting in quadrature the resulting total uncertainty of μ from the uncertainty from the full fit. The total statistical uncertainty is evaluated by fixing all nuisance parameters in the fit. The line "background-model statistical uncertainty" refers to the statistical uncertainties of the MC event samples and in the data-driven determination of the $t\bar{t}$ + jets and the nonprompt and fake-lepton background components. These uncertainties are evaluated after the fit described in Sec. VIII.

Uncertainty source	$\pm\Delta\mu$	
$t\bar{t}$ + jets modeling	+1.2	−0.96
Background-model statistical uncertainty	+0.91	−0.85
Jet energy scale and resolution, jet mass	+0.38	−0.16
Other background modeling	+0.26	−0.20
b-tagging efficiency and mistag rates	+0.33	−0.10
JVT, pileup modeling	+0.18	−0.073
$t\bar{t}$ + H/V modeling	+0.053	−0.055
Luminosity	+0.050	−0.026
Total systematic uncertainty	+1.6	−1.4
Total statistical uncertainty	+1.1	−1.0
Total uncertainty	+1.9	−1.7

prediction (including the SM $t\bar{t}t\bar{t}$ signal) in the signal regions, after the combined fit to data in the signal-plus-background hypothesis in the two channels, are presented in Fig. 7 for the single-lepton channel and in Fig. 8 for the dilepton channel. Good agreement of the extrapolated fit results is observed as well in the validation regions, which are presented in the Appendix.

Table II shows the postfit impact of the largest sources of systematic uncertainty on the signal strength μ after the simultaneous fit to data in the single-lepton and dilepton channels. The leading sources of systematic uncertainty vary depending on the analysis region considered. The largest contributions are due to the uncertainty associated with the choice of $t\bar{t}$ + jets parton shower and hadronization model and that of the $t\bar{t}$ + jets NLO generator, as well as large statistical uncertainties associated with the background prediction.

C. Limits on four-top-quark production in the single-lepton and dilepton channel

No significant excess of events above the SM background prediction, excluding the SM $t\bar{t}t\bar{t}$ production, is found. In the case of $t\bar{t}t\bar{t}$ production with SM kinematics, an observed (expected) 95% C.L. upper limit on the production cross section of 47 fb (33 fb) is obtained, corresponding to an upper limit on $\sigma(t\bar{t}t\bar{t})$ relative to the SM prediction of 5.1 (3.6). The SM fitted signal strength μ, after combination of the single-lepton and dilepton channels, is measured to be $1.7^{+1.9}_{-1.7}$.

The search is used to set limits on BSM four-top-quark production via an EFT model (see Sec. IV). For setting limits on this BSM model, the SM $t\bar{t}t\bar{t}$ process is considered as a background. In the case of $t\bar{t}t\bar{t}$ production via an EFT model with a four-top-quark contact interaction, an observed (expected) 95% C.L. upper limit on the production cross section of 21 fb (22 fb) is obtained. The cross-section limit for the contact interaction case is lower than in the SM because the contact interaction tends to result in final-state objects with slightly larger momenta (see e.g., Fig. 3). The upper limit on the

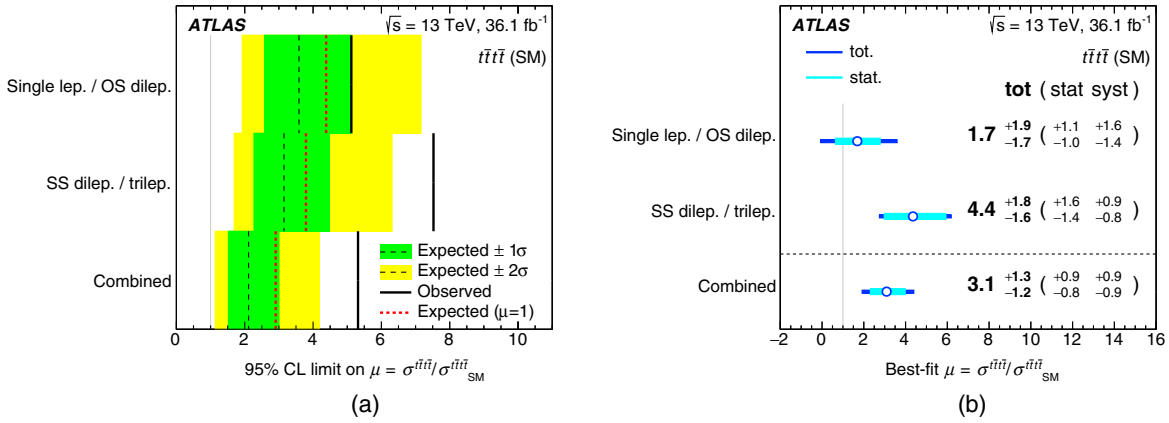

FIG. 9. (a) Summary of the 95% C.L. upper limits on $\sigma(t\bar{t}t\bar{t})$ relative to the SM prediction in the individual channels and for the combination. The observed limits (solid black lines) are shown together with the expected limits in the background-only hypothesis (dashed black lines) and in the SM signal-plus-background hypothesis case (dashed red lines). One- and two-standard-deviation uncertainty bands around the expected limits in the background-only hypothesis are also shown. (b) Summary of the signal-strength measurements in the individual channels and for the combination. The statistical uncertainties are evaluated from a fit to the data performed with all the nuisance parameters associated with systematic uncertainties fixed to their postfit values from the nominal fit.

production cross section can be translated into an observed (expected) limit on the free parameter of the model $|C_{4t}|/\Lambda^2 < 1.9$ TeV^{-2} (1.9 TeV^{-2}).

D. Combination with the same-sign dilepton and multilepton final-state search

The ATLAS Collaboration has carried out a search for new physics using 36.1 fb^{-1} of pp collisions at $\sqrt{s} = 13$ TeV in the same-sign dilepton and multilepton final states (referred to as "SS dilepton/trilepton" channel) [20]. In order to improve the sensitivity to final states containing four top quarks, the results of the search in single-lepton events or dilepton events with two opposite-sign charged leptons reported in Sec. VIII C (referred to as "single lepton/OS dilepton" channel) are combined with the results from the complementary SS dilepton/trilepton channel.

In the combination, all the experimental systematic uncertainties (described in Sec. VII A) are treated as fully correlated between the two channels, while all the background modeling systematic uncertainties described in Sec. VII B are kept uncorrelated with those in the SS dilepton/trilepton channel. This choice is motivated by the different nature of most of the background contributions in the two channels, the different importance of the common background processes and the different techniques used for the data-driven estimates.

The expected sensitivity to the SM $t\bar{t}t\bar{t}$ production from the combination of the two searches, expressed in terms of signal significance relative to the background-only prediction, is 1.0 standard deviation, while the observed value is 2.8 standard deviations. The excess is driven by the SS dilepton/trilepton channel, where the observed (expected) SM $t\bar{t}t\bar{t}$ signal significance amounts to 3.0 (0.8) standard deviations, to be compared with the 1.0 (0.6) standard deviation found in the single lepton/OS dilepton search. The kinematic properties of the SS dilepton/trilepton events were compared with the expectations from the BSM $t\bar{t}t\bar{t}$ production benchmark models studied therein, and found to agree poorly with all of them, in particular for the b-tagged jet multiplicity.

Assuming no signal, an observed (expected) 95% C.L. upper limit on the SM four-top-quark production cross section of 49 fb (19 fb) is obtained. It corresponds to an upper limit on $\sigma(t\bar{t}t\bar{t})$ relative to the SM prediction of 5.3 (2.1). In the signal-plus-background hypothesis, the best-fit value of the SM cross section is found to be $\sigma_{\mathrm{SM}}^{t\bar{t}t\bar{t}} = 28.5^{+12}_{-11}$ fb, to be compared to the theoretical prediction of $9.2^{+2.9}_{-2.4}$ (scale) ± 0.5 (PDF) fb [17]. Figure 9(a) shows the expected and observed upper limits on $\sigma_{\mathrm{SM}}^{t\bar{t}t\bar{t}}$ for the two searches separately and for the combined search, while Fig. 9(b) shows a summary of the signal-strength measurements for each of the two searches and their combination. In the SS dilepton/trilepton channel the uncertainty in μ is mainly statistical, while the systematic uncertainties dominate the sensitivity of the search in the single lepton/OS dilepton channel. The probability that the results of the two searches are compatible is assessed by comparing the maximum-likelihood values for a fit performed after decorrelating the signal-strength parameters in the two channels and for the nominal combined fit with a common signal-strength parameter. The probability of obtaining a discrepancy between the two signal-strength parameters equal to or larger than the one obtained is found to be 31%.

Limits are also set for BSM $t\bar{t}t\bar{t}$ production via an EFT model with a four-top-quark contact interaction. In this benchmark scenario, the SM $t\bar{t}t\bar{t}$ sample is included as a background process. A combined observed (expected) 95% C.L. upper limit on the production cross section of 21 fb (15 fb) is obtained, which translates into an observed (expected) limit on the free parameter of the model of $|C_{4t}|/\Lambda^2 < 1.9$ TeV^{-2} (1.6 TeV^{-2}).

IX. SUMMARY

A search for four-top-quark production in the single-lepton and opposite-sign dilepton channels is presented. The analyzed data sample consists of 36.1 fb^{-1} of proton-proton collisions at $\sqrt{s} = 13$ TeV collected with the ATLAS detector at the Large Hadron Collider during 2015 and 2016. In order to improve the sensitivity of the search, events are categorized according to their jet, b-tagged jet and mass-tagged reclustered large-R jet multiplicities. No significant excess of events above the SM background expectation is found. For the four-top-quark Standard Model production, an observed (expected) 95% C.L. upper limit on the production cross section of 47 fb (33 fb), corresponding to 5.1 (3.6) times the SM prediction, is obtained. The result is combined with the same-sign dilepton and multilepton final-states search carried out by ATLAS [20] and an observed (expected) upper limit of 49 fb (19 fb), corresponding to 5.3 (2.1) times the SM prediction is obtained at 95% C.L. Additionally, in the case of four-top-quark production via an EFT model with a four-top-quark contact interaction, a combined observed (expected) 95% C.L. upper limit on the production cross section of 21 fb (15 fb) is obtained.

ACKNOWLEDGMENTS

We thank CERN for the very successful operation of the LHC, as well as the support staff from our institutions without whom ATLAS could not be operated efficiently. We acknowledge the support of ANPCyT, Argentina; YerPhI, Armenia; ARC, Australia; BMWFW and FWF, Austria; ANAS, Azerbaijan; SSTC, Belarus; CNPq and FAPESP, Brazil; NSERC, NRC and CFI, Canada; CERN; CONICYT, Chile; CAS, MOST and NSFC, China;

COLCIENCIAS, Colombia; MSMT CR, MPO CR and VSC CR, Czech Republic; DNRF and DNSRC, Denmark; IN2P3-CNRS, CEA-DRF/IRFU, France; SRNSFG, Georgia; BMBF, HGF, and MPG, Germany; GSRT, Greece; RGC, Hong Kong SAR, China; ISF and Benoziyo Center, Israel; INFN, Italy; MEXT and JSPS, Japan; CNRST, Morocco; NWO, Netherlands; RCN, Norway; MNiSW and NCN, Poland; FCT, Portugal; MNE/IFA, Romania; MES of Russia and NRC KI, Russian Federation; JINR; MESTD, Serbia; MSSR, Slovakia; ARRS and MIZŠ, Slovenia; DST/NRF, South Africa; MINECO, Spain; SRC and Wallenberg Foundation, Sweden; SERI, SNSF and Cantons of Bern and Geneva, Switzerland; MOST, Taiwan; TAEK, Turkey; STFC, United Kingdom; DOE and NSF, United States of America. In addition, individual groups and members have received support from BCKDF, CANARIE, CRC and Compute Canada, Canada; COST, ERC, ERDF, Horizon 2020, and Marie Skłodowska-Curie Actions, European Union; Investissements d' Avenir Labex and Idex, ANR, France; DFG and AvH Foundation, Germany; Herakleitos, Thales and Aristeia programmes co-financed by EU-ESF and the Greek NSRF, Greece; BSF-NSF and GIF, Israel; CERCA Programme Generalitat de Catalunya, Spain; The Royal Society and Leverhulme Trust, United Kingdom. The crucial computing support from all WLCG partners is acknowledged gratefully, in particular from CERN, the ATLAS Tier-1 facilities at TRIUMF (Canada), NDGF (Denmark, Norway, Sweden), CC-IN2P3 (France), KIT/GridKA (Germany), INFN-CNAF (Italy), NL-T1 (Netherlands), PIC (Spain), ASGC (Taiwan), RAL (UK) and BNL (USA), the Tier-2 facilities worldwide and large non-WLCG resource providers. Major contributors of computing resources are listed in Ref. [115].

APPENDIX: COMPARISON BETWEEN DATA AND PREDICTION OF THE $H_{\mathrm{T}}^{\mathrm{had}}$ DISTRIBUTIONS IN VALIDATION REGIONS AFTER THE FIT TO DATA

Figures 10 and 11 show comparisons of the $H_{\mathrm{T}}^{\mathrm{had}}$ distributions in the validation regions between the data and the postfit prediction in the dilepton and in the single-lepton channels, respectively. The postfit prediction is obtained from the fit to data presented in Sec. VIII in the 20 signal regions and propagated to the validation regions, which are not included in the fit nor used to extract information from the data. The good level of agreement found between data and prediction in these regions is therefore an indication of the validity of the extrapolation of the results of the fit between different regions.

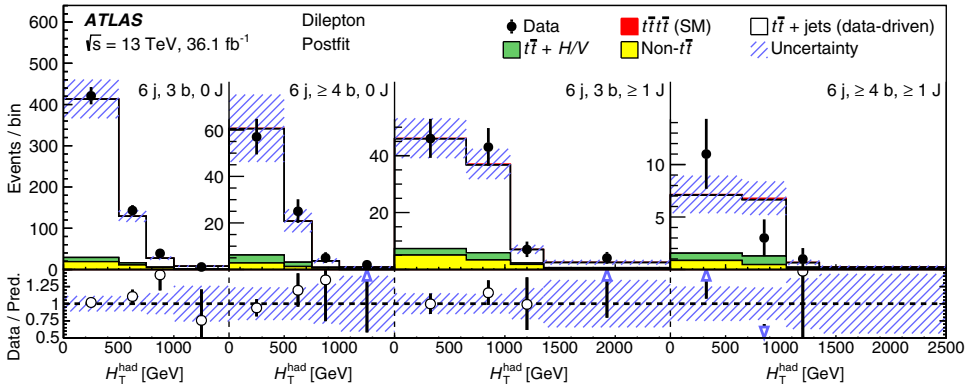

FIG. 10. Comparison between data and prediction of the $H_{\mathrm{T}}^{\mathrm{had}}$ distributions in the dilepton validation regions after the combined fit to data in the single-lepton and dilepton channels. The $t\bar{t}+\mathrm{jets}$ background is estimated with the data-driven method. The $t\bar{t}+V$ and $t\bar{t}+H$ processes are denoted $t\bar{t}+H/V$. Contributions from $W/Z+\mathrm{jets}$, single-top, diboson and multijet backgrounds are combined into a single background source referred to as "Non-$t\bar{t}$". The hashed area represents the combined statistical and systematic uncertainties of the prediction. The last bin in all figures contains the overflow. The lower panel shows the ratio between the data and the total prediction, including the SM $t\bar{t}t\bar{t}$ signal scaled by the best-fit signal strength. An arrow indicates that the point is off scale.

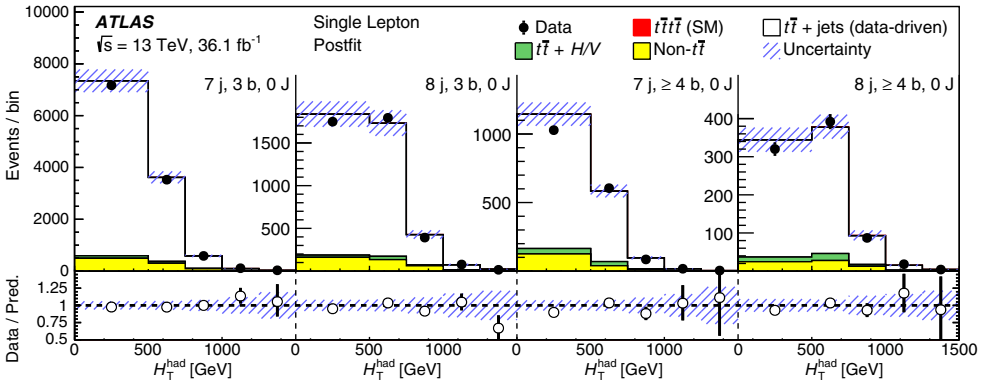

(a)

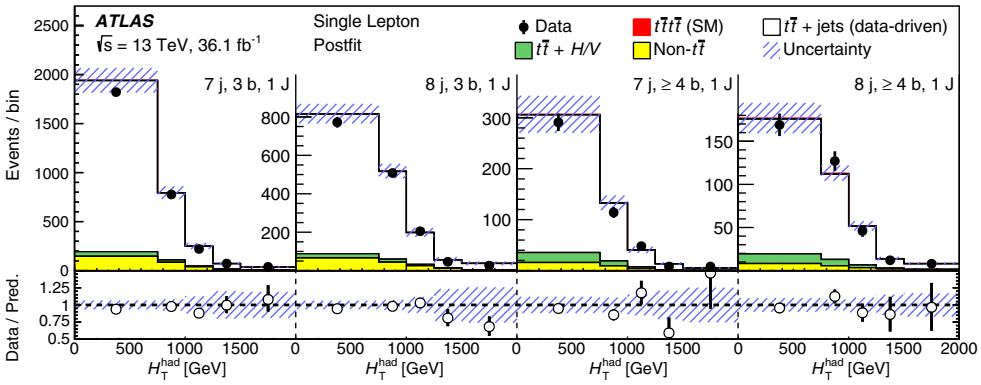

(b)

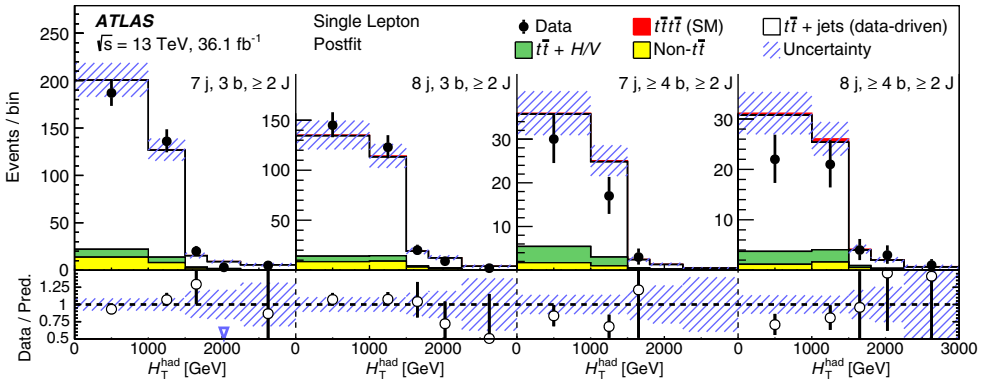

(c)

FIG. 11. Comparison between data and prediction of the $H_{\mathrm{T}}^{\mathrm{had}}$ distributions in the single-lepton validation regions after the combined fit to data in the single-lepton and dilepton channels. The $t\bar{t}+\mathrm{jets}$ background is estimated with the data-driven method. The $t\bar{t}+V$ and $t\bar{t}+H$ processes are denoted $t\bar{t}+H/V$. Contributions from $W/Z+\mathrm{jets}$, single-top, diboson and multijet backgrounds are combined into a single background source referred to as "Non-$t\bar{t}$". The hashed area represents the combined statistical and systematic uncertainties of the prediction. The last bin in all figures contains the overflow. The lower panel shows the ratio between the data and the total prediction, including the SM $t\bar{t}t\bar{t}$ signal scaled by the best-fit signal strength. An arrow indicates that the point is off scale.

[1] CMS Collaboration, Observation of $t\bar{t}H$ Production, Phys. Rev. Lett. **120**, 231801 (2018).

[2] ATLAS Collaboration, Observation of Higgs boson production in association with a top quark pair at the LHC with the ATLAS detector, Phys. Lett. B **784**, 173 (2018).

[3] L. Susskind, Dynamics of spontaneous symmetry breaking in the Weinberg-Salam theory, Phys. Rev. D **20**, 2619 (1979).

[4] D. B. Kaplan, H. Georgi, and S. Dimopoulos, Composite Higgs scalars, Phys. Lett. **136B**, 187 (1984).

[5] N. Arkani-Hamed, A. G. Cohen, E. Katz, and A. E. Nelson, The littlest Higgs, J. High Energy Phys. 07 (2002) 034.

[6] M. Guchait, F. Mahmoudi, and K. Sridhar, Associated production of a Kaluza-Klein excitation of a gluon with a $t\bar{t}$ pair at the LHC, Phys. Lett. B **666**, 347 (2008).

[7] A. Pomarol and J. Serra, Top quark compositeness: Feasibility and implications, Phys. Rev. D **78**, 074026 (2008).

[8] T. Plehn and T. M. P. Tait, Seeking sgluons, J. Phys. G **36**, 075001 (2009).

[9] C. Kilic, T. Okui, and R. Sundrum, Vectorlike confinement at the LHC, J. High Energy Phys. 02 (2010) 018.

[10] C. Degrande, J.-M. Gerard, C. Grojean, F. Maltoni, and G. Servant, Non-resonant new physics in top pair production at hadron colliders, J. High Energy Phys. 03 (2011) 125.

[11] G. Cacciapaglia, R. Chierici, A. Deandrea, L. Panizzi, S. Perries, and S. Tosi, Four tops on the real projective plane at LHC, J. High Energy Phys. 10 (2011) 042.

[12] A. De Simone, O. Matsedonskyi, R. Rattazzi, and A. Wulzer, A first top partner hunter's guide, J. High Energy Phys. 04 (2013) 004.

[13] A. Deandrea and N. Deutschmann, Multi-tops at the LHC, J. High Energy Phys. 08 (2014) 134.

[14] E. Alvarez, D. A. Faroughy, J. F. Kamenik, R. Morales, and A. Szynkman, Four tops for LHC, Nucl. Phys. **B915**, 19 (2017).

[15] G. Cacciapaglia, A. Deandrea, and J. Llodra-Perez, A dark matter candidate from Lorentz invariance in 6D, J. High Energy Phys. 03 (2010) 083.

[16] G. Bevilacqua and M. Worek, Constraining BSM physics at the LHC: Four top final states with NLO accuracy in perturbative QCD, J. High Energy Phys. 07 (2012) 111.

[17] J. Alwall, R. Frederix, S. Frixione, V. Hirschi, F. Maltoni, O. Mattelaer, H.-S. Shao, T. Stelzer, P. Torrielli, and M. Zaro, The automated computation of tree-level and next-to-leading order differential cross sections, and their matching to parton shower simulations, J. High Energy Phys. 07 (2014) 079.

[18] ATLAS Collaboration, Search for new phenomena in a lepton plus high jet multiplicity final state with the ATLAS experiment using $\sqrt{s} = 13$ TeV proton-proton collision data, J. High Energy Phys. 09 (2017) 088.

[19] ATLAS Collaboration, Search for pair production of up-type vector-like quarks and for four-top-quark events in final states with multiple b-jets with the ATLAS detector, J. High Energy Phys. 07 (2018) 089.

[20] ATLAS Collaboration, Search for new phenomena in events with same-charge leptons and b-jets in pp collisions at $\sqrt{s} = 13$ TeV with the ATLAS detector, J. High Energy Phys. 12 (2018) 039.

[21] CMS Collaboration, Search for new physics in same-sign dilepton events in proton-proton collisions at $\sqrt{s} = 13$ TeV, Eur. Phys. J. C **76**, 439 (2016).

[22] CMS Collaboration, Search for standard model production of four top quarks in proton-proton collisions at $\sqrt{s} = 13$ TeV, Phys. Lett. B **772**, 336 (2017).

[23] CMS Collaboration, Search for physics beyond the standard model in events with two leptons of same sign, missing transverse momentum, and jets in proton-proton collisions at $\sqrt{s} = 13$ TeV, Eur. Phys. J. C **77**, 578 (2017).

[24] CMS Collaboration, Search for standard model production of four top quarks with same-sign and multilepton final states in proton-proton collisions at $\sqrt{s} = 13$ TeV, Eur. Phys. J. C **78**, 140 (2018).

[25] B. Nachman, P. Nef, A. Schwartzman, M. Swiatlowski, and C. Wanotayaroj, Jets from jets: Re-clustering as a tool for large radius jet reconstruction and grooming at the LHC, J. High Energy Phys. 02 (2015) 075.

[26] ATLAS Collaboration, Jet reclustering and close-by effects in ATLAS Run 2, Report No. ATLAS-CONF-2017-062, 2017, https://cds.cern.ch/record/2275649.

[27] ATLAS Collaboration, The ATLAS experiment at the CERN large hadron collider, J. Instrum. **3**, S08003 (2008).

[28] M. Capeans *et al.*, ATLAS insertable B-layer technical design, Report No. ATLAS-TDR-19, 2010, https://cds.cern.ch/record/1291633.

[29] ATLAS Collaboration, Production and integration of the ATLAS insertable B-layer, J. Instrum. **13**, T05008 (2018).

[30] ATLAS Collaboration, Performance of the ATLAS trigger system in 2015, Eur. Phys. J. C **77**, 317 (2017).

[31] ATLAS Collaboration, Luminosity determination in pp collisions at $\sqrt{s} = 8$ TeV using the ATLAS detector at the LHC, Eur. Phys. J. C **76**, 653 (2016).

[32] ATLAS Collaboration, Vertex reconstruction performance of the ATLAS detector at $\sqrt{s} = 13$ TeV, Report No. ATL-PHYS-PUB-2015-026, 2015, https://cdsweb.cern.ch/record/2037717.

[33] ATLAS Collaboration, Electron and photon energy calibration with the ATLAS detector using LHC Run 1 data, Eur. Phys. J. C **74**, 3071 (2014).

[34] ATLAS Collaboration, Electron efficiency measurements with the ATLAS detector using the 2015 LHC proton-proton collision data, Report No. ATLAS-CONF-2016-024, 2016, http://cds.cern.ch/record/2157687.

[35] ATLAS Collaboration, Muon reconstruction performance of the ATLAS detector in proton-proton collision data at $\sqrt{s} = 13$ TeV, Eur. Phys. J. C **76**, 292 (2016).

[36] ATLAS Collaboration, Topological cell clustering in the ATLAS calorimeters and its performance in LHC Run 1, Eur. Phys. J. C **77**, 490 (2017).

[37] M. Cacciari, G. P. Salam, and G. Soyez, The anti-k_t jet clustering algorithm, J. High Energy Phys. 04 (2008) 063.

[38] M. Cacciari and G. P. Salam, Dispelling the N^3 myth for the k_t jet-finder, Phys. Lett. B **641**, 57 (2006).

[39] M. Cacciari, G. P. Salam, and G. Soyez, FastJet user manual, Eur. Phys. J. C **72**, 1896 (2012).

[40] ATLAS Collaboration, Expected performance of the ATLAS experiment-detector, trigger and physics, arXiv:0901.0512.
[41] ATLAS Collaboration, Jet energy scale measurements and their systematic uncertainties in proton-proton collisions at $\sqrt{s} = 13$ TeV with the ATLAS detector, Phys. Rev. D **96**, 072002 (2017).
[42] ATLAS Collaboration, Selection of jets produced in 13 TeV proton-proton collisions with the ATLAS detector, Report No. ATLAS-CONF-2015-029, 2015, https://cds.cern.ch/record/2037702.
[43] ATLAS Collaboration, Performance of pile-up mitigation techniques for jets in pp collisions at $\sqrt{s} = 8$ TeV using the ATLAS detector, Eur. Phys. J. C **76**, 581 (2016).
[44] ATLAS Collaboration, Performance of b-jet identification in the ATLAS experiment, J. Instrum. **11**, P04008 (2016).
[45] ATLAS Collaboration, Optimisation of the ATLAS b-tagging performance for the 2016 LHC Run, Report No. ATL-PHYS-PUB-2016-012, 2016, https://cds.cern.ch/record/2160731.
[46] ATLAS Collaboration, Measurements of b-jet tagging efficiency with the ATLAS detector using $t\bar{t}$ events at $\sqrt{s} = 13$ TeV, J. High Energy Phys. 08 (2018) 089.
[47] ATLAS Collaboration, Measurement of b-tagging efficiency of c-jets in $t\bar{t}$ events using a likelihood approach with the ATLAS detector, Report No. ATLAS-CONF-2018-001, 2018, http://cds.cern.ch/record/2306649.
[48] ATLAS Collaboration, Calibration of light-flavour jet b-tagging rates on ATLAS proton-proton collision data at $\sqrt{s} = 13$ TeV, Report No. ATLAS-CONF-2018-006, 2018, https://cds.cern.ch/record/2314418.
[49] D. Krohn, J. Thaler, and L.-T. Wang, Jet trimming, J. High Energy Phys. 02 (2010) 084.
[50] ATLAS Collaboration, Performance of missing transverse momentum reconstruction with the ATLAS detector using proton-proton collisions at $\sqrt{s} = 13$ TeV, Eur. Phys. J. C **78**, 903 (2018).
[51] ATLAS Collaboration, The ATLAS simulation infrastructure, Eur. Phys. J. C **70**, 823 (2010).
[52] S. Agostinelli *et al.*, GEANT4: A simulation toolkit, Nucl. Instrum. Methods Phys. Res., Sect. A **506**, 250 (2003).
[53] ATLAS Collaboration, The simulation principle and performance of the ATLAS fast calorimeter simulation FastCaloSim, Report No. ATL-PHYS-PUB-2010-013, 2010, https://cds.cern.ch/record/1300517.
[54] T. Sjöstrand, S. Mrenna, and P. Z. Skands, A brief introduction to PYTHIA 8.1, Comput. Phys. Commun. **178**, 852 (2008).
[55] D. J. Lange, The EVTGEN particle decay simulation package, Nucl. Instrum. Methods Phys. Res., Sect. A **462**, 152 (2001).
[56] T. Gleisberg, S. Höche, F. Krauss, M. Schönherr, S. Schumann, F. Siegert, and J. Winter, Event generation with SHERPA 1.1, J. High Energy Phys. 02 (2009) 007.
[57] R. D. Ball *et al.*, Parton distributions with LHC data, Nucl. Phys. **B867**, 244 (2013).
[58] ATLAS Collaboration, ATLAS Run 1 PYTHIA 8 tunes, Report No. ATL-PHYS-PUB-2014-021, 2014, https://cds.cern.ch/record/1966419.
[59] S. Frixione, P. Nason, and G. Ridolfi, A positive-weight next-to-leading-order Monte Carlo for heavy flavour hadroproduction, J. High Energy Phys. 09 (2007) 126.
[60] P. Nason, A new method for combining NLO QCD with shower Monte Carlo algorithms, J. High Energy Phys. 11 (2004) 040.
[61] S. Frixione, P. Nason, and C. Oleari, Matching NLO QCD computations with parton shower simulations: The POWHEG method, J. High Energy Phys. 11 (2007) 070.
[62] S. Alioli, P. Nason, C. Oleari, and E. Re, A general framework for implementing NLO calculations in shower Monte Carlo programs: The POWHEG BOX, J. High Energy Phys. 06 (2010) 043.
[63] H.-L. Lai, M. Guzzi, J. Huston, Z. Li, P. M. Nadolsky, J. Pumplin, and C.-P. Yuan, New parton distributions for collider physics, Phys. Rev. D **82**, 074024 (2010).
[64] T. Sjöstrand, S. Mrenna, and P. Z. Skands, PYTHIA 6.4 physics and manual, J. High Energy Phys. 05 (2006) 026.
[65] J. Pumplin, D. Robert Stump, J. Huston, H.-L. Lai, P. Nadolsky, and W.-K. Tung, New generation of parton distributions with uncertainties from global QCD analysis, J. High Energy Phys. 07 (2002) 012.
[66] P. Z. Skands, Tuning Monte Carlo generators: The Perugia tunes, Phys. Rev. D **82**, 074018 (2010).
[67] ATLAS Collaboration, Comparison of Monte Carlo generator predictions to ATLAS measurements of top pair production at 7 TeV, Report No. ATL-PHYS-PUB-2015-002, 2015, https://cds.cern.ch/record/1981319.
[68] M. Czakon and A. Mitov, Top++: A program for the calculation of the top-pair cross-section at hadron colliders, Comput. Phys. Commun. **185**, 2930 (2014).
[69] M. Cacciari, M. Czakon, M. Mangano, A. Mitov, and P. Nason, Top-pair production at hadron colliders with next-to-next-to-leading logarithmic soft-gluon resummation, Phys. Lett. B **710**, 612 (2012).
[70] P. Bärnreuther, M. Czakon, and A. Mitov, Percent Level Precision Physics at the Tevatron: First Genuine NNLO QCD Corrections to $q\bar{q} \to t\bar{t}$, Phys. Rev. Lett. **109**, 132001 (2012).
[71] M. Czakon and A. Mitov, NNLO corrections to top-pair production at hadron colliders: The all-fermionic scattering channels, J. High Energy Phys. 12 (2012) 054.
[72] M. Czakon and A. Mitov, NNLO corrections to top-pair production at hadron colliders: The quark-gluon reaction, J. High Energy Phys. 01 (2013) 080.
[73] M. Czakon, P. Fiedler, and A. Mitov, Total Top-Quark Pair-Production Cross Section at Hadron Colliders through $\mathcal{O}(\alpha_S^4)$, Phys. Rev. Lett. **110**, 252004 (2013).
[74] T. Gleisberg and S. Höche, Comix, a new matrix element generator, J. High Energy Phys. 12 (2008) 039.
[75] F. Cascioli, P. Maierhofer, and S. Pozzorini, Scattering Amplitudes with Open Loops, Phys. Rev. Lett. **108**, 111601 (2012).
[76] S. Schumann and F. Krauss, A parton shower algorithm based on Catani-Seymour dipole factorisation, J. High Energy Phys. 03 (2008) 038.
[77] S. Höche, F. Krauss, M. Schönherr, and F. Siegert, QCD matrix elements + parton showers. The NLO case, J. High Energy Phys. 04 (2013) 027.
[78] K. Melnikov and F. Petriello, Electroweak gauge boson production at hadron colliders through $O(\alpha_s^2)$, Phys. Rev. D **74**, 114017 (2006).

[79] R. Gavin, Y. Li, F. Petriello, and S. Quackenbush, FEWZ 2.0: A code for hadronic Z production at next-to-next-to-leading order, Comput. Phys. Commun. **182**, 2388 (2011).

[80] S. Alioli, P. Nason, C. Oleari, and E. Re, NLO single-top production matched with shower in POWHEG: s- and t-channel contributions, J. High Energy Phys. 09 (2009) 111; 02 (2010) 11(E).

[81] S. Frixione, E. Laenen, P. Motylinski, and B. R. Webber, Single-top production in MCNLO, J. High Energy Phys. 03 (2006) 092.

[82] E. Re, Single-top Wt-channel production matched with parton showers using the POWHEG method, Eur. Phys. J. C **71**, 1547 (2011).

[83] R. Frederix, E. Re, and P. Torrielli, Single-top t-channel hadroproduction in the four-flavour scheme with POWHEG and aMCNLO, J. High Energy Phys. 09 (2012) 130.

[84] N. Kidonakis, Next-to-next-to-leading-order collinear and soft gluon corrections for t-channel single top quark production, Phys. Rev. D **83**, 091503 (2011).

[85] N. Kidonakis, Two-loop soft anomalous dimensions for single top quark associated production with a W^- or H^-, Phys. Rev. D **82**, 054018 (2010).

[86] N. Kidonakis, NNLL resummation for s-channel single top quark production, Phys. Rev. D **81**, 054028 (2010).

[87] R. D. Ball *et al.*, Parton distributions for the LHC Run II, J. High Energy Phys. 04 (2015) 040.

[88] S. Dittmaier *et al.*, Handbook of LHC Higgs cross sections: 1. Inclusive observables, arXiv:1101.0593, DOI: 10.5170/CERN-2011-002.

[89] S. Dittmaier *et al.*, Handbook of LHC Higgs cross sections: 2. Differential distributions, arXiv:1201.3084, DOI: 10.5170/CERN-2012-002.

[90] V. Barger, W.-Y. Keung, and B. Yencho, Triple-top signal of new physics at the LHC, Phys. Lett. B **687**, 70 (2010).

[91] ATLAS Collaboration, Measurement of the top quark-pair production cross section with ATLAS in pp collisions at $\sqrt{s} = 7$ TeV, Eur. Phys. J. C **71**, 1577 (2011).

[92] ATLAS Collaboration, Estimation of non-prompt and fake lepton backgrounds in final states with top quarks produced in proton-proton collisions at $\sqrt{s} = 8$ TeV with the ATLAS detector, Report No. ATLAS-CONF-2014-058, 2014, https://cds.cern.ch/record/1951336.

[93] ATLAS Collaboration, Search for the Standard Model Higgs boson decaying into $b\bar{b}$ produced in association with top quarks decaying hadronically in pp collisions at $\sqrt{s} = 8$ TeV with the ATLAS detector, J. High Energy Phys. 05 (2016) 160.

[94] D0 Collaboration, Measurement of the $t\bar{t}$ production cross section in $p\bar{p}$ collisions at $\sqrt{s} = 1.96$ TeV using secondary vertex b-tagging, Phys. Rev. D **74**, 112004 (2006).

[95] G. Avoni *et al.*, The new LUCID-2 detector for luminosity measurement and monitoring in ATLAS, J. Instrum. **13**, P07017 (2018).

[96] ATLAS Collaboration, Search for the Standard Model Higgs boson produced in association with top quarks and decaying into $b\bar{b}$ in pp collisions at $\sqrt{s} = 8$ TeV with the ATLAS detector, Eur. Phys. J. C **75**, 349 (2015).

[97] F. Cascioli, P. Maierhöfer, N. Moretti, S. Pozzorini, and F. Siegert, NLO matching for $t\bar{t}b\bar{b}$ production with massive b-quarks, Phys. Lett. B **734**, 210 (2014).

[98] M. Bahr *et al.*, Herwig++ physics and manual, Eur. Phys. J. C **58**, 639 (2008).

[99] M. H. Seymour and A. Siodmok, Constraining MPI models using σ_{eff} and recent Tevatron and LHC underlying event data, J. High Energy Phys. 10 (2013) 113.

[100] ATLAS Collaboration, Comparison of Monte Carlo generator predictions from Powheg and Sherpa to ATLAS measurements of top pair production at 7 TeV, Report No. ATL-PHYS-PUB-2015-011, 2015, https://cds.cern.ch/record/2020602.

[101] ATLAS Collaboration, Measurements of top-quark pair differential cross-sections in the lepton + jets channel in pp collisions at $\sqrt{s} = 8$ TeV using the ATLAS detector, Eur. Phys. J. C **76**, 538 (2016).

[102] M. Czakon, D. Heymes, and A. Mitov, High-Precision Differential Predictions for Top-Quark Pairs at the LHC, Phys. Rev. Lett. **116**, 082003 (2016).

[103] M. Czakon, D. Heymes, and A. Mitov, Dynamical scales for multi-TeV top-pair production at the LHC, J. High Energy Phys. 04 (2017) 071.

[104] K. Melnikov and F. Petriello, Electroweak gauge boson production at hadron colliders through $O(\alpha_S^2)$, Phys. Rev. D **74**, 114017 (2006).

[105] J. Alwall *et al.*, Comparative study of various algorithms for the merging of parton showers and matrix elements in hadronic collisions, Eur. Phys. J. C **53**, 473 (2008).

[106] J. M. Campbell, R. K. Ellis, and C. Williams, Vector boson pair production at the LHC, J. High Energy Phys. 07 (2011) 018.

[107] ATLAS Collaboration, Measurement of the $W^{\pm}Z$ boson pair-production cross section in pp collisions at $\sqrt{s} = 13$ TeV with the ATLAS Detector, Phys. Lett. B **762**, 1 (2016).

[108] J. M. Campbell and R. K. Ellis, $t\bar{t}W^{\pm}$ production and decay at NLO, J. High Energy Phys. 07 (2012) 052.

[109] M. V. Garzelli, A. Kardos, C. G. Papadopoulos, and Z. Trocsanyi, $t\bar{t}W^{\pm}$ and $t\bar{t}Z$ hadroproduction at NLO accuracy in QCD with parton shower and Hadronization effects, J. High Energy Phys. 11 (2012) 056.

[110] W. Verkerke and D. P. Kirkby, The RooFit toolkit for data modeling, eConf **C0303241**, MOLT007 (2003).

[111] W. Verkerke and D. Kirkby, RooFit users manual, http://roofit.sourceforge.net/.

[112] T. Junk, Confidence level computation for combining searches with small statistics, Nucl. Instrum. Methods Phys. Res., Sect. A **434**, 435 (1999).

[113] A. L. Read, Presentation of search results: The CL_s technique, J. Phys. G **28**, 2693 (2002).

[114] G. Cowan, K. Cranmer, E. Gross, and O. Vitells, Asymptotic formulae for likelihood-based tests of new physics, Eur. Phys. J. C **71**, 1554 (2011); **73**, 2501(E) (2013).

[115] ATLAS Collaboration, ATLAS computing acknowledgements, Report No. ATL-GEN-PUB-2016-002, https://cds.cern.ch/record/2202407.

M. Aaboud,[34d] G. Aad,[99] B. Abbott,[125] O. Abdinov,[13,a] B. Abeloos,[129] D. K. Abhayasinghe,[91] S. H. Abidi,[164] O. S. AbouZeid,[39] N. L. Abraham,[153] H. Abramowicz,[158] H. Abreu,[157] Y. Abulaiti,[6] B. S. Acharya,[64a,64b,b] S. Adachi,[160] L. Adamczyk,[81a] J. Adelman,[119] M. Adersberger,[112] A. Adiguzel,[12c,c] T. Adye,[141] A. A. Affolder,[143] Y. Afik,[157] C. Agheorghiesei,[27c] J. A. Aguilar-Saavedra,[137f,137a,d] F. Ahmadov,[77,e] G. Aielli,[71a,71b] S. Akatsuka,[83] T. P. A. Åkesson,[94] E. Akilli,[52] A. V. Akimov,[108] G. L. Alberghi,[23b,23a] J. Albert,[173] P. Albicocco,[49] M. J. Alconada Verzini,[86] S. Alderweireldt,[117] M. Aleksa,[35] I. N. Aleksandrov,[77] C. Alexa,[27b] T. Alexopoulos,[10] M. Alhroob,[125] B. Ali,[139] G. Alimonti,[66a] J. Alison,[36] S. P. Alkire,[145] C. Allaire,[129] B. M. M. Allbrooke,[153] B. W. Allen,[128] P. P. Allport,[21] A. Aloisio,[67a,67b] A. Alonso,[39] F. Alonso,[86] C. Alpigiani,[145] A. A. Alshehri,[55] M. I. Alstaty,[99] B. Alvarez Gonzalez,[35] D. Álvarez Piqueras,[171] M. G. Alviggi,[67a,67b] B. T. Amadio,[18] Y. Amaral Coutinho,[78b] L. Ambroz,[132] C. Amelung,[26] D. Amidei,[103] S. P. Amor Dos Santos,[137a,137c] S. Amoroso,[44] C. S. Amrouche,[52] C. Anastopoulos,[146] L. S. Ancu,[52] N. Andari,[142] T. Andeen,[11] C. F. Anders,[59b] J. K. Anders,[20] K. J. Anderson,[36] A. Andreazza,[66a,66b] V. Andrei,[59a] C. R. Anelli,[173] S. Angelidakis,[37] I. Angelozzi,[118] A. Angerami,[38] A. V. Anisenkov,[120b,120a] A. Annovi,[69a] C. Antel,[59a] M. T. Anthony,[146] M. Antonelli,[49] D. J. A. Antrim,[168] F. Anulli,[70a] M. Aoki,[79] J. A. Aparisi Pozo,[171] L. Aperio Bella,[35] G. Arabidze,[104] J. P. Araque,[137a] V. Araujo Ferraz,[78b] R. Araujo Pereira,[78b] A. T. H. Arce,[47] R. E. Ardell,[91] F. A. Arduh,[86] J-F. Arguin,[107] S. Argyropoulos,[75] A. J. Armbruster,[35] L. J. Armitage,[90] A. Armstrong,[168] O. Arnaez,[164] H. Arnold,[118] M. Arratia,[31] O. Arslan,[24] A. Artamonov,[109,a] G. Artoni,[132] S. Artz,[97] S. Asai,[160] N. Asbah,[44] A. Ashkenazi,[158] E. M. Asimakopoulou,[169] L. Asquith,[153] K. Assamagan,[29] R. Astalos,[28a] R. J. Atkin,[32a] M. Atkinson,[170] N. B. Atlay,[148] K. Augsten,[139] G. Avolio,[35] R. Avramidou,[58a] M. K. Ayoub,[15a] G. Azuelos,[107,f] A. E. Baas,[59a] M. J. Baca,[21] H. Bachacou,[142] K. Bachas,[65a,65b] M. Backes,[132] P. Bagnaia,[70a,70b] M. Bahmani,[82] H. Bahrasemani,[149] A. J. Bailey,[171] J. T. Baines,[141] M. Bajic,[39] C. Bakalis,[10] O. K. Baker,[180] P. J. Bakker,[118] D. Bakshi Gupta,[93] E. M. Baldin,[120b,120a] P. Balek,[177] F. Balli,[142] W. K. Balunas,[134] J. Balz,[97] E. Banas,[82] A. Bandyopadhyay,[24] S. Banerjee,[178,g] A. A. E. Bannoura,[179] L. Barak,[158] W. M. Barbe,[37] E. L. Barberio,[102] D. Barberis,[53b,53a] M. Barbero,[99] T. Barillari,[113] M-S. Barisits,[35] J. Barkeloo,[128] T. Barklow,[150] N. Barlow,[31] R. Barnea,[157] S. L. Barnes,[58c] B. M. Barnett,[141] R. M. Barnett,[18] Z. Barnovska-Blenessy,[58a] A. Baroncelli,[72a] G. Barone,[26] A. J. Barr,[132] L. Barranco Navarro,[171] F. Barreiro,[96] J. Barreiro Guimarães da Costa,[15a] R. Bartoldus,[150] A. E. Barton,[87] P. Bartos,[28a] A. Basalaev,[135] A. Bassalat,[129] R. L. Bates,[55] S. J. Batista,[164] S. Batlamous,[34e] J. R. Batley,[31] M. Battaglia,[143] M. Bauce,[70a,70b] F. Bauer,[142] K. T. Bauer,[168] H. S. Bawa,[150,h] J. B. Beacham,[123] T. Beau,[133] P. H. Beauchemin,[167] P. Bechtle,[24] H. C. Beck,[51] H. P. Beck,[20,i] K. Becker,[50] M. Becker,[97] C. Becot,[44] A. Beddall,[12d] A. J. Beddall,[12a] V. A. Bednyakov,[77] M. Bedognetti,[118] C. P. Bee,[152] T. A. Beermann,[35] M. Begalli,[78b] M. Begel,[29] A. Behera,[152] J. K. Behr,[44] A. S. Bell,[92] G. Bella,[158] L. Bellagamba,[23b] A. Bellerive,[33] M. Bellomo,[157] P. Bellos,[9] K. Belotskiy,[110] N. L. Belyaev,[110] O. Benary,[158,a] D. Benchekroun,[34a] M. Bender,[112] N. Benekos,[10] Y. Benhammou,[158] E. Benhar Noccioli,[180] J. Benitez,[75] D. P. Benjamin,[47] M. Benoit,[52] J. R. Bensinger,[26] S. Bentvelsen,[118] L. Beresford,[132] M. Beretta,[49] D. Berge,[44] E. Bergeaas Kuutmann,[169] N. Berger,[5] L. J. Bergsten,[26] J. Beringer,[18] S. Berlendis,[7] N. R. Bernard,[100] G. Bernardi,[133] C. Bernius,[150] F. U. Bernlochner,[24] T. Berry,[91] P. Berta,[97] C. Bertella,[15a] G. Bertoli,[43a,43b] I. A. Bertram,[87] G. J. Besjes,[39] O. Bessidskaia Bylund,[179] M. Bessner,[44] N. Besson,[142] A. Bethani,[98] S. Bethke,[113] A. Betti,[24] A. J. Bevan,[90] J. Beyer,[113] R. M. Bianchi,[136] O. Biebel,[112] D. Biedermann,[19] R. Bielski,[35] K. Bierwagen,[97] N. V. Biesuz,[69a,69b] M. Biglietti,[72a] T. R. V. Billoud,[107] M. Bindi,[51] A. Bingul,[12d] C. Bini,[70a,70b] S. Biondi,[23b,23a] M. Birman,[177] T. Bisanz,[51] J. P. Biswal,[158] C. Bittrich,[46] D. M. Bjergaard,[47] J. E. Black,[150] K. M. Black,[25] T. Blazek,[28a] I. Bloch,[44] C. Blocker,[26] A. Blue,[55] U. Blumenschein,[90] Dr. Blunier,[144a] G. J. Bobbink,[118] V. S. Bobrovnikov,[120b,120a] S. S. Bocchetta,[94] A. Bocci,[47] D. Boerner,[179] D. Bogavac,[112] A. G. Bogdanchikov,[120b,120a] C. Bohm,[43a] V. Boisvert,[91] P. Bokan,[169] T. Bold,[81a] A. S. Boldyrev,[111] A. E. Bolz,[59b] M. Bomben,[133] M. Bona,[90] J. S. Bonilla,[128] M. Boonekamp,[142] A. Borisov,[121] G. Borissov,[87] J. Bortfeldt,[35] D. Bortoletto,[132] V. Bortolotto,[71a,61b,61c,71b] D. Boscherini,[23b] M. Bosman,[14] J. D. Bossio Sola,[30] K. Bouaouda,[34a] J. Boudreau,[136] E. V. Bouhova-Thacker,[87] D. Boumediene,[37] C. Bourdarios,[129] S. K. Boutle,[55] A. Boveia,[123] J. Boyd,[35] D. Boye,[32b] I. R. Boyko,[77] A. J. Bozson,[91] J. Bracinik,[21] N. Brahimi,[99] A. Brandt,[8] G. Brandt,[179] O. Brandt,[59a] F. Braren,[44] U. Bratzler,[161] B. Brau,[100] J. E. Brau,[128] W. D. Breaden Madden,[55] K. Brendlinger,[44] A. J. Brennan,[102] L. Brenner,[44] R. Brenner,[169] S. Bressler,[177] B. Brickwedde,[97] D. L. Briglin,[21] D. Britton,[55] D. Britzger,[59b] I. Brock,[24] R. Brock,[104] G. Brooijmans,[38] T. Brooks,[91] W. K. Brooks,[144b] E. Brost,[119] J. H Broughton,[21] P. A. Bruckman de Renstrom,[82] D. Bruncko,[28b] A. Bruni,[23b] G. Bruni,[23b] L. S. Bruni,[118] S. Bruno,[71a,71b] B. H. Brunt,[31] M. Bruschi,[23b] N. Bruscino,[136] P. Bryant,[36] L. Bryngemark,[44] T. Buanes,[17] Q. Buat,[35] P. Buchholz,[148] A. G. Buckley,[55] I. A. Budagov,[77] M. K. Bugge,[131] F. Bührer,[50] O. Bulekov,[110] D. Bullock,[8] T. J. Burch,[119] S. Burdin,[88] C. D. Burgard,[118]

A. M. Burger,[5] B. Burghgrave,[119] K. Burka,[82] S. Burke,[141] I. Burmeister,[45] J. T. P. Burr,[132] D. Büscher,[50] V. Büscher,[97] E. Buschmann,[51] P. Bussey,[55] J. M. Butler,[25] C. M. Buttar,[55] J. M. Butterworth,[92] P. Butti,[35] W. Buttinger,[35] A. Buzatu,[155] A. R. Buzykaev,[120b,120a] G. Cabras,[23b,23a] S. Cabrera Urbán,[171] D. Caforio,[139] H. Cai,[170] V. M. M. Cairo,[2] O. Cakir,[4a] N. Calace,[52] P. Calafiura,[18] A. Calandri,[99] G. Calderini,[133] P. Calfayan,[63] G. Callea,[40b,40a] L. P. Caloba,[78b] S. Calvente Lopez,[96] D. Calvet,[37] S. Calvet,[37] T. P. Calvet,[152] M. Calvetti,[69a,69b] R. Camacho Toro,[133] S. Camarda,[35] P. Camarri,[71a,71b] D. Cameron,[131] R. Caminal Armadans,[100] C. Camincher,[35] S. Campana,[35] M. Campanelli,[92] A. Camplani,[39] A. Campoverde,[148] V. Canale,[67a,67b] M. Cano Bret,[58c] J. Cantero,[126] T. Cao,[158] Y. Cao,[170] M. D. M. Capeans Garrido,[35] I. Caprini,[27b] M. Caprini,[27b] M. Capua,[40b,40a] R. M. Carbone,[38] R. Cardarelli,[71a] F. C. Cardillo,[146] I. Carli,[140] T. Carli,[35] G. Carlino,[67a] B. T. Carlson,[136] L. Carminati,[66a,66b] R. M. D. Carney,[43a,43b] S. Caron,[117] E. Carquin,[144b] S. Carrá,[66a,66b] G. D. Carrillo-Montoya,[35] D. Casadei,[32b] M. P. Casado,[14,j] A. F. Casha,[164] D. W. Casper,[168] R. Castelijn,[118] F. L. Castillo,[171] V. Castillo Gimenez,[171] N. F. Castro,[137a,137e] A. Catinaccio,[35] J. R. Catmore,[131] A. Cattai,[35] J. Caudron,[24] V. Cavaliere,[29] E. Cavallaro,[14] D. Cavalli,[66a] M. Cavalli-Sforza,[14] V. Cavasinni,[69a,69b] E. Celebi,[12b] F. Ceradini,[72a,72b] L. Cerda Alberich,[171] A. S. Cerqueira,[78a] A. Cerri,[153] L. Cerrito,[71a,71b] F. Cerutti,[18] A. Cervelli,[23b,23a] S. A. Cetin,[12b] A. Chafaq,[34a] D. Chakraborty,[119] S. K. Chan,[57] W. S. Chan,[118] Y. L. Chan,[61a] J. D. Chapman,[31] B. Chargeishvili,[156b] D. G. Charlton,[21] C. C. Chau,[33] C. A. Chavez Barajas,[153] S. Che,[123] A. Chegwidden,[104] S. Chekanov,[6] S. V. Chekulaev,[165a] G. A. Chelkov,[77,k] M. A. Chelstowska,[35] C. Chen,[58a] C. H. Chen,[76] H. Chen,[29] J. Chen,[58a] J. Chen,[38] S. Chen,[134] S. J. Chen,[15c] X. Chen,[15b,l] Y. Chen,[80] Y-H. Chen,[44] H. C. Cheng,[103] H. J. Cheng,[15d] A. Cheplakov,[77] E. Cheremushkina,[121] R. Cherkaoui El Moursli,[34e] E. Cheu,[7] K. Cheung,[62] L. Chevalier,[142] V. Chiarella,[49] G. Chiarelli,[69a] G. Chiodini,[65a] A. S. Chisholm,[35] A. Chitan,[27b] I. Chiu,[160] Y. H. Chiu,[173] M. V. Chizhov,[77] K. Choi,[63] A. R. Chomont,[129] S. Chouridou,[159] Y. S. Chow,[118] V. Christodoulou,[92] M. C. Chu,[61a] J. Chudoba,[138] A. J. Chuinard,[101] J. J. Chwastowski,[82] L. Chytka,[127] D. Cinca,[45] V. Cindro,[89] I. A. Cioară,[24] A. Ciocio,[18] F. Cirotto,[67a,67b] Z. H. Citron,[177] M. Citterio,[66a] A. Clark,[52] M. R. Clark,[38] P. J. Clark,[48] C. Clement,[43a,43b] Y. Coadou,[99] M. Cobal,[64a,64c] A. Coccaro,[53b,53a] J. Cochran,[76] A. E. C. Coimbra,[177] L. Colasurdo,[117] B. Cole,[38] A. P. Colijn,[118] J. Collot,[56] P. Conde Muiño,[137a,m] E. Coniavitis,[50] S. H. Connell,[32b] I. A. Connelly,[98] S. Constantinescu,[27b] F. Conventi,[67a,n] A. M. Cooper-Sarkar,[132] F. Cormier,[172] K. J. R. Cormier,[164] M. Corradi,[70a,70b] E. E. Corrigan,[94] F. Corriveau,[101,o] A. Cortes-Gonzalez,[35] M. J. Costa,[171] D. Costanzo,[146] G. Cottin,[31] G. Cowan,[91] B. E. Cox,[98] J. Crane,[98] K. Cranmer,[122] S. J. Crawley,[55] R. A. Creager,[134] G. Cree,[33] S. Crépé-Renaudin,[56] F. Crescioli,[133] M. Cristinziani,[24] V. Croft,[122] G. Crosetti,[40b,40a] A. Cueto,[96] T. Cuhadar Donszelmann,[146] A. R. Cukierman,[150] J. Cúth,[97] S. Czekierda,[82] P. Czodrowski,[35] M. J. Da Cunha Sargedas De Sousa,[58b] C. Da Via,[98] W. Dabrowski,[81a] T. Dado,[28a,p] S. Dahbi,[34e] T. Dai,[103] F. Dallaire,[107] C. Dallapiccola,[100] M. Dam,[39] G. D'amen,[23b,23a] J. Damp,[97] J. R. Dandoy,[134] M. F. Daneri,[30] N. P. Dang,[178,g] N. D Dann,[98] M. Danninger,[172] V. Dao,[35] G. Darbo,[53b] S. Darmora,[8] O. Dartsi,[5] A. Dattagupta,[128] T. Daubney,[44] S. D'Auria,[55] W. Davey,[24] C. David,[44] T. Davidek,[140] D. R. Davis,[47] E. Dawe,[102] I. Dawson,[146] K. De,[8] R. De Asmundis,[67a] A. De Benedetti,[125] M. De Beurs,[118] S. De Castro,[23b,23a] S. De Cecco,[70a,70b] N. De Groot,[117] P. de Jong,[118] H. De la Torre,[104] F. De Lorenzi,[76] A. De Maria,[51,q] D. De Pedis,[70a] A. De Salvo,[70a] U. De Sanctis,[71a,71b] A. De Santo,[153] K. De Vasconcelos Corga,[99] J. B. De Vivie De Regie,[129] C. Debenedetti,[143] D. V. Dedovich,[77] N. Dehghanian,[3] M. Del Gaudio,[40b,40a] J. Del Peso,[96] Y. Delabat Diaz,[44] D. Delgove,[129] F. Deliot,[142] C. M. Delitzsch,[7] M. Della Pietra,[67a,67b] D. Della Volpe,[52] A. Dell'Acqua,[35] L. Dell'Asta,[25] M. Delmastro,[5] C. Delporte,[129] P. A. Delsart,[56] D. A. DeMarco,[164] S. Demers,[180] M. Demichev,[77] S. P. Denisov,[121] D. Denysiuk,[118] L. D'Eramo,[133] D. Derendarz,[82] J. E. Derkaoui,[34d] F. Derue,[133] P. Dervan,[88] K. Desch,[24] C. Deterre,[44] K. Dette,[164] M. R. Devesa,[30] P. O. Deviveiros,[35] A. Dewhurst,[141] S. Dhaliwal,[26] F. A. Di Bello,[52] A. Di Ciaccio,[71a,71b] L. Di Ciaccio,[5] W. K. Di Clemente,[134] C. Di Donato,[67a,67b] A. Di Girolamo,[35] B. Di Micco,[72a,72b] R. Di Nardo,[100] K. F. Di Petrillo,[57] R. Di Sipio,[164] D. Di Valentino,[33] C. Diaconu,[99] M. Diamond,[164] F. A. Dias,[39] T. Dias Do Vale,[137a] M. A. Diaz,[144a] J. Dickinson,[18] E. B. Diehl,[103] J. Dietrich,[19] S. Díez Cornell,[44] A. Dimitrievska,[18] J. Dingfelder,[24] F. Dittus,[35] F. Djama,[99] T. Djobava,[156b] J. I. Djuvsland,[59a] M. A. B. Do Vale,[78c] M. Dobre,[27b] D. Dodsworth,[26] C. Doglioni,[94] J. Dolejsi,[140] Z. Dolezal,[140] M. Donadelli,[78d] J. Donini,[37] A. D'onofrio,[90] M. D'Onofrio,[88] J. Dopke,[141] A. Doria,[67a] M. T. Dova,[86] A. T. Doyle,[55] E. Drechsler,[51] E. Dreyer,[149] T. Dreyer,[51] Y. Du,[58b] J. Duarte-Campderros,[158] F. Dubinin,[108] M. Dubovsky,[28a] A. Dubreuil,[52] E. Duchovni,[177] G. Duckeck,[112] A. Ducourthial,[133] O. A. Ducu,[107,r] D. Duda,[113] A. Dudarev,[35] A. C. Dudder,[97] E. M. Duffield,[18] L. Duflot,[129] M. Dührssen,[35] C. Dülsen,[179] M. Dumancic,[177] A. E. Dumitriu,[27b,s] A. K. Duncan,[55] M. Dunford,[59a] A. Duperrin,[99] H. Duran Yildiz,[4a] M. Düren,[54] A. Durglishvili,[156b] D. Duschinger,[46] B. Dutta,[44] D. Duvnjak,[1] M. Dyndal,[44] S. Dysch,[98] B. S. Dziedzic,[82] C. Eckardt,[44]

K. M. Ecker,[113] R. C. Edgar,[103] T. Eifert,[35] G. Eigen,[17] K. Einsweiler,[18] T. Ekelof,[169] M. El Kacimi,[34c] R. El Kosseifi,[99] V. Ellajosyula,[99] M. Ellert,[169] F. Ellinghaus,[179] A. A. Elliot,[90] N. Ellis,[35] J. Elmsheuser,[29] M. Elsing,[35] D. Emeliyanov,[141] Y. Enari,[160] J. S. Ennis,[175] M. B. Epland,[47] J. Erdmann,[45] A. Ereditato,[20] S. Errede,[170] M. Escalier,[129] C. Escobar,[171] O. Estrada Pastor,[171] A. I. Etienvre,[142] E. Etzion,[158] H. Evans,[63] A. Ezhilov,[135] M. Ezzi,[34e] F. Fabbri,[55] L. Fabbri,[23b,23a] V. Fabiani,[117] G. Facini,[92] R. M. Faisca Rodrigues Pereira,[137a] R. M. Fakhrutdinov,[121] S. Falciano,[70a] P. J. Falke,[5] S. Falke,[5] J. Faltova,[140] Y. Fang,[15a] M. Fanti,[66a,66b] A. Farbin,[8] A. Farilla,[72a] E. M. Farina,[68a,68b] T. Farooque,[104] S. Farrell,[18] S. M. Farrington,[175] P. Farthouat,[35] F. Fassi,[34e] P. Fassnacht,[35] D. Fassouliotis,[9] M. Faucci Giannelli,[48] A. Favareto,[53b,53a] W. J. Fawcett,[52] L. Fayard,[129] O. L. Fedin,[135,t] W. Fedorko,[172] M. Feickert,[41] S. Feigl,[131] L. Feligioni,[99] C. Feng,[58b] E. J. Feng,[35] M. Feng,[47] M. J. Fenton,[55] A. B. Fenyuk,[121] L. Feremenga,[8] J. Ferrando,[44] A. Ferrari,[169] P. Ferrari,[118] R. Ferrari,[68a] D. E. Ferreira de Lima,[59b] A. Ferrer,[171] D. Ferrere,[52] C. Ferretti,[103] F. Fiedler,[97] A. Filipčič,[89] F. Filthaut,[117] K. D. Finelli,[25] M. C. N. Fiolhais,[137a,137c,u] L. Fiorini,[171] C. Fischer,[14] W. C. Fisher,[104] N. Flaschel,[44] I. Fleck,[148] P. Fleischmann,[103] R. R. M. Fletcher,[134] T. Flick,[179] B. M. Flierl,[112] L. M. Flores,[134] L. R. Flores Castillo,[61a] F. M. Follega,[73a,73b] N. Fomin,[17] G. T. Forcolin,[98] A. Formica,[142] F. A. Förster,[14] A. C. Forti,[98] A. G. Foster,[21] D. Fournier,[129] H. Fox,[87] S. Fracchia,[146] P. Francavilla,[69a,69b] M. Franchini,[23b,23a] S. Franchino,[59a] D. Francis,[35] L. Franconi,[131] M. Franklin,[57] M. Frate,[168] M. Fraternali,[68a,68b] D. Freeborn,[92] S. M. Fressard-Batraneanu,[35] B. Freund,[107] W. S. Freund,[78b] D. Froidevaux,[35] J. A. Frost,[132] C. Fukunaga,[161] E. Fullana Torregrosa,[171] T. Fusayasu,[114] J. Fuster,[171] O. Gabizon,[157] A. Gabrielli,[23b,23a] A. Gabrielli,[18] G. P. Gach,[81a] S. Gadatsch,[52] P. Gadow,[113] G. Gagliardi,[53b,53a] L. G. Gagnon,[107] C. Galea,[27b] B. Galhardo,[137a,137c] E. J. Gallas,[132] B. J. Gallop,[141] P. Gallus,[139] G. Galster,[39] R. Gamboa Goni,[90] K. K. Gan,[123] S. Ganguly,[177] J. Gao,[58a] Y. Gao,[88] Y. S. Gao,[150,h] C. García,[171] J. E. García Navarro,[171] J. A. García Pascual,[15a] M. Garcia-Sciveres,[18] R. W. Gardner,[36] N. Garelli,[150] V. Garonne,[131] K. Gasnikova,[44] A. Gaudiello,[53b,53a] G. Gaudio,[68a] I. L. Gavrilenko,[108] A. Gavrilyuk,[109] C. Gay,[172] G. Gaycken,[24] E. N. Gazis,[10] C. N. P. Gee,[141] J. Geisen,[51] M. Geisen,[97] M. P. Geisler,[59a] K. Gellerstedt,[43a,43b] C. Gemme,[53b] M. H. Genest,[56] C. Geng,[103] S. Gentile,[70a,70b] S. George,[91] D. Gerbaudo,[14] G. Gessner,[45] S. Ghasemi,[148] M. Ghasemi Bostanabad,[173] M. Ghneimat,[24] B. Giacobbe,[23b] S. Giagu,[70a,70b] N. Giangiacomi,[23b,23a] P. Giannetti,[69a] A. Giannini,[67a,67b] S. M. Gibson,[91] M. Gignac,[143] D. Gillberg,[33] G. Gilles,[179] D. M. Gingrich,[3,f] M. P. Giordani,[64a,64c] F. M. Giorgi,[23b] P. F. Giraud,[142] P. Giromini,[57] G. Giugliarelli,[64a,64c] D. Giugni,[66a] F. Giuli,[132] M. Giulini,[59b] S. Gkaitatzis,[159] I. Gkialas,[9,v] E. L. Gkougkousis,[14] P. Gkountoumis,[10] L. K. Gladilin,[111] C. Glasman,[96] J. Glatzer,[14] P. C. F. Glaysher,[44] A. Glazov,[44] M. Goblirsch-Kolb,[26] J. Godlewski,[82] S. Goldfarb,[102] T. Golling,[52] D. Golubkov,[121] A. Gomes,[137a,137b] R. Goncalves Gama,[78a] R. Gonçalo,[137a] G. Gonella,[50] L. Gonella,[21] A. Gongadze,[77] F. Gonnella,[21] J. L. Gonski,[57] S. González de la Hoz,[171] S. Gonzalez-Sevilla,[52] L. Goossens,[35] P. A. Gorbounov,[109] H. A. Gordon,[29] B. Gorini,[35] E. Gorini,[65a,65b] A. Gorišek,[89] A. T. Goshaw,[47] C. Gössling,[45] M. I. Gostkin,[77] C. A. Gottardo,[24] C. R. Goudet,[129] D. Goujdami,[34c] A. G. Goussiou,[145] N. Govender,[32b,w] C. Goy,[5] E. Gozani,[157] I. Grabowska-Bold,[81a] P. O. J. Gradin,[169] E. C. Graham,[88] J. Gramling,[168] E. Gramstad,[131] S. Grancagnolo,[19] V. Gratchev,[135] P. M. Gravila,[27f] F. G. Gravili,[65a,65b] C. Gray,[55] H. M. Gray,[18] Z. D. Greenwood,[93,x] C. Grefe,[24] K. Gregersen,[94] I. M. Gregor,[44] P. Grenier,[150] K. Grevtsov,[44] J. Griffiths,[8] A. A. Grillo,[143] K. Grimm,[150,y] S. Grinstein,[14,z] Ph. Gris,[37] J.-F. Grivaz,[129] S. Groh,[97] E. Gross,[177] J. Grosse-Knetter,[51] G. C. Grossi,[93] Z. J. Grout,[92] C. Grud,[103] A. Grummer,[116] L. Guan,[103] W. Guan,[178] J. Guenther,[35] A. Guerguichon,[129] F. Guescini,[165a] D. Guest,[168] R. Gugel,[50] B. Gui,[123] T. Guillemin,[5] S. Guindon,[35] U. Gul,[55] C. Gumpert,[35] J. Guo,[58c] W. Guo,[103] Y. Guo,[58a,aa] Z. Guo,[99] R. Gupta,[41] S. Gurbuz,[12c] G. Gustavino,[125] B. J. Gutelman,[157] P. Gutierrez,[125] C. Gutschow,[92] C. Guyot,[142] M. P. Guzik,[81a] C. Gwenlan,[132] C. B. Gwilliam,[88] A. Haas,[122] C. Haber,[18] H. K. Hadavand,[8] N. Haddad,[34e] A. Hadef,[58a] S. Hageböck,[24] M. Hagihara,[166] H. Hakobyan,[181,a] M. Haleem,[174] J. Haley,[126] G. Halladjian,[104] G. D. Hallewell,[99] K. Hamacher,[179] P. Hamal,[127] K. Hamano,[173] A. Hamilton,[32a] G. N. Hamity,[146] K. Han,[58a,bb] L. Han,[58a] S. Han,[15d] K. Hanagaki,[79,cc] M. Hance,[143] D. M. Handl,[112] B. Haney,[134] R. Hankache,[133] P. Hanke,[59a] E. Hansen,[94] J. B. Hansen,[39] J. D. Hansen,[39] M. C. Hansen,[24] P. H. Hansen,[39] K. Hara,[166] A. S. Hard,[178] T. Harenberg,[179] S. Harkusha,[105] P. F. Harrison,[175] N. M. Hartmann,[112] Y. Hasegawa,[147] A. Hasib,[48] S. Hassani,[142] S. Haug,[20] R. Hauser,[104] L. Hauswald,[46] L. B. Havener,[38] M. Havranek,[139] C. M. Hawkes,[21] R. J. Hawkings,[35] D. Hayden,[104] C. Hayes,[152] C. P. Hays,[132] J. M. Hays,[90] H. S. Hayward,[88] S. J. Haywood,[141] M. P. Heath,[48] V. Hedberg,[94] L. Heelan,[8] S. Heer,[24] K. K. Heidegger,[50] J. Heilman,[33] S. Heim,[44] T. Heim,[18] B. Heinemann,[44,dd] J. J. Heinrich,[112] L. Heinrich,[122] C. Heinz,[54] J. Hejbal,[138] L. Helary,[35] A. Held,[172] S. Hellesund,[131] S. Hellman,[43a,43b] C. Helsens,[35] R. C. W. Henderson,[87] Y. Heng,[178] S. Henkelmann,[172] A. M. Henriques Correia,[35] G. H. Herbert,[19] H. Herde,[26] V. Herget,[174] Y. Hernández Jiménez,[32c] H. Herr,[97]

M. G. Herrmann,[112] G. Herten,[50] R. Hertenberger,[112] L. Hervas,[35] T. C. Herwig,[134] G. G. Hesketh,[92] N. P. Hessey,[165a] J. W. Hetherly,[41] S. Higashino,[79] E. Higón-Rodriguez,[171] K. Hildebrand,[36] E. Hill,[173] J. C. Hill,[31] K. K. Hill,[29] K. H. Hiller,[44] S. J. Hillier,[21] M. Hils,[46] I. Hinchliffe,[18] M. Hirose,[130] D. Hirschbuehl,[179] B. Hiti,[89] O. Hladik,[138] D. R. Hlaluku,[32c] X. Hoad,[48] J. Hobbs,[152] N. Hod,[165a] M. C. Hodgkinson,[146] A. Hoecker,[35] M. R. Hoeferkamp,[116] F. Hoenig,[112] D. Hohn,[24] D. Hohov,[129] T. R. Holmes,[36] M. Holzbock,[112] M. Homann,[45] S. Honda,[166] T. Honda,[79] T. M. Hong,[136] A. Hönle,[113] B. H. Hooberman,[170] W. H. Hopkins,[128] Y. Horii,[115] P. Horn,[46] A. J. Horton,[149] L. A. Horyn,[36] J-Y. Hostachy,[56] A. Hostiuc,[145] S. Hou,[155] A. Hoummada,[34a] J. Howarth,[98] J. Hoya,[86] M. Hrabovsky,[127] J. Hrdinka,[35] I. Hristova,[19] J. Hrivnac,[129] A. Hrynevich,[106] T. Hryn'ova,[5] P. J. Hsu,[62] S.-C. Hsu,[145] Q. Hu,[29] S. Hu,[58c] Y. Huang,[15a] Z. Hubacek,[139] F. Hubaut,[99] M. Huebner,[24] F. Huegging,[24] T. B. Huffman,[132] E. W. Hughes,[38] M. Huhtinen,[35] R. F. H. Hunter,[33] P. Huo,[152] A. M. Hupe,[33] N. Huseynov,[77,e] J. Huston,[104] J. Huth,[57] R. Hyneman,[103] G. Iacobucci,[52] G. Iakovidis,[29] I. Ibragimov,[148] L. Iconomidou-Fayard,[129] Z. Idrissi,[34e] P. Iengo,[35] R. Ignazzi,[39] O. Igonkina,[118,ee] R. Iguchi,[160] T. Iizawa,[52] Y. Ikegami,[79] M. Ikeno,[79] D. Iliadis,[159] N. Ilic,[117] F. Iltzsche,[46] G. Introzzi,[68a,68b] M. Iodice,[72a] K. Iordanidou,[38] V. Ippolito,[70a,70b] M. F. Isacson,[169] N. Ishijima,[130] M. Ishino,[160] M. Ishitsuka,[162] W. Islam,[126] C. Issever,[132] S. Istin,[12c,ff] F. Ito,[166] J. M. Iturbe Ponce,[61a] R. Iuppa,[73a,73b] A. Ivina,[177] H. Iwasaki,[79] J. M. Izen,[42] V. Izzo,[67a] P. Jacka,[138] P. Jackson,[1] R. M. Jacobs,[24] V. Jain,[2] G. Jäkel,[179] K. B. Jakobi,[97] K. Jakobs,[50] S. Jakobsen,[74] T. Jakoubek,[138] D. O. Jamin,[126] D. K. Jana,[93] R. Jansky,[52] J. Janssen,[24] M. Janus,[51] P. A. Janus,[81a] G. Jarlskog,[94] N. Javadov,[77,e] T. Javůrek,[35] M. Javurkova,[50] F. Jeanneau,[142] L. Jeanty,[18] J. Jejelava,[156a,gg] A. Jelinskas,[175] P. Jenni,[50,hh] J. Jeong,[44] S. Jézéquel,[5] H. Ji,[178] J. Jia,[152] H. Jiang,[76] Y. Jiang,[58a] Z. Jiang,[150,ii] S. Jiggins,[50] F. A. Jimenez Morales,[37] J. Jimenez Pena,[171] S. Jin,[15c] A. Jinaru,[27b] O. Jinnouchi,[162] H. Jivan,[32c] P. Johansson,[146] K. A. Johns,[7] C. A. Johnson,[63] W. J. Johnson,[145] K. Jon-And,[43a,43b] R. W. L. Jones,[87] S. D. Jones,[153] S. Jones,[7] T. J. Jones,[88] J. Jongmanns,[59a] P. M. Jorge,[137a,137b] J. Jovicevic,[165a] X. Ju,[178] J. J. Junggeburth,[113] A. Juste Rozas,[14,z] A. Kaczmarska,[82] M. Kado,[129] H. Kagan,[123] M. Kagan,[150] T. Kaji,[176] E. Kajomovitz,[157] C. W. Kalderon,[94] A. Kaluza,[97] S. Kama,[41] A. Kamenshchikov,[121] L. Kanjir,[89] Y. Kano,[160] V. A. Kantserov,[110] J. Kanzaki,[79] B. Kaplan,[122] L. S. Kaplan,[178] D. Kar,[32c] M. J. Kareem,[165b] E. Karentzos,[10] S. N. Karpov,[77] Z. M. Karpova,[77] V. Kartvelishvili,[87] A. N. Karyukhin,[121] L. Kashif,[178] R. D. Kass,[123] A. Kastanas,[151] Y. Kataoka,[160] C. Kato,[58d,58c] J. Katzy,[44] K. Kawade,[80] K. Kawagoe,[85] T. Kawamoto,[160] G. Kawamura,[51] E. F. Kay,[88] V. F. Kazanin,[120b,120a] R. Keeler,[173] R. Kehoe,[41] J. S. Keller,[33] E. Kellermann,[94] J. J. Kempster,[21] J. Kendrick,[21] O. Kepka,[138] S. Kersten,[179] B. P. Kerševan,[89] R. A. Keyes,[101] M. Khader,[170] F. Khalil-Zada,[13] A. Khanov,[126] A. G. Kharlamov,[120b,120a] T. Kharlamova,[120b,120a] A. Khodinov,[163] T. J. Khoo,[52] E. Khramov,[77] J. Khubua,[156b] S. Kido,[80] M. Kiehn,[52] C. R. Kilby,[91] Y. K. Kim,[36] N. Kimura,[64a,64c] O. M. Kind,[19] B. T. King,[88] D. Kirchmeier,[46] J. Kirk,[141] A. E. Kiryunin,[113] T. Kishimoto,[160] D. Kisielewska,[81a] V. Kitali,[44] O. Kivernyk,[5] E. Kladiva,[28b,a] T. Klapdor-Kleingrothaus,[50] M. H. Klein,[103] M. Klein,[88] U. Klein,[88] K. Kleinknecht,[97] P. Klimek,[119] A. Klimentov,[29] R. Klingenberg,[45,a] T. Klingl,[24] T. Klioutchnikova,[35] F. F. Klitzner,[112] P. Kluit,[118] S. Kluth,[113] E. Kneringer,[74] E. B. F. G. Knoops,[99] A. Knue,[50] A. Kobayashi,[160] D. Kobayashi,[85] T. Kobayashi,[160] M. Kobel,[46] M. Kocian,[150] P. Kodys,[140] T. Koffas,[33] E. Koffeman,[118] N. M. Köhler,[113] T. Koi,[150] M. Kolb,[59b] I. Koletsou,[5] T. Kondo,[79] N. Kondrashova,[58c] K. Köneke,[50] A. C. König,[117] T. Kono,[79] R. Konoplich,[122,jj] V. Konstantinides,[92] N. Konstantinidis,[92] B. Konya,[94] R. Kopeliansky,[63] S. Koperny,[81a] K. Korcyl,[82] K. Kordas,[159] A. Korn,[92] I. Korolkov,[14] E. V. Korolkova,[146] O. Kortner,[113] S. Kortner,[113] T. Kosek,[140] V. V. Kostyukhin,[24] A. Kotwal,[47] A. Koulouris,[10] A. Kourkoumeli-Charalampidi,[68a,68b] C. Kourkoumelis,[9] E. Kourlitis,[146] V. Kouskoura,[29] A. B. Kowalewska,[82] R. Kowalewski,[173] T. Z. Kowalski,[81a] C. Kozakai,[160] W. Kozanecki,[142] A. S. Kozhin,[121] V. A. Kramarenko,[111] G. Kramberger,[89] D. Krasnopevtsev,[58a] M. W. Krasny,[133] A. Krasznahorkay,[35] D. Krauss,[113] J. A. Kremer,[81a] J. Kretzschmar,[88] P. Krieger,[164] K. Krizka,[18] K. Kroeninger,[45] H. Kroha,[113] J. Kroll,[138] J. Kroll,[134] J. Krstic,[16] U. Kruchonak,[77] H. Krüger,[24] N. Krumnack,[76] M. C. Kruse,[47] T. Kubota,[102] S. Kuday,[4b] J. T. Kuechler,[179] S. Kuehn,[35] A. Kugel,[59a] F. Kuger,[174] T. Kuhl,[44] V. Kukhtin,[77] R. Kukla,[99] Y. Kulchitsky,[105] S. Kuleshov,[144b] Y. P. Kulinich,[170] M. Kuna,[56] T. Kunigo,[83] A. Kupco,[138] T. Kupfer,[45] O. Kuprash,[158] H. Kurashige,[80] L. L. Kurchaninov,[165a] Y. A. Kurochkin,[105] M. G. Kurth,[15d] E. S. Kuwertz,[35] M. Kuze,[162] J. Kvita,[127] T. Kwan,[101] A. La Rosa,[113] J. L. La Rosa Navarro,[78d] L. La Rotonda,[40b,40a] F. La Ruffa,[40b,40a] C. Lacasta,[171] F. Lacava,[70a,70b] J. Lacey,[44] D. P. J. Lack,[98] H. Lacker,[19] D. Lacour,[133] E. Ladygin,[77] R. Lafaye,[5] B. Laforge,[133] T. Lagouri,[32c] S. Lai,[51] S. Lammers,[63] W. Lampl,[7] E. Lançon,[29] U. Landgraf,[50] M. P. J. Landon,[90] M. C. Lanfermann,[52] V. S. Lang,[44] J. C. Lange,[14] R. J. Langenberg,[35] A. J. Lankford,[168] F. Lanni,[29] K. Lantzsch,[24] A. Lanza,[68a] A. Lapertosa,[53b,53a] S. Laplace,[133] J. F. Laporte,[142] T. Lari,[66a] F. Lasagni Manghi,[23b,23a] M. Lassnig,[35] T. S. Lau,[61a] A. Laudrain,[129] M. Lavorgna,[67a,67b] A. T. Law,[143] P. Laycock,[88]

M. Lazzaroni,[66a,66b] B. Le,[102] O. Le Dortz,[133] E. Le Guirriec,[99] E. P. Le Quilleuc,[142] M. LeBlanc,[7] T. LeCompte,[6] F. Ledroit-Guillon,[56] C. A. Lee,[29] G. R. Lee,[144a] L. Lee,[57] S. C. Lee,[155] B. Lefebvre,[101] M. Lefebvre,[173] F. Legger,[112] C. Leggett,[18] N. Lehmann,[179] G. Lehmann Miotto,[35] W. A. Leight,[44] A. Leisos,[159,kk] M. A. L. Leite,[78d] R. Leitner,[140] D. Lellouch,[177] B. Lemmer,[51] K. J. C. Leney,[92] T. Lenz,[24] B. Lenzi,[35] R. Leone,[7] S. Leone,[69a] C. Leonidopoulos,[48] G. Lerner,[153] C. Leroy,[107] R. Les,[164] A. A. J. Lesage,[142] C. G. Lester,[31] M. Levchenko,[135] J. Levêque,[5] D. Levin,[103] L. J. Levinson,[177] D. Lewis,[90] B. Li,[103] C-Q. Li,[58a,ll] H. Li,[58b] L. Li,[58c] Q. Li,[15d] Q. Y. Li,[58a] S. Li,[58d,58c] X. Li,[58c] Y. Li,[148] Z. Liang,[15a] B. Liberti,[71a] A. Liblong,[164] K. Lie,[61c] S. Liem,[118] A. Limosani,[154] C. Y. Lin,[31] K. Lin,[104] T. H. Lin,[97] R. A. Linck,[63] J. H. Lindon,[21] B. E. Lindquist,[152] A. L. Lionti,[52] E. Lipeles,[134] A. Lipniacka,[17] M. Lisovyi,[59b] T. M. Liss,[170,mm] A. Lister,[172] A. M. Litke,[143] J. D. Little,[8] B. Liu,[76] B. L Liu,[6] H. B. Liu,[29] H. Liu,[103] J. B. Liu,[58a] J. K. K. Liu,[132] K. Liu,[133] M. Liu,[58a] P. Liu,[18] Y. Liu,[15a] Y. L. Liu,[58a] Y. W. Liu,[58a] M. Livan,[68a,68b] A. Lleres,[56] J. Llorente Merino,[15a] S. L. Lloyd,[90] C. Y. Lo,[61b] F. Lo Sterzo,[41] E. M. Lobodzinska,[44] P. Loch,[7] T. Lohse,[19] K. Lohwasser,[146] M. Lokajicek,[138] B. A. Long,[25] J. D. Long,[170] R. E. Long,[87] L. Longo,[65a,65b] K. A. Looper,[123] J. A. Lopez,[144b] I. Lopez Paz,[14] A. Lopez Solis,[146] J. Lorenz,[112] N. Lorenzo Martinez,[5] M. Losada,[22] P. J. Lösel,[112] A. Lösle,[50] X. Lou,[44] X. Lou,[15a] A. Lounis,[129] J. Love,[6] P. A. Love,[87] J. J. Lozano Bahilo,[171] H. Lu,[61a] M. Lu,[58a] N. Lu,[103] Y. J. Lu,[62] H. J. Lubatti,[145] C. Luci,[70a,70b] A. Lucotte,[56] C. Luedtke,[50] F. Luehring,[63] I. Luise,[133] L. Luminari,[70a] B. Lund-Jensen,[151] M. S. Lutz,[100] P. M. Luzi,[133] D. Lynn,[29] R. Lysak,[138] E. Lytken,[94] F. Lyu,[15a] V. Lyubushkin,[77] H. Ma,[29] L. L. Ma,[58b] Y. Ma,[58b] G. Maccarrone,[49] A. Macchiolo,[113] C. M. Macdonald,[146] J. Machado Miguens,[134,137b] D. Madaffari,[171] R. Madar,[37] W. F. Mader,[46] A. Madsen,[44] N. Madysa,[46] J. Maeda,[80] K. Maekawa,[160] S. Maeland,[17] T. Maeno,[29] A. S. Maevskiy,[111] V. Magerl,[50] C. Maidantchik,[78b] T. Maier,[112] A. Maio,[137a,137b,137d] O. Majersky,[28a] S. Majewski,[128] Y. Makida,[79] N. Makovec,[129] B. Malaescu,[133] Pa. Malecki,[82] V. P. Maleev,[135] F. Malek,[56] U. Mallik,[75] D. Malon,[6] C. Malone,[31] S. Maltezos,[10] S. Malyukov,[35] J. Mamuzic,[171] G. Mancini,[49] I. Mandić,[89] J. Maneira,[137a] L. Manhaes de Andrade Filho,[78a] J. Manjarres Ramos,[46] K. H. Mankinen,[94] A. Mann,[112] A. Manousos,[74] B. Mansoulie,[142] J. D. Mansour,[15a] M. Mantoani,[51] S. Manzoni,[66a,66b] G. Marceca,[30] L. March,[52] L. Marchese,[132] G. Marchiori,[133] M. Marcisovsky,[138] C. A. Marin Tobon,[35] M. Marjanovic,[37] D. E. Marley,[103] F. Marroquim,[78b] Z. Marshall,[18] M. U. F Martensson,[169] S. Marti-Garcia,[171] C. B. Martin,[123] T. A. Martin,[175] V. J. Martin,[48] B. Martin dit Latour,[17] M. Martinez,[14,z] V. I. Martinez Outschoorn,[100] S. Martin-Haugh,[141] V. S. Martoiu,[27b] A. C. Martyniuk,[92] A. Marzin,[35] L. Masetti,[97] T. Mashimo,[160] R. Mashinistov,[108] J. Masik,[98] A. L. Maslennikov,[120b,120a] L. H. Mason,[102] L. Massa,[71a,71b] P. Massarotti,[67a,67b] P. Mastrandrea,[5] A. Mastroberardino,[40b,40a] T. Masubuchi,[160] P. Mättig,[179] J. Maurer,[27b] B. Maček,[89] S. J. Maxfield,[88] D. A. Maximov,[120b,120a] R. Mazini,[155] I. Maznas,[159] S. M. Mazza,[143] N. C. Mc Fadden,[116] G. Mc Goldrick,[164] S. P. Mc Kee,[103] A. McCarn,[103] T. G. McCarthy,[113] L. I. McClymont,[92] E. F. McDonald,[102] J. A. Mcfayden,[35] G. Mchedlidze,[51] M. A. McKay,[41] K. D. McLean,[173] S. J. McMahon,[141] P. C. McNamara,[102] C. J. McNicol,[175] R. A. McPherson,[173,o] J. E. Mdhluli,[32c] Z. A. Meadows,[100] S. Meehan,[145] T. M. Megy,[50] S. Mehlhase,[112] A. Mehta,[88] T. Meideck,[56] B. Meirose,[42] D. Melini,[171,nn] B. R. Mellado Garcia,[32c] J. D. Mellenthin,[51] M. Melo,[28a] F. Meloni,[44] A. Melzer,[24] S. B. Menary,[98] E. D. Mendes Gouveia,[137a] L. Meng,[88] X. T. Meng,[103] A. Mengarelli,[23b,23a] S. Menke,[113] E. Meoni,[40b,40a] S. Mergelmeyer,[19] C. Merlassino,[20] P. Mermod,[52] L. Merola,[67a,67b] C. Meroni,[66a] F. S. Merritt,[36] A. Messina,[70a,70b] J. Metcalfe,[6] A. S. Mete,[168] C. Meyer,[134] J. Meyer,[157] J-P. Meyer,[142] H. Meyer Zu Theenhausen,[59a] F. Miano,[153] R. P. Middleton,[141] L. Mijović,[48] G. Mikenberg,[177] M. Mikestikova,[138] M. Mikuž,[89] M. Milesi,[102] A. Milic,[164] D. A. Millar,[90] D. W. Miller,[36] A. Milov,[177] D. A. Milstead,[43a,43b] A. A. Minaenko,[121] M. Miñano Moya,[171] I. A. Minashvili,[156b] A. I. Mincer,[122] B. Mindur,[81a] M. Mineev,[77] Y. Minegishi,[160] Y. Ming,[178] L. M. Mir,[14] A. Mirto,[65a,65b] K. P. Mistry,[134] T. Mitani,[176] J. Mitrevski,[112] V. A. Mitsou,[171] A. Miucci,[20] P. S. Miyagawa,[146] A. Mizukami,[79] J. U. Mjörnmark,[94] T. Mkrtchyan,[181] M. Mlynarikova,[140] T. Moa,[43a,43b] K. Mochizuki,[107] P. Mogg,[50] S. Mohapatra,[38] S. Molander,[43a,43b] R. Moles-Valls,[24] M. C. Mondragon,[104] K. Mönig,[44] J. Monk,[39] E. Monnier,[99] A. Montalbano,[149] J. Montejo Berlingen,[35] F. Monticelli,[86] S. Monzani,[66a] N. Morange,[129] D. Moreno,[22] M. Moreno Llácer,[35] P. Morettini,[53b] M. Morgenstern,[118] S. Morgenstern,[46] D. Mori,[149] M. Morii,[57] M. Morinaga,[176] V. Morisbak,[131] A. K. Morley,[35] G. Mornacchi,[35] A. P. Morris,[92] J. D. Morris,[90] L. Morvaj,[152] P. Moschovakos,[10] M. Mosidze,[156b] H. J. Moss,[146] J. Moss,[150,oo] K. Motohashi,[162] R. Mount,[150] E. Mountricha,[35] E. J. W. Moyse,[100] S. Muanza,[99] F. Mueller,[113] J. Mueller,[136] R. S. P. Mueller,[112] D. Muenstermann,[87] G. A. Mullier,[20] F. J. Munoz Sanchez,[98] P. Murin,[28b] W. J. Murray,[175,141] A. Murrone,[66a,66b] M. Muškinja,[89] C. Mwewa,[32a] A. G. Myagkov,[121,pp] J. Myers,[128] M. Myska,[139] B. P. Nachman,[18] O. Nackenhorst,[45] K. Nagai,[132] K. Nagano,[79] Y. Nagasaka,[60] M. Nagel,[50] E. Nagy,[99]

A. M. Nairz,[35] Y. Nakahama,[115] K. Nakamura,[79] T. Nakamura,[160] I. Nakano,[124] H. Nanjo,[130] F. Napolitano,[59a] R. F. Naranjo Garcia,[44] R. Narayan,[11] D. I. Narrias Villar,[59a] I. Naryshkin,[135] T. Naumann,[44] G. Navarro,[22] R. Nayyar,[7] H. A. Neal,[103,a] P. Y. Nechaeva,[108] T. J. Neep,[142] A. Negri,[68a,68b] M. Negrini,[23b] S. Nektarijevic,[117] C. Nellist,[51] M. E. Nelson,[132] S. Nemecek,[138] P. Nemethy,[122] M. Nessi,[35,qq] M. S. Neubauer,[170] M. Neumann,[179] P. R. Newman,[21] T. Y. Ng,[61c] Y. S. Ng,[19] H. D. N. Nguyen,[99] T. Nguyen Manh,[107] E. Nibigira,[37] R. B. Nickerson,[132] R. Nicolaidou,[142] J. Nielsen,[143] N. Nikiforou,[11] V. Nikolaenko,[121,pp] I. Nikolic-Audit,[133] K. Nikolopoulos,[21] P. Nilsson,[29] Y. Ninomiya,[79] A. Nisati,[70a] N. Nishu,[58c] R. Nisius,[113] I. Nitsche,[45] T. Nitta,[176] T. Nobe,[160] Y. Noguchi,[83] M. Nomachi,[130] I. Nomidis,[133] M. A. Nomura,[29] T. Nooney,[90] M. Nordberg,[35] N. Norjoharuddeen,[132] T. Novak,[89] O. Novgorodova,[46] R. Novotny,[139] L. Nozka,[127] K. Ntekas,[168] E. Nurse,[92] F. Nuti,[102] F. G. Oakham,[33,f] H. Oberlack,[113] T. Obermann,[24] J. Ocariz,[133] A. Ochi,[80] I. Ochoa,[38] J. P. Ochoa-Ricoux,[144a] K. O'Connor,[26] S. Oda,[85] S. Odaka,[79] S. Oerdek,[51] A. Oh,[98] S. H. Oh,[47] C. C. Ohm,[151] H. Oide,[53b,53a] M. L. Ojeda,[164] H. Okawa,[166] Y. Okazaki,[83] Y. Okumura,[160] T. Okuyama,[79] A. Olariu,[27b] L. F. Oleiro Seabra,[137a] S. A. Olivares Pino,[144a] D. Oliveira Damazio,[29] J. L. Oliver,[1] M. J. R. Olsson,[36] A. Olszewski,[82] J. Olszowska,[82] D. C. O'Neil,[149] A. Onofre,[137a,137e] K. Onogi,[115] P. U. E. Onyisi,[11] H. Oppen,[131] M. J. Oreglia,[36] Y. Oren,[158] D. Orestano,[72a,72b] E. C. Orgill,[98] N. Orlando,[61b] A. A. O'Rourke,[44] R. S. Orr,[164] B. Osculati,[53b,53a,a] V. O'Shea,[55] R. Ospanov,[58a] G. Otero y Garzon,[30] H. Otono,[85] M. Ouchrif,[34d] F. Ould-Saada,[131] A. Ouraou,[142] Q. Ouyang,[15a] M. Owen,[55] R. E. Owen,[21] V. E. Ozcan,[12c] N. Ozturk,[8] J. Pacalt,[127] H. A. Pacey,[31] K. Pachal,[149] A. Pacheco Pages,[14] L. Pacheco Rodriguez,[142] C. Padilla Aranda,[14] S. Pagan Griso,[18] M. Paganini,[180] G. Palacino,[63] S. Palazzo,[40b,40a] S. Palestini,[35] M. Palka,[81b] D. Pallin,[37] I. Panagoulias,[10] C. E. Pandini,[35] J. G. Panduro Vazquez,[91] P. Pani,[35] G. Panizzo,[64a,64c] L. Paolozzi,[52] T. D. Papadopoulou,[10] K. Papageorgiou,[9,v] A. Paramonov,[6] D. Paredes Hernandez,[61b] S. R. Paredes Saenz,[132] B. Parida,[58c] A. J. Parker,[87] K. A. Parker,[44] M. A. Parker,[31] F. Parodi,[53b,53a] J. A. Parsons,[38] U. Parzefall,[50] V. R. Pascuzzi,[164] J. M. P. Pasner,[143] E. Pasqualucci,[70a] S. Passaggio,[53b] F. Pastore,[91] P. Pasuwan,[43a,43b] S. Pataraia,[97] J. R. Pater,[98] A. Pathak,[178,g] T. Pauly,[35] B. Pearson,[113] M. Pedersen,[131] L. Pedraza Diaz,[117] R. Pedro,[137a,137b] S. V. Peleganchuk,[120b,120a] O. Penc,[138] C. Peng,[15d] H. Peng,[58a] B. S. Peralva,[78a] M. M. Perego,[142] A. P. Pereira Peixoto,[137a] D. V. Perepelitsa,[29] F. Peri,[19] L. Perini,[66a,66b] H. Pernegger,[35] S. Perrella,[67a,67b] V. D. Peshekhonov,[77,a] K. Peters,[44] R. F. Y. Peters,[98] B. A. Petersen,[35] T. C. Petersen,[39] E. Petit,[56] A. Petridis,[1] C. Petridou,[159] P. Petroff,[129] M. Petrov,[132] F. Petrucci,[72a,72b] M. Pettee,[180] N. E. Pettersson,[100] A. Peyaud,[142] R. Pezoa,[144b] T. Pham,[102] F. H. Phillips,[104] P. W. Phillips,[141] G. Piacquadio,[152] E. Pianori,[18] A. Picazio,[100] M. A. Pickering,[132] R. H. Pickles,[98] R. Piegaia,[30] J. E. Pilcher,[36] A. D. Pilkington,[98] M. Pinamonti,[71a,71b] J. L. Pinfold,[3] M. Pitt,[177] M.-A. Pleier,[29] V. Pleskot,[140] E. Plotnikova,[77] D. Pluth,[76] P. Podberezko,[120b,120a] R. Poettgen,[94] R. Poggi,[52] L. Poggioli,[129] I. Pogrebnyak,[104] D. Pohl,[24] I. Pokharel,[51] G. Polesello,[68a] A. Poley,[44] A. Policicchio,[70a,70b] R. Polifka,[35] A. Polini,[23b] C. S. Pollard,[44] V. Polychronakos,[29] D. Ponomarenko,[110] L. Pontecorvo,[35] G. A. Popeneciu,[27d] D. M. Portillo Quintero,[133] S. Pospisil,[139] K. Potamianos,[44] I. N. Potrap,[77] C. J. Potter,[31] H. Potti,[11] T. Poulsen,[94] J. Poveda,[35] T. D. Powell,[146] M. E. Pozo Astigarraga,[35] P. Pralavorio,[99] S. Prell,[76] D. Price,[98] M. Primavera,[65a] S. Prince,[101] N. Proklova,[110] K. Prokofiev,[61c] F. Prokoshin,[144b] S. Protopopescu,[29] J. Proudfoot,[6] M. Przybycien,[81a] A. Puri,[170] P. Puzo,[129] J. Qian,[103] Y. Qin,[98] A. Quadt,[51] M. Queitsch-Maitland,[44] A. Qureshi,[1] P. Rados,[102] F. Ragusa,[66a,66b] G. Rahal,[95] J. A. Raine,[52] S. Rajagopalan,[29] A. Ramirez Morales,[90] T. Rashid,[129] S. Raspopov,[5] M. G. Ratti,[66a,66b] D. M. Rauch,[44] F. Rauscher,[112] S. Rave,[97] B. Ravina,[146] I. Ravinovich,[177] J. H. Rawling,[98] M. Raymond,[35] A. L. Read,[131] N. P. Readioff,[56] M. Reale,[65a,65b] D. M. Rebuzzi,[68a,68b] A. Redelbach,[174] G. Redlinger,[29] R. Reece,[143] R. G. Reed,[32c] K. Reeves,[42] L. Rehnisch,[19] J. Reichert,[134] A. Reiss,[97] C. Rembser,[35] H. Ren,[15d] M. Rescigno,[70a] S. Resconi,[66a] E. D. Resseguie,[134] S. Rettie,[172] E. Reynolds,[21] O. L. Rezanova,[120b,120a] P. Reznicek,[140] E. Ricci,[73a,73b] R. Richter,[113] S. Richter,[92] E. Richter-Was,[81b] O. Ricken,[24] M. Ridel,[133] P. Rieck,[113] C. J. Riegel,[179] O. Rifki,[44] M. Rijssenbeek,[152] A. Rimoldi,[68a,68b] M. Rimoldi,[20] L. Rinaldi,[23b] G. Ripellino,[151] B. Ristić,[87] E. Ritsch,[35] I. Riu,[14] J. C. Rivera Vergara,[144a] F. Rizatdinova,[126] E. Rizvi,[90] C. Rizzi,[14] R. T. Roberts,[98] S. H. Robertson,[101,o] D. Robinson,[31] J. E. M. Robinson,[44] A. Robson,[55] E. Rocco,[97] C. Roda,[69a,69b] Y. Rodina,[99] S. Rodriguez Bosca,[171] A. Rodriguez Perez,[14] D. Rodriguez Rodriguez,[171] A. M. Rodríguez Vera,[165b] S. Roe,[35] C. S. Rogan,[57] O. Røhne,[131] R. Röhrig,[113] C. P. A. Roland,[63] J. Roloff,[57] A. Romaniouk,[110] M. Romano,[23b,23a] N. Rompotis,[88] M. Ronzani,[122] L. Roos,[133] S. Rosati,[70a] K. Rosbach,[50] P. Rose,[143] N-A. Rosien,[51] E. Rossi,[44] E. Rossi,[67a,67b] L. P. Rossi,[53b] L. Rossini,[66a,66b] J. H. N. Rosten,[31] R. Rosten,[14] M. Rotaru,[27b] J. Rothberg,[145] D. Rousseau,[129] D. Roy,[32c] A. Rozanov,[99] Y. Rozen,[157] X. Ruan,[32c] F. Rubbo,[150] F. Rühr,[50] A. Ruiz-Martinez,[171] Z. Rurikova,[50] N. A. Rusakovich,[77] H. L. Russell,[101] J. P. Rutherfoord,[7] E. M. Rüttinger,[44,rr] Y. F. Ryabov,[135] M. Rybar,[170] G. Rybkin,[129] S. Ryu,[6] A. Ryzhov,[121] G. F. Rzehorz,[51] P. Sabatini,[51] G. Sabato,[118]

S. Sacerdoti,[129] H. F-W. Sadrozinski,[143] R. Sadykov,[77] F. Safai Tehrani,[70a] P. Saha,[119] M. Sahinsoy,[59a] A. Sahu,[179] M. Saimpert,[44] M. Saito,[160] T. Saito,[160] H. Sakamoto,[160] A. Sakharov,[122,jj] D. Salamani,[52] G. Salamanna,[72a,72b] J. E. Salazar Loyola,[144b] D. Salek,[118] P. H. Sales De Bruin,[169] D. Salihagic,[113] A. Salnikov,[150] J. Salt,[171] D. Salvatore,[40b,40a] F. Salvatore,[153] A. Salvucci,[61a,61b,61c] A. Salzburger,[35] J. Samarati,[35] D. Sammel,[50] D. Sampsonidis,[159] D. Sampsonidou,[159] J. Sánchez,[171] A. Sanchez Pineda,[64a,64c] H. Sandaker,[131] C. O. Sander,[44] M. Sandhoff,[179] C. Sandoval,[22] D. P. C. Sankey,[141] M. Sannino,[53b,53a] Y. Sano,[115] A. Sansoni,[49] C. Santoni,[37] H. Santos,[137a] I. Santoyo Castillo,[153] A. Santra,[171] A. Sapronov,[77] J. G. Saraiva,[137a,137d] O. Sasaki,[79] K. Sato,[166] E. Sauvan,[5] P. Savard,[164,f] N. Savic,[113] R. Sawada,[160] C. Sawyer,[141] L. Sawyer,[93,x] C. Sbarra,[23b] A. Sbrizzi,[23a] T. Scanlon,[92] J. Schaarschmidt,[145] P. Schacht,[113] B. M. Schachtner,[112] D. Schaefer,[36] L. Schaefer,[134] J. Schaeffer,[97] S. Schaepe,[35] U. Schäfer,[97] A. C. Schaffer,[129] D. Schaile,[112] R. D. Schamberger,[152] N. Scharmberg,[98] V. A. Schegelsky,[135] D. Scheirich,[140] F. Schenck,[19] M. Schernau,[168] C. Schiavi,[53b,53a] S. Schier,[143] L. K. Schildgen,[24] Z. M. Schillaci,[26] E. J. Schioppa,[35] M. Schioppa,[40b,40a] K. E. Schleicher,[50] S. Schlenker,[35] K. R. Schmidt-Sommerfeld,[113] K. Schmieden,[35] C. Schmitt,[97] S. Schmitt,[44] S. Schmitz,[97] J. C. Schmoeckel,[44] U. Schnoor,[50] L. Schoeffel,[142] A. Schoening,[59b] E. Schopf,[24] M. Schott,[97] J. F. P. Schouwenberg,[117] J. Schovancova,[35] S. Schramm,[52] A. Schulte,[97] H-C. Schultz-Coulon,[59a] M. Schumacher,[50] B. A. Schumm,[143] Ph. Schune,[142] A. Schwartzman,[150] T. A. Schwarz,[103] H. Schweiger,[98] Ph. Schwemling,[142] R. Schwienhorst,[104] A. Sciandra,[24] G. Sciolla,[26] M. Scornajenghi,[40b,40a] F. Scuri,[69a] F. Scutti,[102] L. M. Scyboz,[113] J. Searcy,[103] C. D. Sebastiani,[70a,70b] P. Seema,[24] S. C. Seidel,[116] A. Seiden,[143] T. Seiss,[36] J. M. Seixas,[78b] G. Sekhniaidze,[67a] K. Sekhon,[103] S. J. Sekula,[41] N. Semprini-Cesari,[23b,23a] S. Sen,[47] S. Senkin,[37] C. Serfon,[131] L. Serin,[129] L. Serkin,[64a,64b] M. Sessa,[72a,72b] H. Severini,[125] F. Sforza,[167] A. Sfyrla,[52] E. Shabalina,[51] J. D. Shahinian,[143] N. W. Shaikh,[43a,43b] L. Y. Shan,[15a] R. Shang,[170] J. T. Shank,[25] M. Shapiro,[18] A. S. Sharma,[1] A. Sharma,[132] P. B. Shatalov,[109] K. Shaw,[153] S. M. Shaw,[98] A. Shcherbakova,[135] Y. Shen,[125] N. Sherafati,[33] A. D. Sherman,[25] P. Sherwood,[92] L. Shi,[155,ss] S. Shimizu,[79] C. O. Shimmin,[180] M. Shimojima,[114] I. P. J. Shipsey,[132] S. Shirabe,[85] M. Shiyakova,[77] J. Shlomi,[177] A. Shmeleva,[108] D. Shoaleh Saadi,[107] M. J. Shochet,[36] S. Shojaii,[102] D. R. Shope,[125] S. Shrestha,[123] E. Shulga,[110] P. Sicho,[138] A. M. Sickles,[170] P. E. Sidebo,[151] E. Sideras Haddad,[32c] O. Sidiropoulou,[35] A. Sidoti,[23b,23a] F. Siegert,[46] Dj. Sijacki,[16] J. Silva,[137a] M. Silva Jr.,[178] M. V. Silva Oliveira,[78a] S. B. Silverstein,[43a] L. Simic,[77] S. Simion,[129] E. Simioni,[97] M. Simon,[97] R. Simoniello,[97] P. Sinervo,[164] N. B. Sinev,[128] M. Sioli,[23b,23a] G. Siragusa,[174] I. Siral,[103] S. Yu. Sivoklokov,[111] J. Sjölin,[43a,43b] P. Skubic,[125] M. Slater,[21] T. Slavicek,[139] M. Slawinska,[82] K. Sliwa,[167] R. Slovak,[140] V. Smakhtin,[177] B. H. Smart,[5] J. Smiesko,[28a] N. Smirnov,[110] S. Yu. Smirnov,[110] Y. Smirnov,[110] L. N. Smirnova,[111] O. Smirnova,[94] J. W. Smith,[51] M. N. K. Smith,[38] M. Smizanska,[87] K. Smolek,[139] A. Smykiewicz,[82] A. A. Snesarev,[108] I. M. Snyder,[128] S. Snyder,[29] R. Sobie,[173,o] A. M. Soffa,[168] A. Soffer,[158] A. Søgaard,[48] D. A. Soh,[155] G. Sokhrannyi,[89] C. A. Solans Sanchez,[35] M. Solar,[139] E. Yu. Soldatov,[110] U. Soldevila,[171] A. A. Solodkov,[121] A. Soloshenko,[77] O. V. Solovyanov,[121] V. Solovyev,[135] P. Sommer,[146] H. Son,[167] W. Song,[141] W. Y. Song,[165b] A. Sopczak,[139] F. Sopkova,[28b] D. Sosa,[59b] C. L. Sotiropoulou,[69a,69b] S. Sottocornola,[68a,68b] R. Soualah,[64a,64c,tt] A. M. Soukharev,[120b,120a] D. South,[44] B. C. Sowden,[91] S. Spagnolo,[65a,65b] M. Spalla,[113] M. Spangenberg,[175] F. Spanò,[91] D. Sperlich,[19] F. Spettel,[113] T. M. Spieker,[59a] R. Spighi,[23b] G. Spigo,[35] L. A. Spiller,[102] D. P. Spiteri,[55] M. Spousta,[140] A. Stabile,[66a,66b] R. Stamen,[59a] S. Stamm,[19] E. Stanecka,[82] R. W. Stanek,[6] C. Stanescu,[72a] B. Stanislaus,[132] M. M. Stanitzki,[44] B. Stapf,[118] S. Stapnes,[131] E. A. Starchenko,[121] G. H. Stark,[36] J. Stark,[56] S. H Stark,[39] P. Staroba,[138] P. Starovoitov,[59a] S. Stärz,[35] R. Staszewski,[82] M. Stegler,[44] P. Steinberg,[29] B. Stelzer,[149] H. J. Stelzer,[35] O. Stelzer-Chilton,[165a] H. Stenzel,[54] T. J. Stevenson,[90] G. A. Stewart,[35] M. C. Stockton,[128] G. Stoicea,[27b] P. Stolte,[51] S. Stonjek,[113] A. Straessner,[46] J. Strandberg,[151] S. Strandberg,[43a,43b] M. Strauss,[125] P. Strizenec,[28b] R. Ströhmer,[174] D. M. Strom,[128] R. Stroynowski,[41] A. Strubig,[48] S. A. Stucci,[29] B. Stugu,[17] J. Stupak,[125] N. A. Styles,[44] D. Su,[150] J. Su,[136] S. Suchek,[59a] Y. Sugaya,[130] M. Suk,[139] V. V. Sulin,[108] D. M. S. Sultan,[52] S. Sultansoy,[4c] T. Sumida,[83] S. Sun,[103] X. Sun,[3] K. Suruliz,[153] C. J. E. Suster,[154] M. R. Sutton,[153] S. Suzuki,[79] M. Svatos,[138] M. Swiatlowski,[36] S. P. Swift,[2] A. Sydorenko,[97] I. Sykora,[28a] T. Sykora,[140] D. Ta,[97] K. Tackmann,[44,uu] J. Taenzer,[158] A. Taffard,[168] R. Tafirout,[165a] E. Tahirovic,[90] N. Taiblum,[158] H. Takai,[29] R. Takashima,[84] E. H. Takasugi,[113] K. Takeda,[80] T. Takeshita,[147] Y. Takubo,[79] M. Talby,[99] A. A. Talyshev,[120b,120a] J. Tanaka,[160] M. Tanaka,[162] R. Tanaka,[129] B. B. Tannenwald,[123] S. Tapia Araya,[144b] S. Tapprogge,[97] A. Tarek Abouelfadl Mohamed,[133] S. Tarem,[157] G. Tarna,[27b,s] G. F. Tartarelli,[66a] P. Tas,[140] M. Tasevsky,[138] T. Tashiro,[83] E. Tassi,[40b,40a] A. Tavares Delgado,[137a,137b] Y. Tayalati,[34e] A. C. Taylor,[116] A. J. Taylor,[48] G. N. Taylor,[102] P. T. E. Taylor,[102] W. Taylor,[165b] A. S. Tee,[87] P. Teixeira-Dias,[91] H. Ten Kate,[35] P. K. Teng,[155] J. J. Teoh,[118] F. Tepel,[179] S. Terada,[79] K. Terashi,[160] J. Terron,[96] S. Terzo,[14] M. Testa,[49] R. J. Teuscher,[164,o] S. J. Thais,[180] T. Theveneaux-Pelzer,[44] F. Thiele,[39]

D. W. Thomas,[91] J. P. Thomas,[21] A. S. Thompson,[55] P. D. Thompson,[21] L. A. Thomsen,[180] E. Thomson,[134] Y. Tian,[38] R. E. Ticse Torres,[51] V. O. Tikhomirov,[108,vv] Yu. A. Tikhonov,[120b,120a] S. Timoshenko,[110] P. Tipton,[180] S. Tisserant,[99] K. Todome,[162] S. Todorova-Nova,[5] S. Todt,[46] J. Tojo,[85] S. Tokár,[28a] K. Tokushuku,[79] E. Tolley,[123] K. G. Tomiwa,[32c] M. Tomoto,[115] L. Tompkins,[150,ii] K. Toms,[116] B. Tong,[57] P. Tornambe,[50] E. Torrence,[128] H. Torres,[46] E. Torró Pastor,[145] C. Tosciri,[132] J. Toth,[99,ww] F. Touchard,[99] D. R. Tovey,[146] C. J. Treado,[122] T. Trefzger,[174] F. Tresoldi,[153] A. Tricoli,[29] I. M. Trigger,[165a] S. Trincaz-Duvoid,[133] M. F. Tripiana,[14] W. Trischuk,[164] B. Trocmé,[56] A. Trofymov,[129] C. Troncon,[66a] M. Trovatelli,[173] F. Trovato,[153] L. Truong,[32b] M. Trzebinski,[82] A. Trzupek,[82] F. Tsai,[44] J. C-L. Tseng,[132] P. V. Tsiareshka,[105] A. Tsirigotis,[159] N. Tsirintanis,[9] V. Tsiskaridze,[152] E. G. Tskhadadze,[156a] I. I. Tsukerman,[109] V. Tsulaia,[18] S. Tsuno,[79] D. Tsybychev,[152] Y. Tu,[61b] A. Tudorache,[27b] V. Tudorache,[27b] T. T. Tulbure,[27a] A. N. Tuna,[57] S. Turchikhin,[77] D. Turgeman,[177] I. Turk Cakir,[4b,xx] R. T. Turra,[66a] P. M. Tuts,[38] E. Tzovara,[97] G. Ucchielli,[23b,23a] I. Ueda,[79] M. Ughetto,[43a,43b] F. Ukegawa,[166] G. Unal,[35] A. Undrus,[29] G. Unel,[168] F. C. Ungaro,[102] Y. Unno,[79] K. Uno,[160] J. Urban,[28b] P. Urquijo,[102] P. Urrejola,[97] G. Usai,[8] J. Usui,[79] L. Vacavant,[99] V. Vacek,[139] B. Vachon,[101] K. O. H. Vadla,[131] A. Vaidya,[92] C. Valderanis,[112] E. Valdes Santurio,[43a,43b] M. Valente,[52] S. Valentinetti,[23b,23a] A. Valero,[171] L. Valéry,[44] R. A. Vallance,[21] A. Vallier,[5] J. A. Valls Ferrer,[171] T. R. Van Daalen,[14] W. Van Den Wollenberg,[118] H. Van der Graaf,[118] P. Van Gemmeren,[6] J. Van Nieuwkoop,[149] I. Van Vulpen,[118] M. Vanadia,[71a,71b] W. Vandelli,[35] A. Vaniachine,[163] P. Vankov,[118] R. Vari,[70a] E. W. Varnes,[7] C. Varni,[53b,53a] T. Varol,[41] D. Varouchas,[129] K. E. Varvell,[154] G. A. Vasquez,[144b] J. G. Vasquez,[180] F. Vazeille,[37] D. Vazquez Furelos,[14] T. Vazquez Schroeder,[101] J. Veatch,[51] V. Vecchio,[72a,72b] L. M. Veloce,[164] F. Veloso,[137a,137c] S. Veneziano,[70a] A. Ventura,[65a,65b] M. Venturi,[173] N. Venturi,[35] V. Vercesi,[68a] M. Verducci,[72a,72b] C. M. Vergel Infante,[76] W. Verkerke,[118] A. T. Vermeulen,[118] J. C. Vermeulen,[118] M. C. Vetterli,[149,f] N. Viaux Maira,[144b] M. Vicente Barreto Pinto,[52] I. Vichou,[170,a] T. Vickey,[146] O. E. Vickey Boeriu,[146] G. H. A. Viehhauser,[132] S. Viel,[18] L. Vigani,[132] M. Villa,[23b,23a] M. Villaplana Perez,[66a,66b] E. Vilucchi,[49] M. G. Vincter,[33] V. B. Vinogradov,[77] A. Vishwakarma,[44] C. Vittori,[23b,23a] I. Vivarelli,[153] S. Vlachos,[10] M. Vogel,[179] P. Vokac,[139] G. Volpi,[14] S. E. von Buddenbrock,[32c] E. Von Toerne,[24] V. Vorobel,[140] K. Vorobev,[110] M. Vos,[171] J. H. Vossebeld,[88] N. Vranjes,[16] M. Vranjes Milosavljevic,[16] V. Vrba,[139] M. Vreeswijk,[118] T. Šfiligoj,[89] R. Vuillermet,[35] I. Vukotic,[36] T. Ženiš,[28a] L. Živković,[16] P. Wagner,[24] W. Wagner,[179] J. Wagner-Kuhr,[112] H. Wahlberg,[86] S. Wahrmund,[46] K. Wakamiya,[80] V. M. Walbrecht,[113] J. Walder,[87] R. Walker,[112] S. D. Walker,[91] W. Walkowiak,[148] V. Wallangen,[43a,43b] A. M. Wang,[57] C. Wang,[58b,s] F. Wang,[178] H. Wang,[18] H. Wang,[3] J. Wang,[154] J. Wang,[59b] P. Wang,[41] Q. Wang,[125] R.-J. Wang,[133] R. Wang,[58a] R. Wang,[6] S. M. Wang,[155] W. T. Wang,[58a] W. Wang,[15c,yy] W. X. Wang,[58a,yy] Y. Wang,[58a,ll] Z. Wang,[58c] C. Wanotayaroj,[44] A. Warburton,[101] C. P. Ward,[31] D. R. Wardrope,[92] A. Washbrook,[48] P. M. Watkins,[21] A. T. Watson,[21] M. F. Watson,[21] G. Watts,[145] S. Watts,[98] B. M. Waugh,[92] A. F. Webb,[11] S. Webb,[97] C. Weber,[180] M. S. Weber,[20] S. A. Weber,[33] S. M. Weber,[59a] A. R. Weidberg,[132] B. Weinert,[63] J. Weingarten,[45] M. Weirich,[97] C. Weiser,[50] P. S. Wells,[35] T. Wenaus,[29] T. Wengler,[35] S. Wenig,[35] N. Wermes,[24] M. D. Werner,[76] P. Werner,[35] M. Wessels,[59a] T. D. Weston,[20] K. Whalen,[128] N. L. Whallon,[145] A. M. Wharton,[87] A. S. White,[103] A. White,[8] M. J. White,[1] R. White,[144b] D. Whiteson,[168] B. W. Whitmore,[87] F. J. Wickens,[141] W. Wiedenmann,[178] M. Wielers,[141] C. Wiglesworth,[39] L. A. M. Wiik-Fuchs,[50] A. Wildauer,[113] F. Wilk,[98] H. G. Wilkens,[35] L. J. Wilkins,[91] H. H. Williams,[134] S. Williams,[31] C. Willis,[104] S. Willocq,[100] J. A. Wilson,[21] I. Wingerter-Seez,[5] E. Winkels,[153] F. Winklmeier,[128] O. J. Winston,[153] B. T. Winter,[24] M. Wittgen,[150] M. Wobisch,[93] A. Wolf,[97] T. M. H. Wolf,[118] R. Wolff,[99] M. W. Wolter,[82] H. Wolters,[137a,137c] V. W. S. Wong,[172] N. L. Woods,[143] S. D. Worm,[21] B. K. Wosiek,[82] K. W. Woźniak,[82] K. Wraight,[55] M. Wu,[36] S. L. Wu,[178] X. Wu,[52] Y. Wu,[58a] T. R. Wyatt,[98] B. M. Wynne,[48] S. Xella,[39] Z. Xi,[103] L. Xia,[175] D. Xu,[15a] H. Xu,[58a,s] L. Xu,[29] T. Xu,[142] W. Xu,[103] B. Yabsley,[154] S. Yacoob,[32a] K. Yajima,[130] D. P. Yallup,[92] D. Yamaguchi,[162] Y. Yamaguchi,[162] A. Yamamoto,[79] T. Yamanaka,[160] F. Yamane,[80] M. Yamatani,[160] T. Yamazaki,[160] Y. Yamazaki,[80] Z. Yan,[25] H. J. Yang,[58c,58d] H. T. Yang,[18] S. Yang,[75] Y. Yang,[160] Z. Yang,[17] W-M. Yao,[18] Y. C. Yap,[44] Y. Yasu,[79] E. Yatsenko,[58c,58d] J. Ye,[41] S. Ye,[29] I. Yeletskikh,[77] E. Yigitbasi,[25] E. Yildirim,[97] K. Yorita,[176] K. Yoshihara,[134] C. J. S. Young,[35] C. Young,[150] J. Yu,[8] J. Yu,[76] X. Yue,[59a] S. P. Y. Yuen,[24] B. Zabinski,[82] G. Zacharis,[10] E. Zaffaroni,[52] R. Zaidan,[14] A. M. Zaitsev,[121,pp] T. Zakareishvili,[156b] N. Zakharchuk,[44] J. Zalieckas,[17] S. Zambito,[57] D. Zanzi,[35] D. R. Zaripovas,[55] S. V. Zeißner,[45] C. Zeitnitz,[179] G. Zemaityte,[132] J. C. Zeng,[170] Q. Zeng,[150] O. Zenin,[121] D. Zerwas,[129] M. Zgubič,[132] D. F. Zhang,[58b] D. Zhang,[103] F. Zhang,[178] G. Zhang,[58a] H. Zhang,[15c] J. Zhang,[6] L. Zhang,[15c] L. Zhang,[58a] M. Zhang,[170] P. Zhang,[15c] R. Zhang,[58a] R. Zhang,[24] X. Zhang,[58b] Y. Zhang,[15d] Z. Zhang,[129] P. Zhao,[47] X. Zhao,[41] Y. Zhao,[58b,129,bb] Z. Zhao,[58a] A. Zhemchugov,[77] B. Zhou,[103] C. Zhou,[178] L. Zhou,[41] M. S. Zhou,[15d] M. Zhou,[152] N. Zhou,[58c] Y. Zhou,[7] C. G. Zhu,[58b] H. L. Zhu,[58a] H. Zhu,[15a] J. Zhu,[103] Y. Zhu,[58a] X. Zhuang,[15a]

K. Zhukov,[108] V. Zhulanov,[120b,120a] A. Zibell,[174] D. Zieminska,[63] N. I. Zimine,[77] S. Zimmermann,[50] Z. Zinonos,[113] M. Zinser,[97] M. Ziolkowski,[148] G. Zobernig,[178] A. Zoccoli,[23b,23a] K. Zoch,[51] T. G. Zorbas,[146] R. Zou,[36] M. Zur Nedden,[19] and L. Zwalinski[35]

(ATLAS Collaboration)

[1]*Department of Physics, University of Adelaide, Adelaide, Australia*
[2]*Physics Department, SUNY Albany, Albany, New York, USA*
[3]*Department of Physics, University of Alberta, Edmonton, Alberta, Canada*
[4a]*Department of Physics, Ankara University, Ankara, Turkey*
[4b]*Istanbul Aydin University, Istanbul, Turkey*
[4c]*Division of Physics, TOBB University of Economics and Technology, Ankara, Turkey*
[5]*LAPP, Université Grenoble Alpes, Université Savoie Mont Blanc, CNRS/IN2P3, Annecy, France*
[6]*High Energy Physics Division, Argonne National Laboratory, Argonne, Illinois, USA*
[7]*Department of Physics, University of Arizona, Tucson, Arizona, USA*
[8]*Department of Physics, University of Texas at Arlington, Arlington, Texas, USA*
[9]*Physics Department, National and Kapodistrian University of Athens, Athens, Greece*
[10]*Physics Department, National Technical University of Athens, Zografou, Greece*
[11]*Department of Physics, University of Texas at Austin, Austin, Texas, USA*
[12a]*Bahcesehir University, Faculty of Engineering and Natural Sciences, Istanbul, Turkey*
[12b]*Istanbul Bilgi University, Faculty of Engineering and Natural Sciences, Istanbul, Turkey*
[12c]*Department of Physics, Bogazici University, Istanbul, Turkey*
[12d]*Department of Physics Engineering, Gaziantep University, Gaziantep, Turkey*
[13]*Institute of Physics, Azerbaijan Academy of Sciences, Baku, Azerbaijan*
[14]*Institut de Física d'Altes Energies (IFAE), Barcelona Institute of Science and Technology, Barcelona, Spain*
[15a]*Institute of High Energy Physics, Chinese Academy of Sciences, Beijing, China*
[15b]*Physics Department, Tsinghua University, Beijing, China*
[15c]*Department of Physics, Nanjing University, Nanjing, China*
[15d]*University of Chinese Academy of Science (UCAS), Beijing, China*
[16]*Institute of Physics, University of Belgrade, Belgrade, Serbia*
[17]*Department for Physics and Technology, University of Bergen, Bergen, Norway*
[18]*Physics Division, Lawrence Berkeley National Laboratory and University of California, Berkeley, California, USA*
[19]*Institut für Physik, Humboldt Universität zu Berlin, Berlin, Germany*
[20]*Albert Einstein Center for Fundamental Physics and Laboratory for High Energy Physics, University of Bern, Bern, Switzerland*
[21]*School of Physics and Astronomy, University of Birmingham, Birmingham, United Kingdom*
[22]*Centro de Investigaciónes, Universidad Antonio Nariño, Bogota, Colombia*
[23a]*Dipartimento di Fisica e Astronomia, Università di Bologna, Bologna, Italy*
[23b]*INFN Sezione di Bologna, Bologna, Italy*
[24]*Physikalisches Institut, Universität Bonn, Bonn, Germany*
[25]*Department of Physics, Boston University, Boston, Massachusetts, USA*
[26]*Department of Physics, Brandeis University, Waltham, Massachusetts, USA*
[27a]*Transilvania University of Brasov, Brasov, Romania*
[27b]*Horia Hulubei National Institute of Physics and Nuclear Engineering, Bucharest, Romania*
[27c]*Department of Physics, Alexandru Ioan Cuza University of Iasi, Iasi, Romania*
[27d]*National Institute for Research and Development of Isotopic and Molecular Technologies, Physics Department, Cluj-Napoca, Romania*
[27e]*University Politehnica Bucharest, Bucharest, Romania*
[27f]*West University in Timisoara, Timisoara, Romania*
[28a]*Faculty of Mathematics, Physics and Informatics, Comenius University, Bratislava, Slovak Republic*
[28b]*Department of Subnuclear Physics, Institute of Experimental Physics of the Slovak Academy of Sciences, Kosice, Slovak Republic*
[29]*Physics Department, Brookhaven National Laboratory, Upton, New York, USA*
[30]*Departamento de Física, Universidad de Buenos Aires, Buenos Aires, Argentina*
[31]*Cavendish Laboratory, University of Cambridge, Cambridge, United Kingdom*
[32a]*Department of Physics, University of Cape Town, Cape Town, South Africa*

[32b]*Department of Mechanical Engineering Science, University of Johannesburg, Johannesburg, South Africa*
[32c]*School of Physics, University of the Witwatersrand, Johannesburg, South Africa*
[33]*Department of Physics, Carleton University, Ottawa, Ontario, Canada*
[34a]*Faculté des Sciences Ain Chock, Réseau Universitaire de Physique des Hautes Energies - Université Hassan II, Casablanca, Morocco*
[34b]*Centre National de l'Energie des Sciences Techniques Nucleaires (CNESTEN), Rabat, Morocco*
[34c]*Faculté des Sciences Semlalia, Université Cadi Ayyad, LPHEA-Marrakech, Morocco*
[34d]*Faculté des Sciences, Université Mohamed Premier and LPTPM, Oujda, Morocco*
[34e]*Faculté des sciences, Université Mohammed V, Rabat, Morocco*
[35]*CERN, Geneva, Switzerland*
[36]*Enrico Fermi Institute, University of Chicago, Chicago, Illinois, USA*
[37]*LPC, Université Clermont Auvergne, CNRS/IN2P3, Clermont-Ferrand, France*
[38]*Nevis Laboratory, Columbia University, Irvington, New York, USA*
[39]*Niels Bohr Institute, University of Copenhagen, Copenhagen, Denmark*
[40a]*Dipartimento di Fisica, Università della Calabria, Rende, Italy*
[40b]*INFN Gruppo Collegato di Cosenza, Laboratori Nazionali di Frascati, Italy*
[41]*Physics Department, Southern Methodist University, Dallas, Texas, USA*
[42]*Physics Department, University of Texas at Dallas, Richardson, Texas, USA*
[43a]*Department of Physics, Stockholm University, Sweden*
[43b]*Oskar Klein Centre, Stockholm, Sweden*
[44]*Deutsches Elektronen-Synchrotron DESY, Hamburg and Zeuthen, Germany*
[45]*Lehrstuhl für Experimentelle Physik IV, Technische Universität Dortmund, Dortmund, Germany*
[46]*Institut für Kern- und Teilchenphysik, Technische Universität Dresden, Dresden, Germany*
[47]*Department of Physics, Duke University, Durham, North Carolina, USA*
[48]*SUPA - School of Physics and Astronomy, University of Edinburgh, Edinburgh, United Kingdom*
[49]*INFN e Laboratori Nazionali di Frascati, Frascati, Italy*
[50]*Physikalisches Institut, Albert-Ludwigs-Universität Freiburg, Freiburg, Germany*
[51]*II. Physikalisches Institut, Georg-August-Universität Göttingen, Göttingen, Germany*
[52]*Département de Physique Nucléaire et Corpusculaire, Université de Genève, Genève, Switzerland*
[53a]*Dipartimento di Fisica, Università di Genova, Genova, Italy*
[53b]*INFN Sezione di Genova, Genova, Italy*
[54]*II. Physikalisches Institut, Justus-Liebig-Universität Giessen, Giessen, Germany*
[55]*SUPA - School of Physics and Astronomy, University of Glasgow, Glasgow, United Kingdom*
[56]*LPSC, Université Grenoble Alpes, CNRS/IN2P3, Grenoble INP, Grenoble, France*
[57]*Laboratory for Particle Physics and Cosmology, Harvard University, Cambridge, Massachusetts, USA*
[58a]*Department of Modern Physics and State Key Laboratory of Particle Detection and Electronics, University of Science and Technology of China, Hefei, China*
[58b]*Institute of Frontier and Interdisciplinary Science and Key Laboratory of Particle Physics and Particle Irradiation (MOE), Shandong University, Qingdao, China*
[58c]*School of Physics and Astronomy, Shanghai Jiao Tong University, KLPPAC-MoE, SKLPPC, Shanghai, China*
[58d]*Tsung-Dao Lee Institute, Shanghai, China*
[59a]*Kirchhoff-Institut für Physik, Ruprecht-Karls-Universität Heidelberg, Heidelberg, Germany*
[59b]*Physikalisches Institut, Ruprecht-Karls-Universität Heidelberg, Heidelberg, Germany*
[60]*Faculty of Applied Information Science, Hiroshima Institute of Technology, Hiroshima, Japan*
[61a]*Department of Physics, Chinese University of Hong Kong, Shatin, N.T., Hong Kong, China*
[61b]*Department of Physics, University of Hong Kong, Hong Kong, China*
[61c]*Department of Physics and Institute for Advanced Study, Hong Kong University of Science and Technology, Clear Water Bay, Kowloon, Hong Kong, China*
[62]*Department of Physics, National Tsing Hua University, Hsinchu, Taiwan*
[63]*Department of Physics, Indiana University, Bloomington, Indiana, USA*
[64a]*INFN Gruppo Collegato di Udine, Sezione di Trieste, Udine, Italy*
[64b]*ICTP, Trieste, Italy*
[64c]*Dipartimento di Chimica, Fisica e Ambiente, Università di Udine, Udine, Italy*
[65a]*INFN Sezione di Lecce, Lecce, Italy*
[65b]*Dipartimento di Matematica e Fisica, Università del Salento, Lecce, Italy*
[66a]*INFN Sezione di Milano, Milano, Italy*
[66b]*Dipartimento di Fisica, Università di Milano, Milano, Italy*
[67a]*INFN Sezione di Napoli, Napoli, Italy*

[67b]Dipartimento di Fisica, Università di Napoli, Napoli, Italy
[68a]INFN Sezione di Pavia, Pavia, Italy
[68b]Dipartimento di Fisica, Università di Pavia, Pavia, Italy
[69a]INFN Sezione di Pisa, Pisa, Italy
[69b]Dipartimento di Fisica E. Fermi, Università di Pisa, Pisa, Italy
[70a]INFN Sezione di Roma, Roma, Italy
[70b]Dipartimento di Fisica, Sapienza Università di Roma, Roma, Italy
[71a]INFN Sezione di Roma Tor Vergata, Roma, Italy
[71b]Dipartimento di Fisica, Università di Roma Tor Vergata, Roma, Italy
[72a]INFN Sezione di Roma Tre, Roma, Italy
[72b]Dipartimento di Matematica e Fisica, Università Roma Tre, Roma, Italy
[73a]INFN-TIFPA, Trento, Italy
[73b]Università degli Studi di Trento, Trento, Italy
[74]Institut für Astro- und Teilchenphysik, Leopold-Franzens-Universität, Innsbruck, Austria
[75]University of Iowa, Iowa City, Iowa, USA
[76]Department of Physics and Astronomy, Iowa State University, Ames, Iowa, USA
[77]Joint Institute for Nuclear Research, Dubna, Russia
[78a]Departamento de Engenharia Elétrica, Universidade Federal de Juiz de Fora (UFJF), Juiz de Fora, Brazil
[78b]Universidade Federal do Rio De Janeiro COPPE/EE/IF, Rio de Janeiro, Brazil
[78c]Universidade Federal de São João del Rei (UFSJ), São João del Rei, Brazil
[78d]Instituto de Física, Universidade de São Paulo, São Paulo, Brazil
[79]KEK, High Energy Accelerator Research Organization, Tsukuba, Japan
[80]Graduate School of Science, Kobe University, Kobe, Japan
[81a]AGH University of Science and Technology, Faculty of Physics and Applied Computer Science, Krakow, Poland
[81b]Marian Smoluchowski Institute of Physics, Jagiellonian University, Krakow, Poland
[82]Institute of Nuclear Physics Polish Academy of Sciences, Krakow, Poland
[83]Faculty of Science, Kyoto University, Kyoto, Japan
[84]Kyoto University of Education, Kyoto, Japan
[85]Research Center for Advanced Particle Physics and Department of Physics, Kyushu University, Fukuoka, Japan
[86]Instituto de Física La Plata, Universidad Nacional de La Plata and CONICET, La Plata, Argentina
[87]Physics Department, Lancaster University, Lancaster, United Kingdom
[88]Oliver Lodge Laboratory, University of Liverpool, Liverpool, United Kingdom
[89]Department of Experimental Particle Physics, Jožef Stefan Institute and Department of Physics, University of Ljubljana, Ljubljana, Slovenia
[90]School of Physics and Astronomy, Queen Mary University of London, London, United Kingdom
[91]Department of Physics, Royal Holloway University of London, Egham, United Kingdom
[92]Department of Physics and Astronomy, University College London, London, United Kingdom
[93]Louisiana Tech University, Ruston, Louisiana, USA
[94]Fysiska institutionen, Lunds universitet, Lund, Sweden
[95]Centre de Calcul de l'Institut National de Physique Nucléaire et de Physique des Particules (IN2P3), Villeurbanne, France
[96]Departamento de Física Teorica C-15 and CIAFF, Universidad Autónoma de Madrid, Madrid, Spain
[97]Institut für Physik, Universität Mainz, Mainz, Germany
[98]School of Physics and Astronomy, University of Manchester, Manchester, United Kingdom
[99]CPPM, Aix-Marseille Université, CNRS/IN2P3, Marseille, France
[100]Department of Physics, University of Massachusetts, Amherst, Massachusetts, USA
[101]Department of Physics, McGill University, Montreal, Québec, Canada
[102]School of Physics, University of Melbourne, Victoria, Australia
[103]Department of Physics, University of Michigan, Ann Arbor, Michigan, USA
[104]Department of Physics and Astronomy, Michigan State University, East Lansing, Michigan, USA
[105]B.I. Stepanov Institute of Physics, National Academy of Sciences of Belarus, Minsk, Belarus
[106]Research Institute for Nuclear Problems of Byelorussian State University, Minsk, Belarus
[107]Group of Particle Physics, University of Montreal, Montreal, Québec, Canada
[108]P.N. Lebedev Physical Institute of the Russian Academy of Sciences, Moscow, Russia
[109]Institute for Theoretical and Experimental Physics (ITEP), Moscow, Russia
[110]National Research Nuclear University MEPhI, Moscow, Russia

[111]*D.V. Skobeltsyn Institute of Nuclear Physics, M.V. Lomonosov Moscow State University, Moscow, Russia*
[112]*Fakultät für Physik, Ludwig-Maximilians-Universität München, München, Germany*
[113]*Max-Planck-Institut für Physik (Werner-Heisenberg-Institut), München, Germany*
[114]*Nagasaki Institute of Applied Science, Nagasaki, Japan*
[115]*Graduate School of Science and Kobayashi-Maskawa Institute, Nagoya University, Nagoya, Japan*
[116]*Department of Physics and Astronomy, University of New Mexico, Albuquerque, New Mexico, USA*
[117]*Institute for Mathematics, Astrophysics and Particle Physics, Radboud University Nijmegen/Nikhef, Nijmegen, Netherlands*
[118]*Nikhef National Institute for Subatomic Physics and University of Amsterdam, Amsterdam, Netherlands*
[119]*Department of Physics, Northern Illinois University, DeKalb, Illinois, USA*
[120a]*Budker Institute of Nuclear Physics and NSU, SB RAS, Novosibirsk, Russia*
[120b]*Novosibirsk State University Novosibirsk, Russia*
[121]*Institute for High Energy Physics of the National Research Centre Kurchatov Institute, Protvino, Russia*
[122]*Department of Physics, New York University, New York, New York, USA*
[123]*The Ohio State University, Columbus, Ohio, USA*
[124]*Faculty of Science, Okayama University, Okayama, Japan*
[125]*Homer L. Dodge Department of Physics and Astronomy, University of Oklahoma, Norman, Oklahoma, USA*
[126]*Department of Physics, Oklahoma State University, Stillwater, Oklahoma, USA*
[127]*Palacký University, RCPTM, Joint Laboratory of Optics, Olomouc, Czech Republic*
[128]*Center for High Energy Physics, University of Oregon, Eugene, Oregon, USA*
[129]*LAL, Université Paris-Sud, CNRS/IN2P3, Université Paris-Saclay, Orsay, France*
[130]*Graduate School of Science, Osaka University, Osaka, Japan*
[131]*Department of Physics, University of Oslo, Oslo, Norway*
[132]*Department of Physics, Oxford University, Oxford, United Kingdom*
[133]*LPNHE, Sorbonne Université, Paris Diderot Sorbonne Paris Cité, CNRS/IN2P3, Paris, France*
[134]*Department of Physics, University of Pennsylvania, Philadelphia, Pennsylvania, USA*
[135]*Konstantinov Nuclear Physics Institute of National Research Centre "Kurchatov Institute", PNPI, St. Petersburg, Russia*
[136]*Department of Physics and Astronomy, University of Pittsburgh, Pittsburgh, Pennsylvania, USA*
[137a]*Laboratório de Instrumentação e Física Experimental de Partículas - LIP, Portugal*
[137b]*Departamento de Física, Faculdade de Ciências, Universidade de Lisboa, Lisboa, Portugal*
[137c]*Departamento de Física, Universidade de Coimbra, Coimbra, Portugal*
[137d]*Centro de Física Nuclear da Universidade de Lisboa, Lisboa, Portugal*
[137e]*Departamento de Física, Universidade do Minho, Braga, Portugal*
[137f]*Departamento de Física Teorica y del Cosmos, Universidad de Granada, Granada (Spain), Spain*
[137g]*Dep Física and CEFITEC of Faculdade de Ciências e Tecnologia, Universidade Nova de Lisboa, Caparica, Portugal*
[138]*Institute of Physics, Academy of Sciences of the Czech Republic, Prague, Czech Republic*
[139]*Czech Technical University in Prague, Prague, Czech Republic*
[140]*Charles University, Faculty of Mathematics and Physics, Prague, Czech Republic*
[141]*Particle Physics Department, Rutherford Appleton Laboratory, Didcot, United Kingdom*
[142]*IRFU, CEA, Université Paris-Saclay, Gif-sur-Yvette, France*
[143]*Santa Cruz Institute for Particle Physics, University of California Santa Cruz, Santa Cruz, California, USA*
[144a]*Departamento de Física, Pontificia Universidad Católica de Chile, Santiago, Chile*
[144b]*Departamento de Física, Universidad Técnica Federico Santa María, Valparaíso, Chile*
[145]*Department of Physics, University of Washington, Seattle, Washington, USA*
[146]*Department of Physics and Astronomy, University of Sheffield, Sheffield, United Kingdom*
[147]*Department of Physics, Shinshu University, Nagano, Japan*
[148]*Department Physik, Universität Siegen, Siegen, Germany*
[149]*Department of Physics, Simon Fraser University, Burnaby, British Columbia, Canada*
[150]*SLAC National Accelerator Laboratory, Stanford, California, USA*
[151]*Physics Department, Royal Institute of Technology, Stockholm, Sweden*
[152]*Departments of Physics and Astronomy, Stony Brook University, Stony Brook, New York, USA*
[153]*Department of Physics and Astronomy, University of Sussex, Brighton, United Kingdom*
[154]*School of Physics, University of Sydney, Sydney, Australia*
[155]*Institute of Physics, Academia Sinica, Taipei, Taiwan*
[156a]*E. Andronikashvili Institute of Physics, Iv. Javakhishvili Tbilisi State University, Tbilisi, Georgia*

[156b]*High Energy Physics Institute, Tbilisi State University, Tbilisi, Georgia*
[157]*Department of Physics, Technion, Israel Institute of Technology, Haifa, Israel*
[158]*Raymond and Beverly Sackler School of Physics and Astronomy, Tel Aviv University, Tel Aviv, Israel*
[159]*Department of Physics, Aristotle University of Thessaloniki, Thessaloniki, Greece*
[160]*International Center for Elementary Particle Physics and Department of Physics, University of Tokyo, Tokyo, Japan*
[161]*Graduate School of Science and Technology, Tokyo Metropolitan University, Tokyo, Japan*
[162]*Department of Physics, Tokyo Institute of Technology, Tokyo, Japan*
[163]*Tomsk State University, Tomsk, Russia*
[164]*Department of Physics, University of Toronto, Toronto, Ontario, Canada*
[165a]*TRIUMF, Vancouver, British Columbia, Canada*
[165b]*Department of Physics and Astronomy, York University, Toronto, Ontario, Canada*
[166]*Division of Physics and Tomonaga Center for the History of the Universe, Faculty of Pure and Applied Sciences, University of Tsukuba, Tsukuba, Japan*
[167]*Department of Physics and Astronomy, Tufts University, Medford, Massachusetts, USA*
[168]*Department of Physics and Astronomy, University of California Irvine, Irvine, California, USA*
[169]*Department of Physics and Astronomy, University of Uppsala, Uppsala, Sweden*
[170]*Department of Physics, University of Illinois, Urbana, Illinois, USA*
[171]*Instituto de Física Corpuscular (IFIC), Centro Mixto Universidad de Valencia - CSIC, Valencia, Spain*
[172]*Department of Physics, University of British Columbia, Vancouver, British Columbia, Canada*
[173]*Department of Physics and Astronomy, University of Victoria, Victoria, British Columbia, Canada*
[174]*Fakultät für Physik und Astronomie, Julius-Maximilians-Universität Würzburg, Würzburg, Germany*
[175]*Department of Physics, University of Warwick, Coventry, United Kingdom*
[176]*Waseda University, Tokyo, Japan*
[177]*Department of Particle Physics, Weizmann Institute of Science, Rehovot, Israel*
[178]*Department of Physics, University of Wisconsin, Madison, Wisconsin, USA*
[179]*Fakultät für Mathematik und Naturwissenschaften, Fachgruppe Physik, Bergische Universität Wuppertal, Wuppertal, Germany*
[180]*Department of Physics, Yale University, New Haven, Connecticut, USA*
[181]*Yerevan Physics Institute, Yerevan, Armenia*

[a]Deceased.
[b]Also at Department of Physics, King's College London, London, United Kingdom.
[c]Also at Istanbul University, Department of Physics, Istanbul, Turkey.
[d]Also at Instituto de Física Teórica de la Universidad Autónoma de Madrid, Spain.
[e]Also at Institute of Physics, Azerbaijan Academy of Sciences, Baku, Azerbaijan.
[f]Also at TRIUMF, Vancouver, British Columbia, Canada.
[g]Also at Department of Physics and Astronomy, University of Louisville, Louisville, Kentucky, USA.
[h]Also at Department of Physics, California State University, Fresno, California, USA.
[i]Also at Department of Physics, University of Fribourg, Fribourg, Switzerland.
[j]Also at Departament de Fisica de la Universitat Autonoma de Barcelona, Barcelona, Spain.
[k]Also at Tomsk State University, Tomsk, and Moscow Institute of Physics and Technology State University, Dolgoprudny, Russia.
[l]Also at The Collaborative Innovation Center of Quantum Matter (CICQM), Beijing, China.
[m]Also at Departamento de Física, Instituto Superior Técnico, Universidade de Lisboa, Lisboa, Portugal.
[n]Also at Universita di Napoli Parthenope, Napoli, Italy.
[o]Also at Institute of Particle Physics (IPP), Victoria, BC, Canada.
[p]Also at II. Physikalisches Institut, Georg-August-Universität Göttingen, Göttingen, Germany.
[q]Also at Dipartimento di Fisica E. Fermi, Università di Pisa, Pisa, Italy.
[r]Also at Horia Hulubei National Institute of Physics and Nuclear Engineering, Bucharest, Romania.
[s]Also at CPPM, Aix-Marseille Université, CNRS/IN2P3, Marseille, France.
[t]Also at Department of Physics, St. Petersburg State Polytechnical University, St. Petersburg, Russia.
[u]Also at Borough of Manhattan Community College, City University of New York, New York, USA.
[v]Also at Department of Financial and Management Engineering, University of the Aegean, Chios, Greece.
[w]Also at Centre for High Performance Computing, CSIR Campus, Rosebank, Cape Town, South Africa.
[x]Also at Louisiana Tech University, Ruston, Louisiana, USA.
[y]Also at California State University, East Bay, California, USA.
[z]Also at Institucio Catalana de Recerca i Estudis Avancats, ICREA, Barcelona, Spain.
[aa]Also at Department of Physics, University of Michigan, Ann Arbor, Michigan, USA.
[bb]Also at LAL, Université Paris-Sud, CNRS/IN2P3, Université Paris-Saclay, Orsay, France.
[cc]Also at Graduate School of Science, Osaka University, Osaka, Japan.

[dd]Also at Physikalisches Institut, Albert-Ludwigs-Universität Freiburg, Freiburg, Germany.
[ee]Also at Institute for Mathematics, Astrophysics and Particle Physics, Radboud University Nijmegen/Nikhef, Nijmegen, Netherlands.
[ff]Also at Near East University, Nicosia, North Cyprus, Mersin, Turkey.
[gg]Also at Institute of Theoretical Physics, Ilia State University, Tbilisi, Georgia.
[hh]Also at CERN, Geneva, Switzerland.
[ii]Also at Department of Physics, Stanford University, Stanford, California, USA.
[jj]Also at Manhattan College, New York, New York, USA.
[kk]Also at Hellenic Open University, Patras, Greece.
[ll]Also at LPNHE, Sorbonne Université, Paris Diderot Sorbonne Paris Cité, CNRS/IN2P3, Paris, France.
[mm]Also at The City College of New York, New York, New York, USA.
[nn]Also at Departamento de Física Teorica y del Cosmos, Universidad de Granada, Granada (Spain), Spain.
[oo]Also at Department of Physics, California State University, Sacramento, California, USA.
[pp]Also at Moscow Institute of Physics and Technology State University, Dolgoprudny, Russia.
[qq]Also at Département de Physique Nucléaire et Corpusculaire, Université de Genève, Genève, Switzerland.
[rr]Also at Department of Physics and Astronomy, University of Sheffield, Sheffield, United Kingdom.
[ss]Also at School of Physics, Sun Yat-sen University, Guangzhou, China.
[tt]Also at Department of Applied Physics and Astronomy, University of Sharjah, Sharjah, United Arab Emirates.
[uu]Also at Institut für Experimentalphysik, Universität Hamburg, Hamburg, Germany.
[vv]Also at National Research Nuclear University MEPhI, Moscow, Russia.
[ww]Also at Institute for Particle and Nuclear Physics, Wigner Research Centre for Physics, Budapest, Hungary.
[xx]Also at Giresun University, Faculty of Engineering, Giresun, Turkey.
[yy]Also at Institute of Physics, Academia Sinica, Taipei, Taiwan.